

ACKNOWLEDGMENT

I am grateful to my research supervisor, Dr. F. D. F. Talbot, for his counsel and encouragement throughout the progress of this work. I wish also to thank Environment Canada and the National Research Council of Canada for providing financial assistance.

I dedicate this thesis to my wife Trinh Khiet and my parents.

ABSTRACT

The removal of copper, lead and cadmium ions from aqueous solution by foam fractionation using sodium dodecylbenzene sulphonate (NaDBS) has been experimentally studied and theoretically predicted for solutions with a pH less than 4. A mathematical model of the system consisting of the equilibrium relations of chemical reactions occurring in the system was solved for the equilibrium concentration of all ions in the solution. Based on this equilibrium concentration and the effective radius of the hydrated ion, a modified theory of the Gouy-Chapman diffuse double layer developed by Jorne and Rubin (9) was used to predict the distribution factor of the metal ions. The work was extended to systems containing two metal ions for the determination of the separability of the ions with respect to each other.

It was found that the distribution factor for solutions containing one metal ion could be predicted theoretically for a bulk solution pH less than four. Deviation of results above this pH was attributed to the limitations of the bulk solution reaction model because it did not include reactions for the formation of poly hydroxyl and poly nuclear hydroxyl complexes. Good agreement was also obtained between experiment and theory in the separability study. The results indicate that the order of removal of the ions from solution is  $Pb^{++} > Cd^{++} > Cu^{++}$ . This sequence is the reverse order of the effective radii of the hydrated ions. The results support the fact that the mechanism for removal of the ions from solution is that of electrical attraction and that selectivity depends upon the charge and size of the hydrated ion.

TABLE OF CONTENTS

	Page
ACKNOWLEDGMENT	i
ABSTRACT	ii
TABLE OF CONTENTS	iii
LIST OF FIGURES	v
LIST OF TABLES	vii
NOMENCLATURE	x
CHAPTER	
1. INTRODUCTION	1
2. LITERATURE SURVEY	3
3. THEORETICAL BACKGROUND	11
3.1 Measurement of the Distribution Factor	11
3.2 Estimation of Bulk Liquid Ionic Composition	13
3.3 The Gouy-Chapman Diffuse Double Layer Model	21
4. EXPERIMENTAL INVESTIGATION	36
4.1 Foam Fractionation	36
4.2 Equilibrium Constant Determination	40
4.3 Instrument and Material	43
5. RESULTS	44
5.1 Results of Equilibrium Constants	44
5.2 Results of Foam Fractionation	47
6. DISCUSSION	67
6.1 Error Analysis	79

	Page
7. CONCLUSIONS	82
8. RECOMMENDATIONS FOR FUTURE WORK	83
REFERENCES	84
GLOSSARY	89
APPENDIX A	91
A.1 A Mathematical Model of the System Containing Two Metal Ions	92
A.2 Derivation of Equation (3.7)	97
A.3 Method of Continuous Variation	99
A.4 Derivation of Equation (3.34)	101
A.5 Derivation of Equation (3.42)	103
A.6 Derivation of Equation (3.44)	104
A.7 Determination of the Effective Radii of Hydrated Ions	105
APPENDIX B Tables of Experimental and Calculated Data	107
APPENDIX C Computer Programs	137

LIST OF FIGURES

<u>Figure</u>		<u>Page</u>
1	A Schematic Representation of the Variation of Interface Concentration With Distance.	24
2	A Lamina in the Solution, Parallel to An Interface.	26
3	Surface Adsorption Model for Small Ions of Charge $z_1$ and Large Ions of Charge $z_2$ to Monolayer of Surfactant of Charge $z_s$ at $x = 0$ .	32
4	Schematic Diagram of the Experimental Apparatus.	37
5	Spectrophotometric Analysis for the Determination of $k_p$ of Cu-NaDBS System.	48
6	Spectrophotometric Analysis for the Determination of $k_p$ of Pb-NaDBS System.	49
7	Spectrophotometric Analysis for the Determination of $k_p$ of Cd-NaDBS System.	50
8	Method of Continuous Variation for the Determination of the value of $n$ in $Cd(DBS)_n$	53
9	Effect of pH on the Distribution Factor of Copper, $[Cu] = 10$ ppm, $[NaDBS] = 0.50$ gm/l.	57
10	Effect of pH on the Distribution Factor of Cadmium, $[Cd] = 10$ ppm, $[NaDBS] = 0.50$ gm/l.	58
11	Effect of pH on the Distribution Factor of Lead, $[Pb] = 10$ ppm, $[NaDBS] = 0.50$ gm/l.	59
12	Effect of Bulk Copper Concentration on Distribution Factor, $pH = 4.70 \pm 0.05$ , $[NaDBS] = 0.50$ gm/l.	60
13	Effect of Bulk Cadmium Concentration on Distribution Factor, $pH = 5.00 \pm 0.05$ , $[NaDBS] = 0.50$ gm/l.	61

Figure

Page

14	Effect of Bulk Lead Concentration on Distribution Factor, $\text{pH} = 5.15 \pm 0.07$ , $[\text{NaDBS}] = 0.50 \text{ gm/l.}$	62
15	Comparison of Predicted and Measured Selectivity Coefficients of Pb-Cu-NaDBS System, $\text{pH} = 4.10 \pm 0.05$ , $[\text{NaDBS}] = 0.50 \text{ gm/l.}$	63
16	Comparison of Predicted and Measured Selectivity Coefficients of Cd-Cu-NaDBS System, $\text{pH} = 4.10 \pm 0.05$ , $[\text{NaDBS}] = 0.50 \text{ gm/l.}$	64
17	Comparison of Predicted and Measured Selectivity Coefficients of Pb-Cd-NaDBS System, $\text{pH} = 4.10 \pm 0.05$ , $[\text{NaDBS}] = 0.50 \text{ gm/l.}$	65
18	pH Change of Cu-NaDBS System : $\text{pHF}$ , pH of Foamate; $\text{pHB}$ , pH of Bulk.	71
19	pH Change of Pb-NaDBS System : $\text{pHF}$ , pH of Foamate; $\text{pHB}$ , pH of Bulk.	72
20	pH Change of Cd-NaDBS System : $\text{pHF}$ , pH of Foamate; $\text{pHB}$ , pH of Bulk.	73

LIST OF TABLES

<u>Table</u>		<u>Page</u>
1	Various Adsorption Bubble Separation Methods Classified on the Basis of Mechanism of Separation and Size of the Material Separated.	4
2	Instrumental Parameters for the Analysis of Metal Ions.	41
3	Equilibrium Constants $k_a$ and $k_d$ of Three Metal Ions.	45
4	Equilibrium Constant of Acetic Acid Measured by Spectrophotometric Analysis.	46
5	Equilibrium Constant $k_c$ of HDDBS	51
6	Slopes and Intercepts of Figures 5 to 7 and the Results of $k_b$	52
7	The Effective Radii of Hydrated Ions	56
8	Comparison of Selectivity Coefficients Measured from Mixture Systems and That Calculated from Pure Component Systems.	66
9	pH Change of Foaming NaDBS Solution Without Metal Ions.	78
A-1	Equilibrium Constants of the Model of Mixture Systems	93
B-1	Spectrophotometric Analysis for the Determination of $k_b$ of Cu-NaDBS System.	108
B-2	Spectrophotometric Analysis for the Determination of $k_b$ of Pb-NaDBS System.	109
B-3	Spectrophotometric Analysis for the Determination of $k_b$ of Cd-NaDBS System.	110
B-4	Spectrophotometric Measurements for the Method of Continuous Variation.	111

<u>Table</u>		<u>Page</u>
B-5	Spectrophotometric Measurements of EDDBS Solution.	112
B-6	Effect of pH on the Distribution Factor of $\text{Cu}^{++}$ and $\text{CuOH}^+$ .	113
B-7	Effect of Bulk Copper Concentration on the Distribution Factor of $\text{Cu}^{++}$ and $\text{CuOH}^+$ .	114
B-8	Effect of pH on the Distribution Factor of $\text{Pb}^{++}$ and $\text{PbOH}^+$ .	115
B-9	Effect of Bulk Lead Concentration on the Distribution Factor of $\text{Pb}^{++}$ and $\text{PbOH}^+$ .	116
B-10	Effect of pH on the Distribution Factor of $\text{Cd}^{++}$ and $\text{CdOH}^+$ .	117
B-11	Effect of Bulk Cadmium Concentration on the Distribution Factor of $\text{Cd}^{++}$ and $\text{CdOH}^+$ .	118
B-12	Theoretical Prediction of Distribution Factor of $\text{Cu}^{++}$ and $\text{CuOH}^+$ vs. Bulk Concentration.	119
B-13	Theoretical Prediction of Distribution Factor of $\text{Cu}^{++}$ and $\text{CuOH}^+$ vs. pH.	120
B-14	Theoretical Prediction of Distribution Factor of $\text{Pb}^{++}$ and $\text{PbOH}^+$ vs. pH.	121
B-15	Theoretical Prediction of Distribution Factor of $\text{Pb}^{++}$ and $\text{PbOH}^+$ vs. Bulk Concentration.	122
B-16	Theoretical Prediction of Distribution Factor of $\text{Cd}^{++}$ and $\text{CdOH}^+$ vs. pH.	123



<u>Table</u>		<u>Page</u>
B-17	Theoretical Prediction of Distribution Factor of $Cd^{++}$ and $CdOH^+$ vs. Bulk Concentration.	124
B-18	Experimental and Predicted Selectivity Coefficient of Cd-Cu-NaDBS System.	125
B-19	Experimental and Predicted Selectivity Coefficient of Pb-Cu-NaDBS System.	126
B-20	Experimental and Predicted Selectivity Coefficient of Pb-Cd-NaDBS System.	127
B-21	Spectrophotometric Measurements of Cu-NaDBS System.	128
B-22	Spectrophotometric Measurements of Pb-NaDBS System.	129
B-23	Spectrophotometric Measurements of Cd-NaDBS System.	130
B-24	Experimental Data of Cu-NaDBS System.	131
B-25	Experimental Data of Pb-NaDBS System.	132
B-26	Experimental Data of Cd-NaDBS System.	133
B-27	Experimental Data of Cu-Cd-NaDBS System.	134
B-28	Experimental Data of Cu-Pb-NaDBS System.	135
B-29	Experimental Data of Cd-Pb-NaDBS System.	136

NOMENCLATURE

- $a_i$  activity of species  $i$  (moles/l.)
- $A(i)$  equilibrium concentration of ions in solution (moles/l.)
- $C_i$  Concentration of solute  $i$  in solution (moles/l.)
- $d$  diameter of individual bubbles (cm.)
- $D$  distribution factor of metal ion
- $e_0$  electronic charge =  $1.602 \times 10^{-19}$  coul.  
=  $4.8029 \times 10^{-10}$  esu.
- $G$  volumetric gas rate ( $\text{cm}^3/\text{min}$ )
- $G(x_i)$  equations of the mathematical model
- $k$  Boltzmann constant =  $1.3805 \times 10^{-16}$  erg/molecule.  $^{\circ}\text{K}$
- $K_1$  equilibrium constant of chemical reaction in solution
- $K$  the Debye-Huckel reciprocal length  
=  $(8\pi e_0^2 z^2 n_1^0 / \epsilon kT)^{1/2}$
- $l$  length of the optical path
- $n$  number of capillaries in a bubbler
- $N$  bubble emission frequency (bubbles/minute/capillary)
- $n_i$  concentration of species  $i$  (moles/l.)
- $n_i^0$  concentration of species  $i$  in bulk liquid
- $P$  volume of solution (liter)
- $Q$  volumetric rate of foam overflow on a gas-free (collapsed) basis
- $S$  surface generation rate ( $\text{cm}^2/\text{min}$ )
- $T$  absolute temperature ( $^{\circ}\text{K}$ )
- $v$  the Boltzmann correction for ions at potential  $\phi$   
 $\phi = \exp(-e_0\phi/kT)$

UNIVERSITY OF UTAH  
LIBRARY

$v_0$	$v$ at $x = x_0$
$w_1$	uncertainty in the independent variable
$x$	distance from interface into the interstitial liquid (cm.)
$x_1$	independent variable
$x_0$	distance of closest approach (cm.)
$y$	the difference between the optical density found and calculated for no reaction
$z_i$	charge of species $i$

Subscripts

b	bulk liquid
d	diffuse layer
f	foamate
s	surfactant

Greek Letters

$\Gamma_1$	surface excess of species $i$ (moles/cm <sup>2</sup> )
$\alpha_{AB}$	selective separation coefficient of element A to B
$\epsilon$	molar extinction coefficient (cm <sup>2</sup> /mole), or dielectrical constant of water = 81 at 18 °C ( 69 )
$\rho$	charge density at distance $x$ from interface (esu/cm <sup>3</sup> )
$\phi$	electrical potential at distance $x$ from interface (erg/coul.)
$\sigma$	surface charge density (esu/cm <sup>2</sup> )

Abbreviations

M <sup>++</sup>	free form of metal ions in solution
DES <sup>-</sup>	anionic surfactant ion
E	experimental result
T	theoretical prediction
OD	optical density
TM	transmittance

Unit

esu	electrostatic unit. ( $\text{gm}^{1/2}\text{cm}^{3/2}\text{sec}^{-1}$ ) = $3.336 \times 10^{-10}$ coul.
erg	$\text{gm cm}^2\text{sec}^{-2}$ = dyne-cm



CHAPTER 1

INTRODUCTION

The use of foaming as a separation technique is well documented. General references concerning the technique have been published by Sebba ( 1 ), Lemlich ( 2 ) and Rubin et al ( 3 ). The separation of ions from aqueous solution using foam fractionation is based on the fact that surface-active materials accumulate at an air-liquid interface. Finally dispersed air bubbles introduced into such a solution will effectively remove the surface-active substance from the solution into the foam. Surface inactive ions, such as metal ions used in this study, can be removed using an ionic surfactant of opposite charge. The actual mechanism of attachment of the surface inactive ion to the surfactant ion depends on the system. Experimental evidence from metal ion removal studies reported by Walling et al ( 4 ), Rubin et al ( 5,6,7 ), and Dick and Talbot ( 8 ) indicate the mechanism to be one of electrical attraction. That is, the layer of anionic surfactant adsorbed at the air-liquid interface has associated with it a diffuse layer of ions of opposite charge in order to maintain electrical neutrality. The fact that counterions associated with the anion layer could consist of a mixture of all the cation species in solution complicates the matter. Preferential attraction of cations to the layer depends on concentration, physical size, and electrical charge.

Application of foaming to the extraction of nonsurface-active species requires a method of predicting the specificity of the foam surface for individual ions in the solution. This specificity may arise from charge interactions between the adsorbed surfactant layer and a diffuse-double-layer of counterions or from bonded interactions of a complex type between surfactant and solution species. Competitive coadsorption of ions of opposite charge to the surfactant based on the diffuse-double-layer theory of Gouy and Chapman and allowing for the difference in the distance of closest approach of ions of different size has been reported by Jorne and Rubin ( 9 ). The theory enables one to predict the distribution factor of each species between a solution of mixed electrolytes and a surface layer, and therefore to calculate the selective separation coefficient between two elements. They reported that the diffuse-double-layer theory agreed well with experimental results for solutions containing  $Sr^{++}$  or  $UO_2^{++}$  in the presence of monobutyl biphenyl sodium sulfonate as the collector.

This study consists of the application of the above principles reported by Jorne and Rubin combined with an equilibrium model of the solution to predict the surface specificity of copper, lead and cadmium in dilute aqueous solution using sodium dodecylbenzene sulfonate as collector. The work represents a variety of bulk solution conditions, different metal ion species, and mixtures of metal ions.

CHAPTER 2

LITERATURE SURVEY

It is difficult to separate soluble materials from solutions when their concentrations are relatively small as most of the separation techniques become inefficient. A number of separation methods which appear to be useful for separating any material particularly when its bulk concentration is low, are called adsorptive bubble separation techniques and are discussed by Lemlich ( 2 ). These methods are based on the fact that the surface-active materials are preferentially concentrated at air-liquid interface and certain other components that are not surface active are associated with these materials so that they can be enriched in the foam phase. The classification of these techniques based on the particle size of the material and the mechanism by which it is separated are listed in table 1. If a species is naturally surface active, it can be separated simply by providing enough air-liquid interface and by collecting the resultant foam. Such a separation is called " foam fractionation " for the separation of surface-active molecules, " foam flotation " for that of hydrophobic colloids, " froth flotation " for that of sieve-size particles of crushed naturally hydrophobic minerals such as sulphur and graphite. If the species to be separated is not naturally surface active, a surface active agent that would associate with the species in some manner is added and

VANIER LIBRARY  
UNIVERSITY OF TORONTO

Table 1. Various Adsorptive Bubble Separation Methods Classified on the Basis of Mechanism of Separation and Size of the Material Separated (10).

MECHANISM	SIZE RANGE		
	MOLECULAR	MICROSCOPIC	MACROSCOPIC
Natural surface activity	FOAM FRACTIONATION ex: detergent from aqueous solutions	FOAM FLOTATION ex: micro-organisms, proteins, dyes	FROTH FLOTATION of non-polar minerals ex: sulfur
	ION FLOTATION MOLECULAR FLOTATION ex: $Sr^{++}$ , $Cu^{++}$ , $Cd^{++}$ , $Pb^{++}$ , $Hg^{++}$ , Cyanides, Phosphates	MICRO FLOTATION ex: particulates in waste, micro-organisms	FROTH FLOTATION ex: minerals such as silica PRECIPITATE FLOTATION ex: ferric hydroxide





then foaming is conducted. This process is called "ion flotation" for the separation of submicro species. The separation of particulates of colloid size by this technique is called "micro flotation" and of sieve-size particles of naturally hydrophilic minerals such as silica and alumina is called "froth flotation".

In the early stage of exploring the foam separation technique, all the experiments reported deal with the separation or purification of naturally surface active substances such as proteins, enzymes, various fatty acids, salts, and detergents. In recent years, the foam separation method has found increasing application in water treatment and the recovery of valuable substances. The former is mainly in the removal of radio-active materials ( 11,12,13 ) and organic substances ( 14 ) from waste waters; an example of the latter is the uranium and vanadium extraction from carbonate solution ( 15 ). A comprehensive review of the materials separated by foam separation techniques was summarized by Rubin and Gaden ( 3 ) in 1962 and by Somasundaran ( 10 ) in 1972.

Copper, cadmium and lead ions were chosen for this study, and it is appropriate to review all the works that have been done on these elements. Rubin et al ( 6,7 ) studied the effect of pH on the separation of copper from dilute aqueous solution using stearylamine or sodium lauryl sulfate ( NaLS ). The mechanism of ion flotation they proposed was that attraction

between the cation and anionic surfactant must be due to specific ion-pair interaction or complex formation, that is the charge on  $LS^-$  is neutralized so that electroneutrality in the foam is maintained. Dick and Talbot ( 8 ) also worked on the same system but more factors were studied. The optimum conditions of removal were found to be as follows : pH range between 5.8 and 5.7 and surfactant concentration of 0.5 gm/l.. It was also found in this work that as the ratio of molar concentration of sodium ion to cupric ion was increased, the distribution factor of copper decreased. A similar decrease was noted for the hydronium ion. This behavior supports the ion attraction mechanism proposed by Rubin et al ( 6,7 ) for the removal of cupric ion from solution using NaLS. The work was extended to study the effect of the addition of an auxiliary ligand and the results indicated that under certain conditions the separation efficiency was improved.

Rubin and Lapp ( 16 ) reported the study on the removal of lead from Pb(II)-NaLS system. An attempt was made to relate the mechanism of the process to the hydrolytic behavior of the metal and the solution pH as well as the ionic strength and collector concentration. The results presented in the per cent removal demonstrate the applicability of hydrolysis data to estimating maximum removals by foam separation. It also mentioned that increasing the ionic strength results in a reduction in lead(II) removal at all pH values. This reduction is attributed to a reduction in the activity of the lead species and increased competition between cations for the collector.

There are no reports available in the literature on the separation of cadmium ion, and this is the first work on this element.

Grieves et al have reported a number of extensive studies on the foam separation process in an effort to establish the effects on the extent of separation of each of the following independent variables : surfactant concentration, temperature, pH and ionic strength etc. The systems they have studied include the separation of orthophosphate ( 17 ), phenol ( 18,19 ), chromium(IV) ( 20,21 ), cyanide complexed by iron ( 22 ), colloidal ferric oxide ( 23 ), bacteria ( 24,25 ), clay ( 26 ) and active carbon ( 27 ). All the works have been summarized and discussed in the book ( 2 ).

Robertson ( 28 ) investigated the foam fractionation of rare-earth elements by extraction of their EDTA chelates with a cationic surfactant, and the foam fractionation of an anionic surfactant. The results suggested that appreciable separation improvement was achieved by blocking foam with stacks of screen or plastic bead packings. The published research on ion flotation done by Sebba ( 1,29,30,31 ) and others ( 32,33 ) has concentrated largely on extraction of individual ion. Little work has been done to investigate interionic separation.

Walling et al ( 4 ) reported a study of the relative adsorption of calcium and sodium ion by N-palmitoyl methyl taurine. The result indicated a strong preferential adsorption of calcium ion by the anionic surface layer. The results among

the univalent ions suggest an order of increasing adsorption  $H^+ < Na^+ < K^+ < NH_4^+$ . A selective extraction of copper from solution containing zinc by using increased pH has been investigated by Jacobelli-Turi et al ( 2a ). This is based on the difference in values of stability constant of the two metallic complexes. In this case, at pH values above 10.5 the copper surfactant complex is stable while the zinc complex is less stable.

From the above experimental evidence of metal ion removal it can be concluded that the specificity depends on charge interaction and complex formation that occur at the gas-liquid interface between the adsorbed surfactant layer and a diffuse-double-layer of counterions in solution. The adsorption model was first given independently by Gouy ( 34 ) and Chapman ( 35 ). The basic assumptions are that the charged surface is impenetrable, that the charge is uniformly spread over it, and that the counterions behave as point charges, being able to approach right up to the plane of the charges. On the basis of these assumptions, they solved the Boltzmann equation for the distribution of cations and anions in terms of a potential near the charged surface relative to the bulk of the solution.

In the above theory, it is assumed that the ions are point charges and therefore no selectivity exists between ions of the same valency. However, a recent paper ( 4 ) indicated that there is selectivity between different ions of the same valency. It was Jorne and Rubin ( 9 ) who first modified the

theory that enables one to predict the distribution factor of each species between a solution of mixed electrolytes and a surface layer. The basis of this modification is that the distances of closest approach of the hydrated ions to the air-liquid interface are different. They reported that the diffuse-double-layer theory agreed well with experimental results for solutions containing  $\text{Sr}^{++}$  or  $\text{UO}_2^{++}$  in the presence of monobutyl biphenyl sodium sulfonate as the collector.

Various modes of the foam separation column have been used in research and are summarized by Lemlich (36) and Rubin et al (3). They include foam fractionation in the simple mode with batchwise and continuous flow operation, and in the higher modes with enriching, stripping and combined enriching and stripping. Since the goal of this work was to study the separation mechanism of ions at the air-liquid interface, a reliable one theoretical stage foam fractionating column was chosen. Operating conditions of the column must fulfil the requirements for a theoretical stage as discussed by Lemlich (2b); they are, the liquid pool is well mixed, sparger submergence is over 30 cm, and there is no coalescence in the rising foam. Usually, such coalescence would release adsorbed solute which would run back down through the rising foam as internal reflux, thus enriching the foam overflow beyond that of a single stage of separation. Coalescence of bubbles in the liquid just before they enter the foam can also make for a richer foam.

Foam fractionation of copper, lead and cadmium ions was investigated in this study using sodium dodecylbenzene sulfonate (NaDBS) as the collector. For the systems containing one of above elements, distribution factor of that element was measured as function of the

acidity of solution or the concentration of the element. For the systems containing two or above three elements, selective separation coefficient between the two elements was measured. All the experimental results were predicted by the modified diffuse-double-layer theory. Since the effect of ionic interactions is essential to the efficiency of extraction, the chemistry of the solution foamed was examined, that is, the equilibrium composition of species were determined by considering all the equilibrium reactions occurring in the solution.

UNIVERSITY OF TORONTO  
LIBRARY

## CHAPTER 3

### THEORETICAL BACKGROUND

The original theory of Gouy-Chapman diffuse layer predicts that like-charged ions have like distribution coefficients. But, this is not usually true, since the relative separability exists between like charged ions. Jorne and Rubin (9) was then the first to modify the theory allowing for the difference of closest approach of ions of different diameter. The physical size of the hydrated ions in a solution depends upon the conditions of the solution such as pH, ionic concentration, etc. Hence, a fundamental investigation on the chemistry of the solution foamed was thought to be essential to the study of foam fractionation. It is known that ionic size increases as solution pH is increased due to the formation of poly nuclear species. A bulk solution reaction model has been developed to estimate the equilibrium concentrations of variously charged ions at different bulk conditions.

#### 3.1 Measurement of the Distribution Factor

The distribution factor of a surfactant or colligend adsorbed on the surface layer is a measure of the degree of separation and is defined as the ratio of the surface excess to the bulk concentration of the species in question. It can be measured experimentally using a single, equilibrium stage foam fractionation column. The method consists of bubbling

prehumidified air through a large volume of solution containing the surfactant and colligend to be studied and collecting a relatively small volume of foam. Assuming no bubble coalescence in the foam and that the interstitial liquid is identical to that of the bulk, a mass balance carried out on the collapsed foam produces the following relationship :

$$Q C_f = S \Gamma + Q C_b \quad (3.1)$$

where  $Q$  is the volumetric rate of foam overflow on a gas-free ( collapsed ) basis,  $S$  is the surface overflow in the foam,  $C_f$  is the concentration of the collapsed foam, and  $C_b$  is the bulk liquid composition. If the air bubble is designed such that the bubbles are spherical and uniform, the surface rate generated from a bubbler of  $n$  capillaries can be estimated by :

$$S = n N \pi d^2 \quad (3.2)$$

where  $d$  is the bubble diameter,  $N$  is the bubble emission frequency and  $\pi d^2$  is the surface of a sphere. Since the volume of a sphere is  $\pi d^3/6$  and the gas rate  $G$  is known, the bubble diameter can be calculated from :

$$d = \left( \frac{6 G}{n N \pi} \right)^{1/3} \quad (3.3)$$



Rearranging equation (3.1) yields equation (3.4)

$$\Gamma = \frac{Q (C_f - C_b)}{S} \quad (3.4)$$

Thus, from measurements of  $Q$ ,  $N$ ,  $G$ ,  $C_f$  and  $C_b$ ,  $\Gamma$  can be found. The distribution factor, indicating the possible extent or degree of separation, of the solute is then determined by the relation

$$D = \frac{\Gamma}{C_b} \quad (3.5)$$

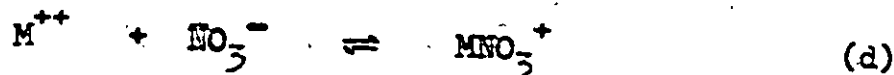
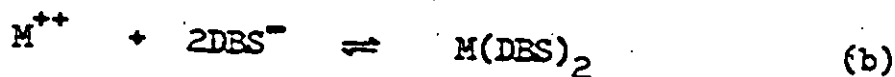
A selective separation coefficient of element A to element B is defined as the ratio of their individual distribution factors:

$$\alpha_{AB} = \frac{(\Gamma / C_b)_A}{(\Gamma / C_b)_B} \quad (3.6)$$

### 3.2 Estimation of Bulk Liquid Ionic Composition

In this study, an attempt has been made to estimate the concentration of all ionic species in the bulk solution by postulating a set of equilibrium reactions and calculating the equilibrium composition. The metal ions, copper, cadmium and lead, used in this study form poly hydroxy complexes and in

the case of lead and copper, polynuclear complexes in basic solution ( 37 ). In order to keep the system as simple as possible only acidic solutions with  $\text{pH} < 4$  were considered. In this region the equilibrium reactions present in solution were assumed to be :



The equilibrium expressions for the above reactions, including their respective equilibrium constant,  $k_a$ ,  $k_b$ ,  $k_c$ , and  $k_d$ , plus the following material balances constitutes the model assumed in this study.

$$[\text{M}^{++}] + [\text{MOH}^+] + [\text{M}(\text{DBS})_2] + [\text{MNO}_3^+] = C_{\text{M}^{++}} \quad (\text{e})$$

$$[\text{DBS}^-] + [2\text{M}(\text{DBS})_2] + [\text{HDBS}] = C_{\text{DBS}^-} \quad (\text{f})$$

$$[\text{NO}_3^-] + [\text{MNO}_3^+] = C_{\text{NO}_3^-} \quad (\text{g})$$

$C_{\text{M}^{++}}$ ,  $C_{\text{DBS}^-}$  and  $C_{\text{NO}_3^-}$  are the total concentration of metal ions, surfactant, and nitrate added to the solution, respectively. Such a mathematical model can be solved on a digital

computer, using an iterative technique, to estimate equilibrium concentration of all the molecular species defined in the model. It is noted that for the systems containing two different metal ions, in addition to equations (a) to (g), four more equations are required for the mathematical model. This is shown in appendix A.1. The equilibrium constants  $k_b$  and  $k_c$  were not available in the literature and were determined experimentally by the author.

### 3.2.1 Determination of Equilibrium Constants

Studies of the absorption of visual and ultraviolet radiation have long been used to obtain information about equilibria in solution. Many species undergo electronic transition in the near-ultraviolet and visual regions of the spectrum, and the intensities of the corresponding absorption bands of a solution have been widely used as a measure of the concentration of the various species present. The quantity measured

is the optical density which can be expressed as  $OD = l \epsilon_s [s]$ , where  $l$  is the length of the optical path, and  $\epsilon_s$  is the molar extinction coefficient of species  $s$ .

Determination of  $k_c$  consider a monobasic acid reaction  $HDBS \rightleftharpoons H^+ + DBS^-$ . When the two conjugate forms, HDBS and  $DBS^-$ , coexist in solution, the observed molar extinction coefficient for the solute at any wavelength is equal to the sum of the products of mole fraction and molar extinction

coefficient of each form. This has provided a convenient means of determining the equilibrium constant of such a reaction.

However, the molar extinction coefficients of pure conjugate forms are difficult to determine. A method proposed ( 38 ) for the calculation of the equilibrium constant does not require pure conjugate forms. A general equation was derived ( see appendix A.2 ) as :

$$a_n \epsilon_n ( 1/k_c ) - a_n ( \epsilon_p/k_c ) - (\epsilon_r) = -\epsilon_n \quad (3.7)$$

where  $\epsilon_p$  is molar extinction coefficient of HDBS,  $\epsilon_r$  is that of  $\text{DBS}^-$ , and  $\epsilon_n$  is that of a mixture at hydrogen ion activity  $a_n$  and containing solute concentration of  $[\text{HDBS}]_n$  and  $[\text{DBS}^-]_n$ . This is a linear equation in four terms and three unknowns ( the latter in parentheses ), since  $\epsilon_n$  and  $a_n$  are measurable quantities. Solution for the unknown  $k_c$  requires three simultaneous equations which may be solved with determinants.

$$k_c = \frac{\begin{vmatrix} a_1 \epsilon_1 & a_1 & 1 \\ a_2 \epsilon_2 & a_2 & 1 \\ a_3 \epsilon_3 & a_3 & 1 \end{vmatrix}}{\begin{vmatrix} a_1 & \epsilon_1 & 1 \\ a_2 & \epsilon_2 & 1 \\ a_3 & \epsilon_3 & 1 \end{vmatrix}} \quad (3.8)$$

Optical density, OD, is the instrumentally measured quantity. If the light path and total concentration of absorbing solute are the same in each measurement, then  $[s]$  and  $l$  will cancel out, and OD may then be substituted for  $\epsilon$  in equation (3.8). This means that the optical densities were measured at a particular wavelength for three solutions with different hydrogen ion concentration and that  $k_c$  can be calculated from equation (3.8).

Determination of  $k_b$  Equilibrium constant  $k_b$  was determined by using a spectrophotometric method which combines the method of continuous variation (39, 40) with logarithmic analysis similar to that used by Bent et al (41) and Kingery et al (42). The method can be used to demonstrate the existence of metal-DBS complex in a solution and to determine its equilibrium constant.

For the application of the method of continuous variation, consider an equilibrium reaction such as



In general, a series of equimolar mixtures prepared by adding  $p$  liters of DBS to  $(1-p)$  liters of  $M$  will have varying optical densities. If the difference between the value of optical density found and the value calculated for no reaction, is plotted against  $p$ , a maximum will be obtained. The complex number  $n$  can be calculated using the relationship  $n = p / (1-p)$ . (see appendix A.3).

Also in above equilibrium reaction (h), the mass action expression  $k_p = [M(DBS)_n] / [M] [DBS]^n$  can be converted to the logarithmic form :

$$\log \frac{[M(DBS)_n]}{[DBS]^n} = \log k_p + \log [M] \quad (3.9)$$

It is seen that a plot of  $\log [M(DBS)_n] / [DBS]^n$  against  $\log [M]$  should yield a straight line with a slope of one and an intercept equal to  $\log k_p$ . This method was applied to solutions containing only uncomplexed metal ion.

Once all the equilibrium constants are known, the equilibrium model of the system can be simulated using the modified Reguli-falsi iterative method ( 45, 75, 76 )

### 3.2.2 Simulation of the Equilibrium Model

Assuming the identities  $A(1) = [M^{++}]$ ,  $A(2) = [MOH^+]$ ,  $A(3) = [M(DBS)_2]$ ,  $A(4) = [DBS^-]$ ,  $A(5) = [HDBS]$ ,  $A(6) = [NO_3^-]$  and  $A(7) = [MNO_3^+]$ , the equilibrium expressions for the reactions (a) to (d) plus the material balance ( equations (e) to (g) ) can be rewritten as :

$$\frac{[H^+] A(2)}{A(1) k_a} = 1.0 \quad (3.10)$$

$$\frac{A(3)}{A(1) A(4)^2 k_b} = 1.0 \quad (3.11)$$

$$\frac{[H^+] A(4)}{A(5) k_c} = 1.0 \quad (3.12)$$

$$\frac{A(7)}{A(1) A(6) k_d} = 1.0 \quad (3.13)$$

$$\frac{A(1) + A(2) + A(3) + A(7)}{C_{M^{++}}} = 1.0 \quad (3.14)$$

$$\frac{A(4) + 2A(3) + A(5)}{C_{DBS^-}} = 1.0 \quad (3.15)$$

$$\frac{A(6) + A(7)}{C_{NO_3^-}} = 1.0 \quad (3.16)$$

Assuming a function  $G(x_1)$  which is equal to any one of above equations and is defined to satisfy the condition of

$$\lim_{x_1 \rightarrow 0} G(x_1) = 0 \quad (3.17)$$

For example, the variable  $A(2)$  in equation (3.10) is equivalent to the independent variable  $X_1$  in the above equation, and in the case of equation (3.11), it is  $A(3)$ , etc. The mathematical solution of the model is then obtained when the conditions of  $G(X_1)$  equal to one are met simultaneously.

From the iterative process, the  $r^{\text{th}}$  approximation is given by

$$x_1^{r+1} = \frac{x_1^r}{G(x_1)^r} \quad (3.18)$$

To prevent from the divergency of iteration, the following improvement is made.

$$x_1^{r+1} = \frac{1}{2} (x_1^{r+1} + x_1^r) \quad (3.19)$$

Substituting equation (3.18) into (3.19), it becomes

$$x_1^{r+1} = \frac{1}{2} x_1^r \left( 1.0 + \frac{1}{G(x_1)^r} \right) \quad (3.20)$$

Based on this development, the mathematical model can be rewritten for simulation as :

$$A(2)^{r+1} = \frac{1}{2} A(2)^r \left( 1.0 + \frac{A(1) k_a}{[H^+] A(2)} \right)^r \quad (3.21)$$

$$A(5)^{r+1} = \frac{1}{2} A(5)^r \left( 1.0 + \frac{A(1) A(4)^2 k_b}{A(5)} \right)^r \quad (3.22)$$

$$A(4)^{r+1} = \frac{1}{2} A(4)^r \left( 1.0 + \frac{A(5) k_c}{A(4) [H^+]} \right)^r \quad (3.23)$$



$$A(7)^{r+1} = \frac{1}{2} A(7)^r \left( 1.0 + \frac{A(1) A(6) k_d}{A(7)} \right)^r \quad (3.24)$$

$$A(1)^{r+1} = \frac{1}{2} A(1)^r \left( 1.0 + \frac{C_{M^{++}}}{A(1)+A(2)+A(3)+A(7)} \right)^r \quad (3.25)$$

$$A(5)^{r+1} = \frac{1}{2} A(5)^r \left( 1.0 + \frac{C_{DBS^-}}{A(4)+2A(3)+A(5)} \right)^r \quad (3.26)$$

and

$$A(6)^{r+1} = \frac{1}{2} A(6)^r \left( 1.0 + \frac{C_{NO_2^-}}{A(6) + A(7)} \right)^r \quad (3.27)$$

In summary, the simulation started with the reasonably initial guesses of variables, then followed by successive approximations until the process converged. The final values of the variables are the equilibrium concentration of species in the solution.

### 3.3 The Gouy-Chapman Diffuse Double Layer Model

A deeper level of understanding of the separation process is gained if the double-layer structure can be predicted on the basis of the properties of the bulk phase. The Gouy and Chapman treatment of the behavior of ions in the vicinity of the charged surface is that the ions are affected by the electrical force arising from the charge on the interface and by thermal jostling. The ionic distribution is known after the equilibrium between electric and thermal forces is attained.

UNIVERSITY OF CALIFORNIA LIBRARY

The ions are scattered so much that it is imagined that only scattered particles existed in the interphase and none of the rigidly fixed charges of the simple double-layer model is left ( 44,45,46,47,48 ).

It is noted that the concept of surface excess is different from that of adsorption, though the surface excess may become nearly identical to the total amount adsorbed under certain limiting conditions ( i.e., bulk concentration equal to zero ). The surface excess of a particular species is the excess of that species present in the surface phase relative to the amount that would be present if the double layer were not there. The surface excess, therefore, represents the accumulation of the species in the entire interphase region.

Application of the diffuse-double-layer theory to foam separation process was first proposed by Jorne and Rubin ( 9 ). In the foaming process, if the air is bubbling in water containing surface active material, an excess of this material will generally be present on the air-liquid interface and an equivalent amount of ions of opposite charge will be distributed in the solution near the interface. The charge on the air-liquid interface is treated as a surface charge spread uniformly over the surface. The charge in solution is considered to be composed of an unequal distribution of point-like ions. The solvent influences the double layer only through its dielectric constant. According to the Gouy-Chapman treatment,

the distribution of the ions in the solution is governed by a Boltzmann relation. Positive ions are concentrated at places of negative potential and repelled at places of positive potential. The reverse occurs for negative ions.

Consider a solution of an anionic surfactant and several species of cations and anions. The surfactant adsorbs to the air-liquid interface forming a negatively charged interfacial layer. The ionic atmosphere near the charged interface consisting of an excess of ions of positive charge represents a falling-off, with distance from the interface, of the net charge density in a lamina parallel to the interface and at increasing distances out into the solution.

Gibbs conceived the idea of measuring adsorption in the interphase by using the integral of the perturbation in concentration with distance. A schematic representation of these perturbations is shown in figure 1. The surface excess of ions of species  $i$  of valence  $z_i$  is given as

$$\begin{aligned}\Gamma_i &= \int_{x_0}^{\infty} n_i(x) dx \\ &= \int_{x_0}^{\infty} (n_i^1(x) - n_i^0) dx\end{aligned}\tag{3.28}$$

where  $x_0$  is the distance of closest approach of ions to the

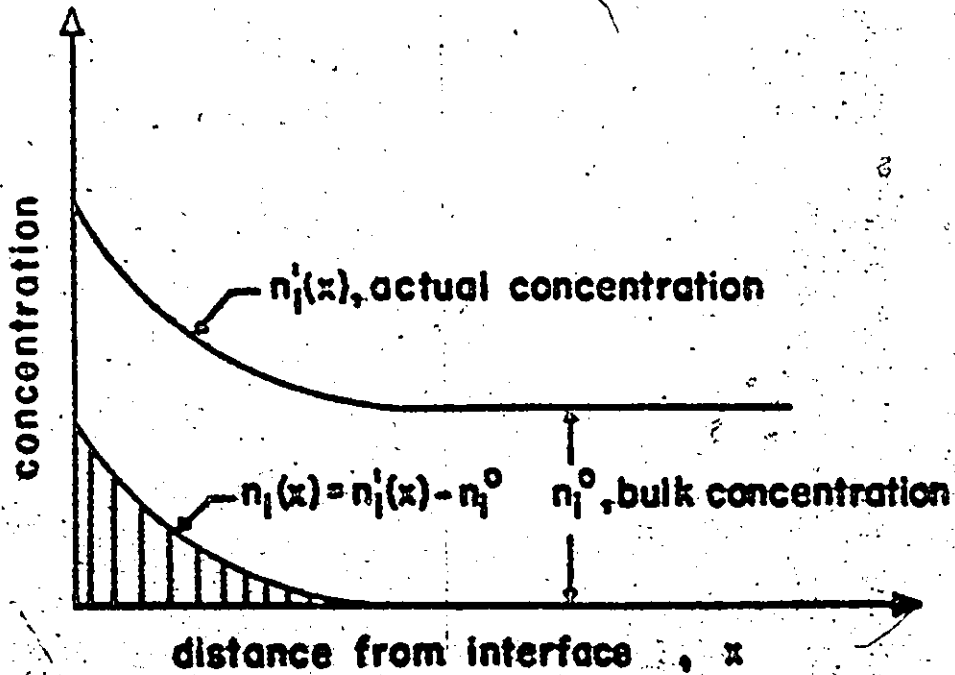


Figure 1. A Schematic Representation of the Variation of Interface Concentration With Distance. ( after Brockris and Reddy (47)).

surface. Introducing the Boltzmann relation, equation (3.28) yields equation (3.29).

$$\Gamma_1 = \int_{x_0}^{\infty} n_1^0 \left( v^{\frac{z_1}{2}} - 1 \right) dx \quad (3.29)$$

where  $v = \exp(-e_0 \phi / k T)$ ,  $\phi$  is the outer potential difference between a distance  $x$  from the interface and the bulk of the solution (taken as  $\phi_{x \rightarrow \infty} = 0$ ),  $e_0$  is the electronic charge,  $n_1^0$  is the bulk concentration of ions of species 1.

Consider a lamina parallel to the interface and at distance  $x$  from it (figure 2). The charge density  $\rho$  in this lamina can be expressed in two ways: (1) in terms of the Poisson equation for the  $x$  dimension in rectangular coordinates

$$\rho = - \frac{\epsilon}{4\pi} \frac{d^2 \phi}{dx^2} \quad (3.30)$$

where  $\epsilon$  is the dielectric constant of the medium and is taken to be that of bulk water, <sup>and</sup> (2) in terms of the Boltzmann equation

$$\begin{aligned} \rho &= \sum_1 n_1 z_1 e_0 \\ &= \sum_1 n_1^0 z_1 e_0 \exp(-z_1 e_0 \phi / k T) \end{aligned} \quad (3.31)$$

where the factor  $z_1 e_0 \phi / k T$  represents the ratio of the electrical and thermal energies of an ion at the distance  $x$  from the interface. From the two expressions ( equations (3.30) and (3.31) ) for the charge density, one obtains the Poisson-Boltzmann equation ( 47a )

$$\frac{d^2 \phi}{dx^2} = - \frac{4\pi}{\epsilon} \sum_1 n_1^0 z_1 e_0 \exp(-z_1 e_0 \phi / k T) \quad (3.32)$$

Solving for the solution of the nonlinear differential equation ( equation (3.32) ), a simple transformation can be used. Consider the steps

$$\begin{aligned} \frac{1}{2} \frac{d}{d\phi} \left( \frac{d\phi}{dx} \right)^2 &= \frac{1}{2} 2 \left( \frac{d}{d\phi} \frac{d\phi}{dx} \right) \frac{d\phi}{dx} \\ &= \left( \frac{dx}{d\phi} \frac{d}{dx} \frac{d\phi}{dx} \right) \frac{d\phi}{dx} \\ &= \frac{d^2 \phi}{dx^2} \end{aligned} \quad (3.33)$$

UNIVERSITY OF OTTAWA  
OTTAWA, ONTARIO  
K1N 6N5

Thus, the identity, equation (3.33), can be used in the equation (3.32) which can then be integrated ( see appendix A.4 ) to give :

$$\frac{d\phi}{dx} = \pm \left( \frac{8\pi k T}{\epsilon} \right)^{\frac{1}{2}} \left[ \sum_1 n_1^0 (v^{\frac{z_1}{2}} - 1) \right]^{\frac{1}{2}} \quad (3.34)$$

To decide which root is to be taken, one remembers that, at the positively charged interface,  $\phi > 0$ , but  $d\phi / dx < 0$ , while, at the negatively charged interface,  $\phi < 0$ , and  $d\phi / dx > 0$ . Hence, it is clear that only the positive root of equation (3.34) corresponds to the physical situation.

Equation (3.34) represents the field ( or gradient of potential ) at a distance  $x$  from the interface according to the diffuse-charge model of Gouy and Chapman, and spells out the relation between the electric field and the potential at any distance  $x$  from the interface.

Differentiating  $v$  with respect to  $x$ , one obtains a relation

$$\begin{aligned} \frac{dv}{dx} &= \frac{-e_0}{k T} e^{-e_0 \phi / k T} \frac{d\phi}{dx} \\ &= -\frac{e_0 v}{k T} \frac{d\phi}{dx} \end{aligned} \quad (3.35)$$

By change of variables, equations (3.29), (3.34) and (3.35) reduce to equation (3.36).

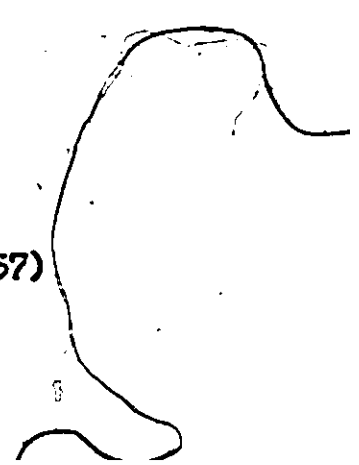
$$\left(\frac{\Gamma}{n}\right)_i = - \left(\frac{k T \epsilon}{8\pi e_0^2}\right)^{\frac{1}{2}} \int_{v_0}^1 \frac{(v^{z_i} - 1) dv}{v \left[\sum_1 z_i^0 (v^{z_i} - 1)\right]^{\frac{1}{2}}} \quad (3.36)$$

This is an equation to calculate the distribution factor  $\left(\frac{\Gamma}{n}\right)_i$  of ions of species  $i$  in a multicomponent solution (9). The lower limit of the above integration,  $v_0$ , can be determined in the later development.

Instead of the field, it is preferable to have an expression for the total charge in the solution in terms of the potential. This diffuse charge is obtained as follows. According to Gauss' theorem assuming that no specific adsorption exists and there is no oriented dipole layer at the boundary or the potential due to such a layer is negligible at  $x > x_0$ ,

$$\begin{aligned} q &= - \int_{x_0}^{\infty} \rho \, dx = - \frac{\epsilon}{4\pi} \int_{x_0}^{\infty} \left(\frac{d^2\psi}{dx^2}\right) dx \\ &= - \frac{\epsilon}{4\pi} \left(\frac{d\psi}{dx}\right)_{x_0} \end{aligned} \quad (3.37)$$

UNIVERSITY OF CHICAGO  
 LIBRARY  
 575 EAST 58TH STREET  
 CHICAGO, ILLINOIS 60637





where  $\sigma$  is the surface charge density at the surface expressed in (esu/cm<sup>2</sup>).

Therefore from equation (3.34) and (3.37)

$$\sigma = - \left( \frac{kCT}{2\pi} \right)^{\frac{1}{2}} \left[ \sum_i n_i^0 (v_0^{z_i} - 1) \right]^{\frac{1}{2}} \quad (3.38)$$

where  $v_0$  is the value of  $v$  when  $\phi = \phi_0$  at distance  $z_0$  from the interface, or at the outer Helmholtz plane. The negative sign in equation (3.38) is chosen for the case of negatively charged surface (anionic surfactant). The surface charge density can be calculated from knowing surface excess of the ionic surfactant,  $\Gamma_s$ :

$$\sigma = z_s e_0 \Gamma_s \quad (3.39)$$

From equation (3.38) and (3.39),  $v_0$  (or  $\phi_0$ ) can be calculated by trial and error. Taking  $v_0$  as the lower limit, equation (3.36) can be integrated to give the distribution factor of ions of species  $i$  in a solution. It is important to note that the summation over all the ionic species includes the cations, the anions, and the surfactant ions.

Assumptions that have been made in the development of the above theory are as follows: (1) the dielectrical constant

is constant over the diffuse double layer, (2) the ions are points of charge. The latter means that no selectivity exists between ions of the same valency. However, it was found experimentally that there is selectivity between different ions of the same valency ( 4, 49, 50 ). The modification which enables one to distinguish the selectivity was first done by Jorne and Rubin ( 9 ).

### 3.3.1 Modified Diffuse Model

The concept of difference in the distance of closest approach,  $x_0$ , was incorporated into the diffuse model, because, in general, cations that are strongly solvated have larger  $x_0$  than those that are weakly solvated. Figure 3 presents a physical picture of the hypothetical interface in which a surfactant monolayer of charge  $z_B$  is formed at  $x = 0$ , a layer of small counterions with charge  $z_1$  is formed no closer than  $x_0^1$ , and a layer of larger counterions with charge  $z_2$  is formed no closer than  $x_0^2$ . The diffuse layer can then be divided into two regions:  $x_0^2 < x < \infty$ , all ions are present;  $x_0^1 < x < x_0^2$ , only smaller ions are present. Therefore, a correction term  $\Delta \Gamma_B$  in addition to the excess of the smaller ion between the limits  $x_0^1 < x < x_0^2$  is required. For z-z electrolyte

$$\Delta \Gamma_B = \int_{x_0^1}^{x_0^2} z_B \left[ \exp\left(-\frac{z_1 z_2 \psi}{k T}\right) - 1 \right] dx \quad (3.40)$$

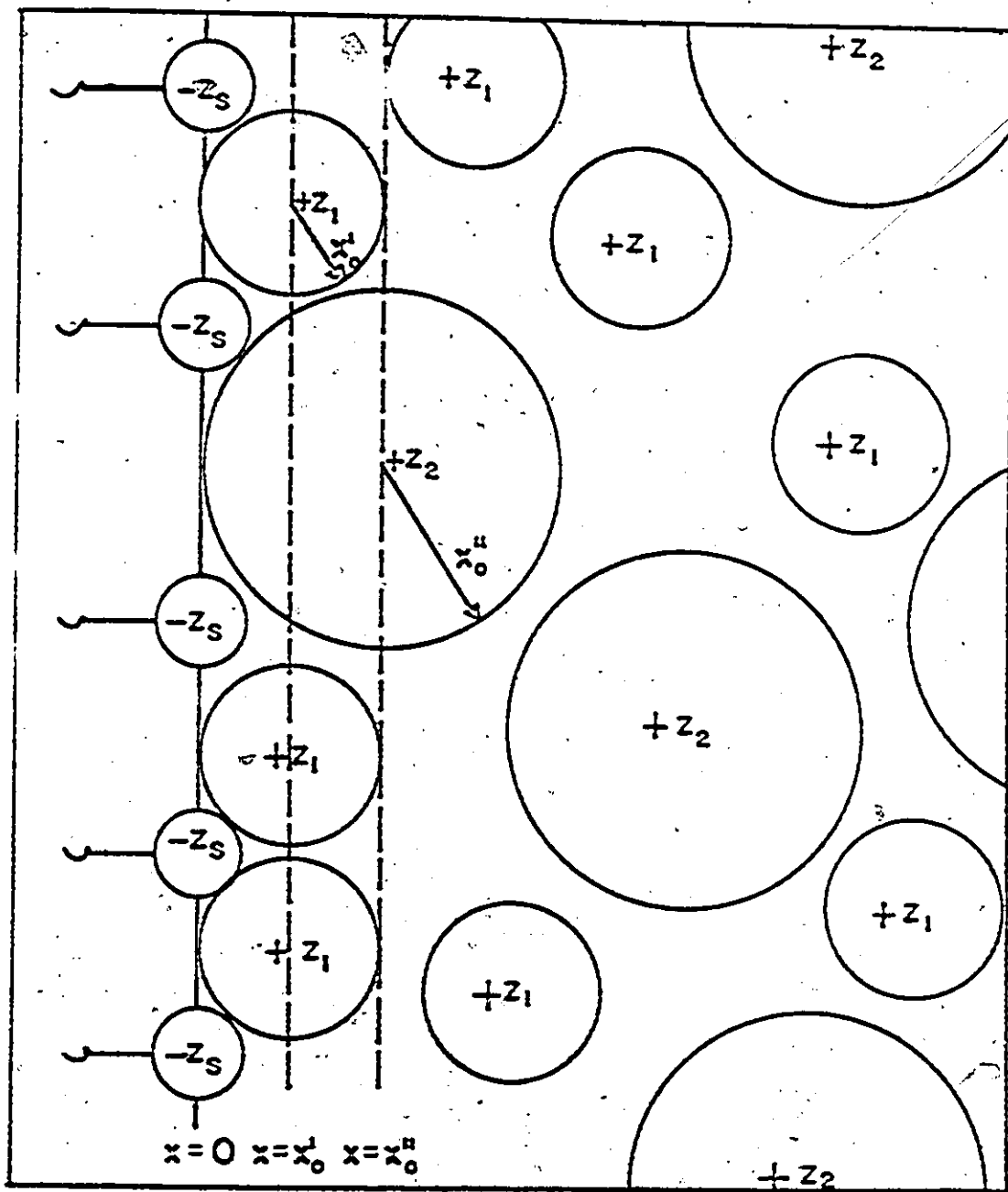


Figure 3. Surface Adsorption Model for Small Ions of Charge  $z_1$  and Large Ions of Charge  $z_2$  to Monolayer of Surfactant of Charge  $z_s$  at  $x = 0$  ( 28 ).

This integral can be evaluated analytically to give

$$\Delta \Gamma_B = \left( \frac{k T \epsilon n_B}{2 \pi \epsilon_0^2} \right)^{\frac{1}{2}} \left[ (v_0')^{\frac{1}{2}} - (v_0'')^{\frac{1}{2}} \right] \quad (3.41)$$

In order to evaluate  $\Delta \Gamma_B$ , it is necessary to find that relation between  $\phi_0'$  and  $\phi_0''$  ( or equivalently  $v_0'$  and  $v_0''$  ). For z-z electrolyte, the total diffuse-charge density scattered in the solution under the interplay of thermal and electrical forces is obtained ( see appendix A.5 ) as :

$$\sigma = \left( \frac{2 k T \epsilon n_1^0}{\pi} \right)^{\frac{1}{2}} \sinh \left( \frac{z \epsilon_0 \phi}{2 k T} \right) \quad (3.42)$$

Again, from equation (3.37) and (3.42), the result is

$$\left( \frac{d\sigma}{dz} \right)_{z=0} = - \left( \frac{2 k T}{z \epsilon_0} \right) K \sinh \left( \frac{z \epsilon_0 \phi}{2 k T} \right) \quad (3.45)$$

where  $K$  is the Debye-Hückel reciprocal length and  $K^2 = 8 \pi \epsilon_0^2 z^2 n_1^0 / \epsilon k T$ . The physical meaning of  $K^{-1}$  is the effective

thickness of the diffuse double layer. By integration with the boundary conditions  $x = x_0'$ ,  $\phi = \phi_0'$ ;  $x = x_0''$ ,  $\phi = \phi_0''$ ; we get the desired relationship (see appendix A.6) :

$$\tanh\left(\frac{z e_0 \phi_0'}{4 k T}\right) = \exp[K (x_0'' - x_0')] \tanh\left(\frac{z e_0 \phi_0''}{4 k T}\right) \quad (3.44)$$

where  $(x_0' - x_0'')$  is the difference in closest approach to the surface.

The distribution factors of the two cationic species are :

$$\left(\frac{\Gamma}{n}\right)_A = \left(\frac{k T \epsilon}{8 \pi e_0^2}\right)^{\frac{1}{2}} \int_{v_0''}^1 \frac{(v^{z_A} - 1) dv}{v \left[ \sum_1 n_1^0 (v^{z_1} - 1) \right]^{\frac{1}{2}}} \quad (3.45)$$

$$\left(\frac{\Gamma}{n}\right)_B = \left(\frac{k T \epsilon}{8 \pi e_0^2}\right)^{\frac{1}{2}} \left\{ \int_{v_0''}^1 \frac{(v^{z_B} - 1) dv}{v \left[ \sum_1 n_1^0 (v^{z_1} - 1) \right]^{\frac{1}{2}}} + 2 \left(\frac{1}{n_B}\right)^{\frac{1}{2}} \left[ (v_0')^{\frac{1}{2}} - (v_0'')^{\frac{1}{2}} \right] \right\} \quad (3.46)$$

where A is the larger ion and B is the smaller ion.

In summary, the above discussion has outlined a method to predict the distribution factor of an ion in a dilute aqueous solution. The procedure is to estimate the equilibrium composition of all ions in the solution, calculate the surface potential, then integrate equations (3.45) or (3.46) to obtain the distribution factor of the ion.



CHAPTER 4

EXPERIMENTAL INVESTIGATION

This chapter consists of two parts; first, the description of apparatus and experimental procedure for foam fractionation, and second, the spectrophotometric analysis for the determination of equilibrium constants of a reaction. The instruments and materials used for the study are also listed.

4.1 Foam Fractionation

The distribution factor of a surfactant or colligend adsorbed on the surface layer can be measured experimentally using a single stage foam fractionation column. The method consists of bubbling prehumidified air through a large volume of solution containing the surfactant and colligend to be studied and collecting a relatively small volume of foam.

Experimental apparatus similar to that developed by Dick and Talbot ( 8 ) was used in this study to measure the distribution factor of the various metal ions. A schematic diagram of the equipment is shown in figure 4.

Description of Apparatus

For all runs, oil-free compressed air from cylinders was first reduced to 9 psig and then humidified using a gas wash bottle followed by a saturator

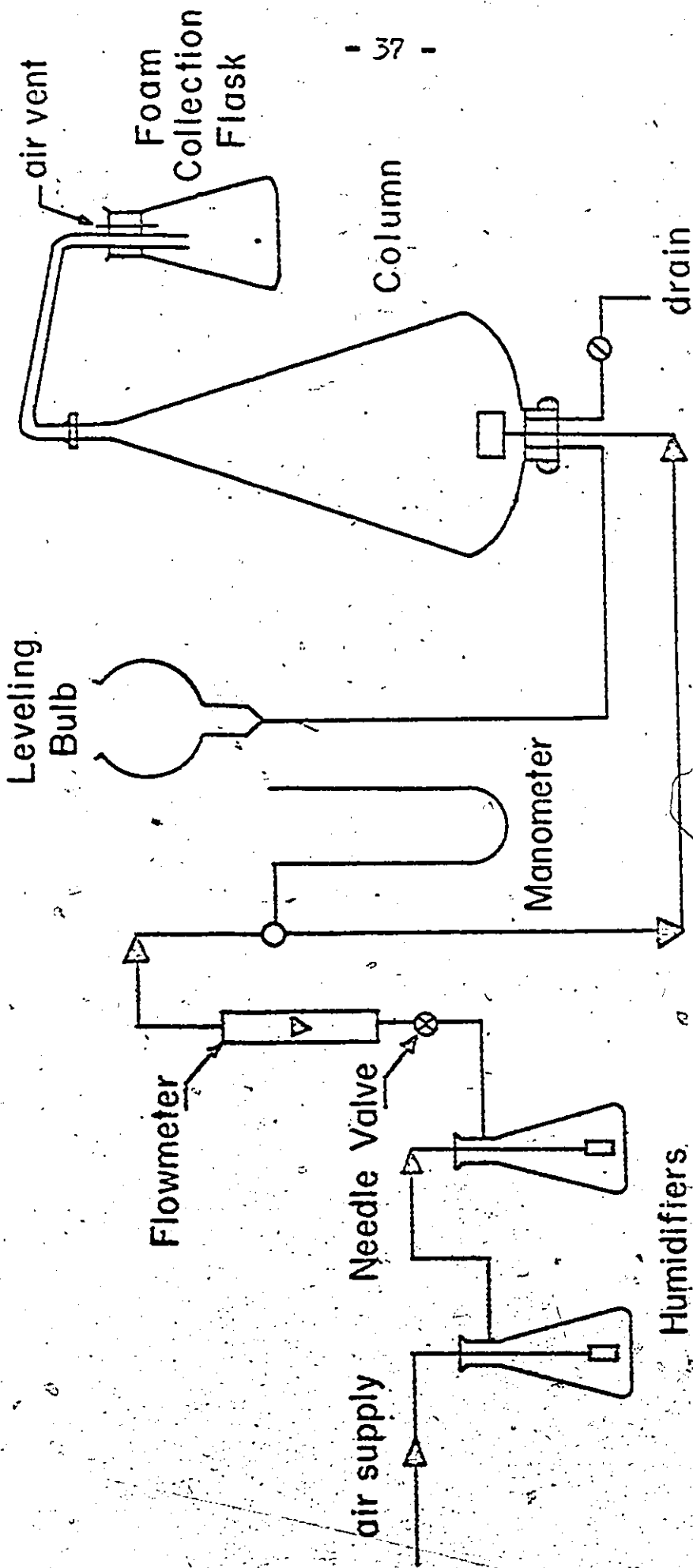


Figure 4. Schematic Diagram of the Experimental Apparatus.



made of a fritted sparger contained in a flask of distilled water. The flow rate of the humidified air was then adjusted with a needle valve, measured with a calibrated flowmeter. The downstream pressure of <sup>the</sup> calibrated flowmeter was recorded using a manometer. The humidified air then passed to the bubbler in the foam column. Because a stroboscope was used to determine the bubble diameters, it was necessary to utilize a bubbler capable of producing bubbles of a uniform size. This requirement was met using a bubbler consisting of five glass capillary tubes 0.240 in. long and 0.007 in. i.d. imbedded in a teflon chamber.

The column was constructed of an inverted 3-liter separatory funnel with the stopcock portion removed and replaced by a foam delivery tube and the bubbler inserted into the bottom. The liquid pool depth was approximately 33 cm. above the bubbler, and the foam/liquid interface height was controlled by means of a 300-ml leveling bulb and adjusting screw. The calibrated air flowrate was controlled by keeping constant readings in both calibrated manometer and flowmeter.

On leaving the column, the foam was directed along a 15-cm long by 0.9-cm i.d. foam delivery tube to a weighed 1000-ml erlenmeyer flask. The foam delivery tube was adjusted so that it had a declination of about  $10^{\circ}$ . Drainage was therefore toward the flask. The overall foam height in the apparatus, including the vertical portion of the delivery tube, was about 6 cm.

Experimental Procedure

Four liters of feed solution were prepared for each run using deionized distilled water, which was prepared by passing the distilled water through a Barnstead mixed ion exchanger. After addition of the required quantities of chemicals, the pH was then adjusted to the desired value using  $\text{HNO}_3$ .

Prior to charging the column, the foam receiver was weighed to 0.1 mg. The air was turned on then the column was filled through the leveling bulb. The air flowrate was then adjusted to the exact value desired after the foam-liquid interface height had been set at the mark.

The air flowrate was kept constant during the run. Once steady state had been reached, the foam receiver was placed in position and the timer started. Bubble rate was measured by means of the stroboscope.

On completion of a run ( approximately 15 min. ), the foam receiver was removed, stoppered, weighed, and allowed to sit so that the foam broke naturally.

Since the solute concentration were so low, a density of 1.0 was assumed so that foam weight was equivalent to foam volume.

Analytical Technique

Surfactant concentration was determined using the methylene blue method ( 51 ). This tedious, but reliable, extraction method was used because it was found that the direct measurement of absorption of the solution at ultraviolet wavelength region ( 52 ) was interfered by the

presence of metal ions and the pH of solution.

Methylene blue is a cationic dye which, in the form of an inorganic salt such as the chloride or sulfate, does not extract from water into an organic liquid such as chloroform. But if an anionic surfactant is present, a salt of much lower water solubility is formed with the surfactant anion, a salt which is readily extractable into organic solvents.

Absorption measurements were made at a wavelength of 652 m $\mu$  with a Bausch & Lomb precision spectrophotometer. The intensity of blue color in the solvent gives a measure of the amount of anionic surfactant present, one molecule for each molecule of methylene blue. Its intense color makes for adequate sensitivity: 10  $\mu$ g of surfactant is readily detected, corresponding to a 100 ml sample of 0.1 ppm concentration.

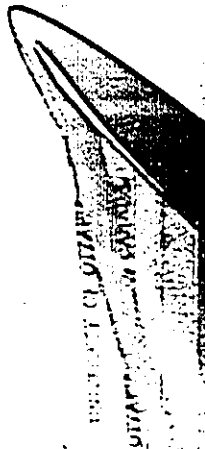
The concentration of heavy metals studied were determined using atomic absorption spectrophotometer, UNICAM SP 90. It was found that the presence of surfactant did not interfere with the absorption readings of the heavy metals. Operating conditions of the analysis are tabulated in table 2.

#### 4.2 Equilibrium Constant Determination

Transmittance measurements were made with a Bausch & Lomb precision spectrophotometer equipped with a digital readout. The same cells were used for all measurements and oriented in the same direction. In all cases, measurements were made with

Table 2. Instrumental Parameters for the Analysis of Metal Ions ( 53 ).

element	wavelength ( m $\mu$ )	slit width ( mm )	fuel ( ml/min )	oxidant, air ( l/min )	sensitivity ( ppm )
copper	324.8	0.08	propane (450)	5.0	0.1
cadmium	228.8	0.10	propane (400)	5.0	0.04
lead	217.0	0.30	propane (400)	5.0	0.3



reference to a blank solution containing all constituents save one, namely, the complex forming constituent in lowest concentration. All measurements were made at room temperature, 20 - 25 °C .

Determination of  $k_p$  for Metal-DBS

Solutions were

prepared from mixing 100 ml, 1.0 gm/l NaDBS and 100 ml, 1 M perchloric acid. Different amounts of 0.1 M metal nitrate were added to each of 20 ml of above solution. In order to repress hydrolysis of the metal in the more concentrated solutions, it was necessary to work in 0.5 M perchloric acid, which brought the pH of solution down to 0.5. Perchloric acid is known to have little or no tendency to form complexes and transmits well in the ultraviolet as well as in the visible section of the spectrum.

All measurements were performed at wavelength 260 to 320 m $\mu$  . It was found that 300 m $\mu$  was a peak wavelength for the optical density. Therefore, the plot determining the value of  $k_p$  is based on the measurements at this wavelength.

Determination of  $k_c$  for HDBS

The acid HDBS was prepared

by passing NaDBS solution through an ion exchanger, REXYN 101(H) resin, to remove sodium ion. Ninety-eight percent removal was obtained. Three HDBS solutions with different pH adjusted by 0.1 N NaOH were examined with a precision spectrophotometer at wavelengths of 300, 320 and 340 m $\mu$  .



Deionized water was used in the reference cell for all the measurements.

#### 4.3 Instruments and Materials

The instruments used in the study were as follows :

- 1) Precision spectrophotometer; Bausch & Lomb, Cat. No. 33-26-50.
- 2) Digital readout; AT-20, Bausch & Lomb, Cat. No. 33-26-58, for used with the precision spectrophotometer.
- 3) Digital pH/mv meter; model 801, Orion Research Inc.
- 4) Strobotac electronic stroboscope; type 1538-A, General Radio Company.
- 5) Atomic absorption spectrophotometer ; Unicam SP 90, Unicam Instruments Ltd., England.

The material and reagent used were listed as follows :

- 1) Copper nitrate;  $0.1000 \pm 0.0005$  moles per liter, Orion Research Inc.
- 2) Cadmium nitrate; Fisher Scientific Company, Lot No. 706011.
- 3) Lead nitrate; Fisher Scientific Company, Lot No. 712226.
- 4)  $\text{HNO}_3$  , NaOH ; research and analytic grade.
- 5) Sodium dodecylbenzene sulfonate; K & K Laboratories, Inc., Lot No. 60959.
- 6) Perchloric acid; analytical grade, The British Drug Houses Ltd., Lot No. 44993.
- 7) Chloroform; certified A.C.S. spectranalyzed, Fisher Scientific Company, Lot No. 711938.
- 8) Methylene blue; u.s.p., Fisher Scientific Company, Lot No. 790255.

It is noted that all the chemicals were used directly without further treatment.

CHAPTER 5

RESULTS

This chapter presents all the experimental foaming results and the theoretical predictions of distribution factor, both are plotted on the same figure for easy comparison. The detailed discussion of the results are presented in the next chapter. The complete tabulation of data is shown in appendix B. Computer programs for the pure component and mixture systems are presented separately in appendix C.

5.1 Results of Equilibrium Constants

The equilibrium constants of the model  $k_a$  and  $k_d$  have been reported and are summarized in table 3. The values of  $k_b$  and  $k_c$  were not available in the literature and were determined by the author using spectrophotometric analysis. The quantity measured was the optical density which can be calculated from the transmittance measurement of a solution at wavelengths near ultraviolet region. Experimental details have been given in section 4.2 .

In order to verify the applicability of the spectrophotometric analysis for determining  $k_b$  of HDBS, an acid with the known value of equilibrium constant was tested. Acetic acid was chosen and the measured data are presented in table 4.

Table 3. Equilibrium Constants  $k_a$  and  $k_d$  of Three Metal Ions.

element	$k_a$	$k_d$
copper	$3.400 \times 10^{-7}$ (54)	$4.237 \times 10^{-17}$ (57)
cadmium	$4.565 \times 10^{-9}$ (55)	$7.413 \times 10^{-1}$ (58)
lead	$6.760 \times 10^{-7}$ (56)	2.291 (59)



Table 4. Equilibrium Constant of Acetic Acid Measured by Spectrophotometric Analysis.

hydrogen ion activity, a	optical density			$k_{HAC} \times 10^5$ ( average )
	230 m $\mu$	235 m $\mu$	240 m $\mu$	
$8.811 \times 10^{-4}$	0.2233	0.1107	0.0395	
$9.638 \times 10^{-5}$	0.2055	0.0980	0.0362	
$1.037 \times 10^{-5}$	0.1409	0.0630	0.0232	
$k_{HAC} \times 10^5$	1.675	2.569	1.455	1.899

The average equilibrium constant is equal to  $1.899 \times 10^{-5}$ , which is close to the known value of  $1.800 \times 10^{-5}$  (60). It is therefore assumed that the spectrophotometric analysis method was suitable.

The results for the determination of  $k_b$  and  $k_c$  are presented in figures 5 to 7 and in table 5. In figures 5 to 7, slopes and intercepts of the lines were obtained by the least square correlation and the results are tabulated in table 6. The slope close to one demonstrates the existence of  $M(DBS)_n$  in the solution. The value of  $n$  in the complex species  $M(DBS)_n$  was determined by the method of continuous variation (39). The result is shown in figure 8, from which it is known that the value of  $n$  is equal to 2.

## 5.2 Results of Foam Fractionation

Experiments for the systems containing one metal ion were carried out to study the effect of solution pH and bulk metal concentrations on the distribution factor of the ions. The systems containing two metal ions were used to study the selectivity between them and to find out what factor controlled the selectivity. The solutions used in the mixture studies were made up in such a way that pH and surfactant concentration was constant. In these solutions the metal concentrations were varied, however, the total concentration was kept constant.

Experiments were performed at room temperature, constant surfactant concentration and constant gas flow rate. A surfactant concentration of 0.50 gm/l was used because it was found to produce a stable foam and the most efficient separation. The

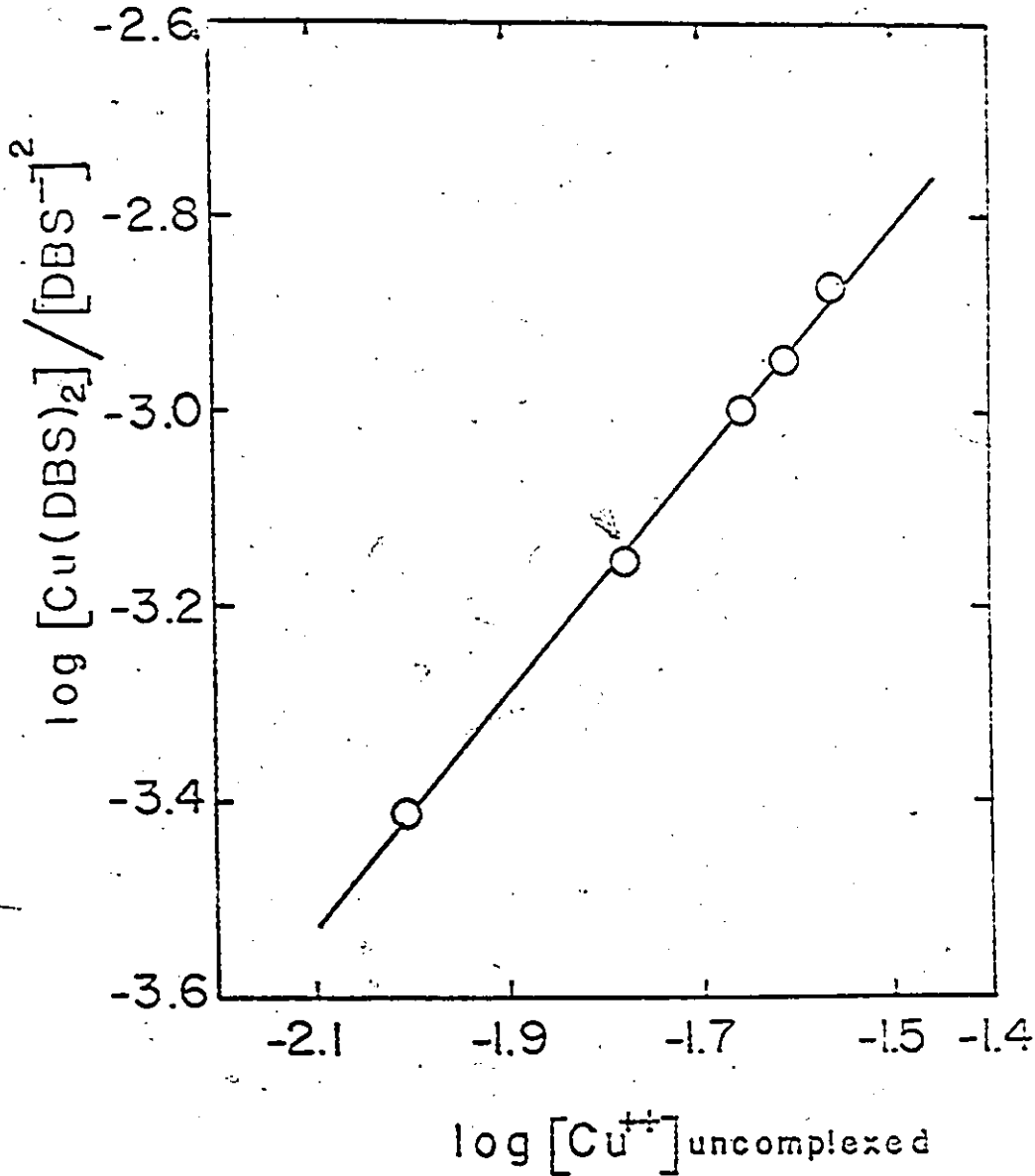


Figure 5. Spectrophotometric Analysis for the Determination of  $k_p$  of Cu-NaDBS System.

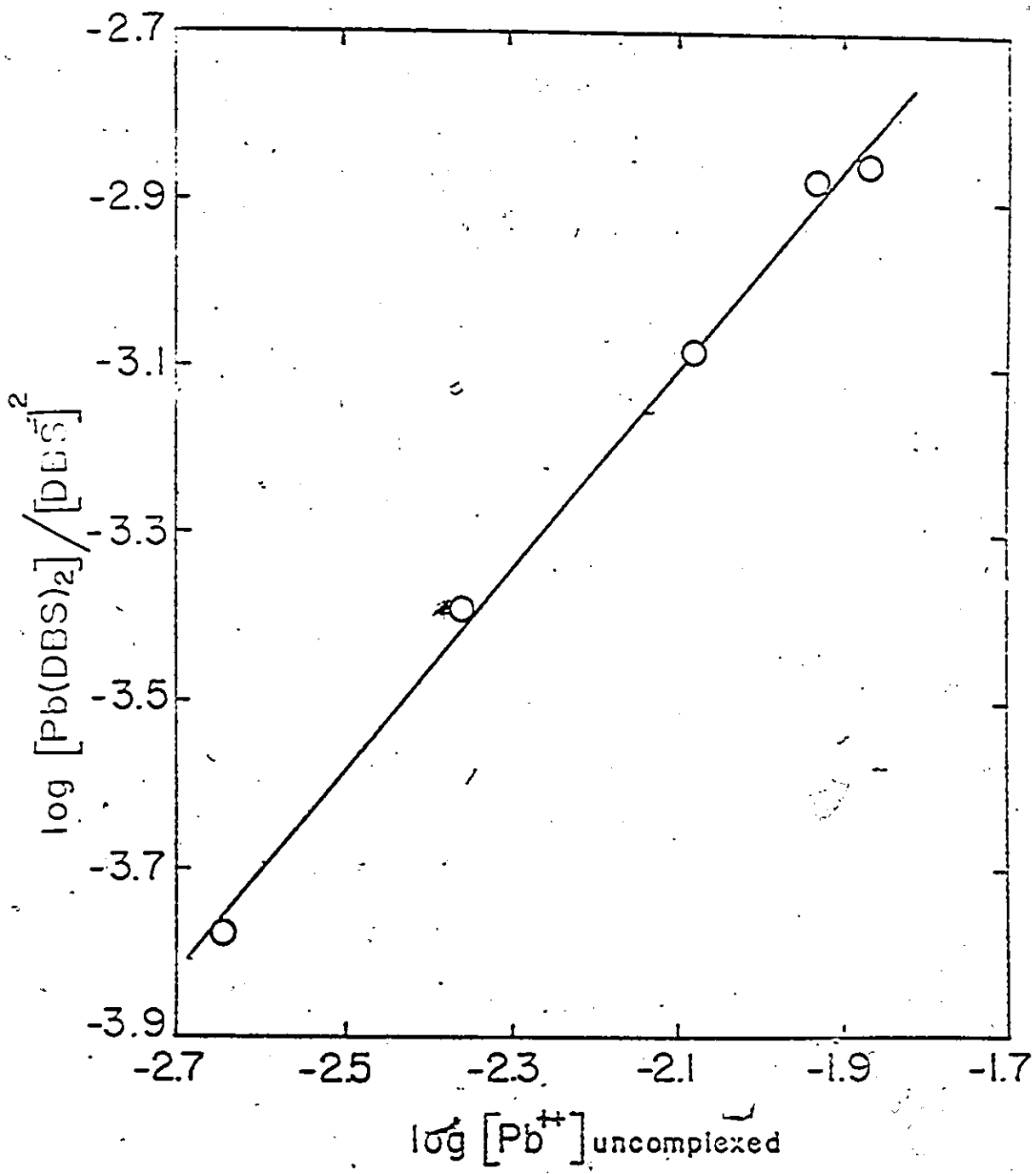


Figure 6. Spectrophotometric Analysis for the Determination of  $k_p$  of Pb-NaDBS System.

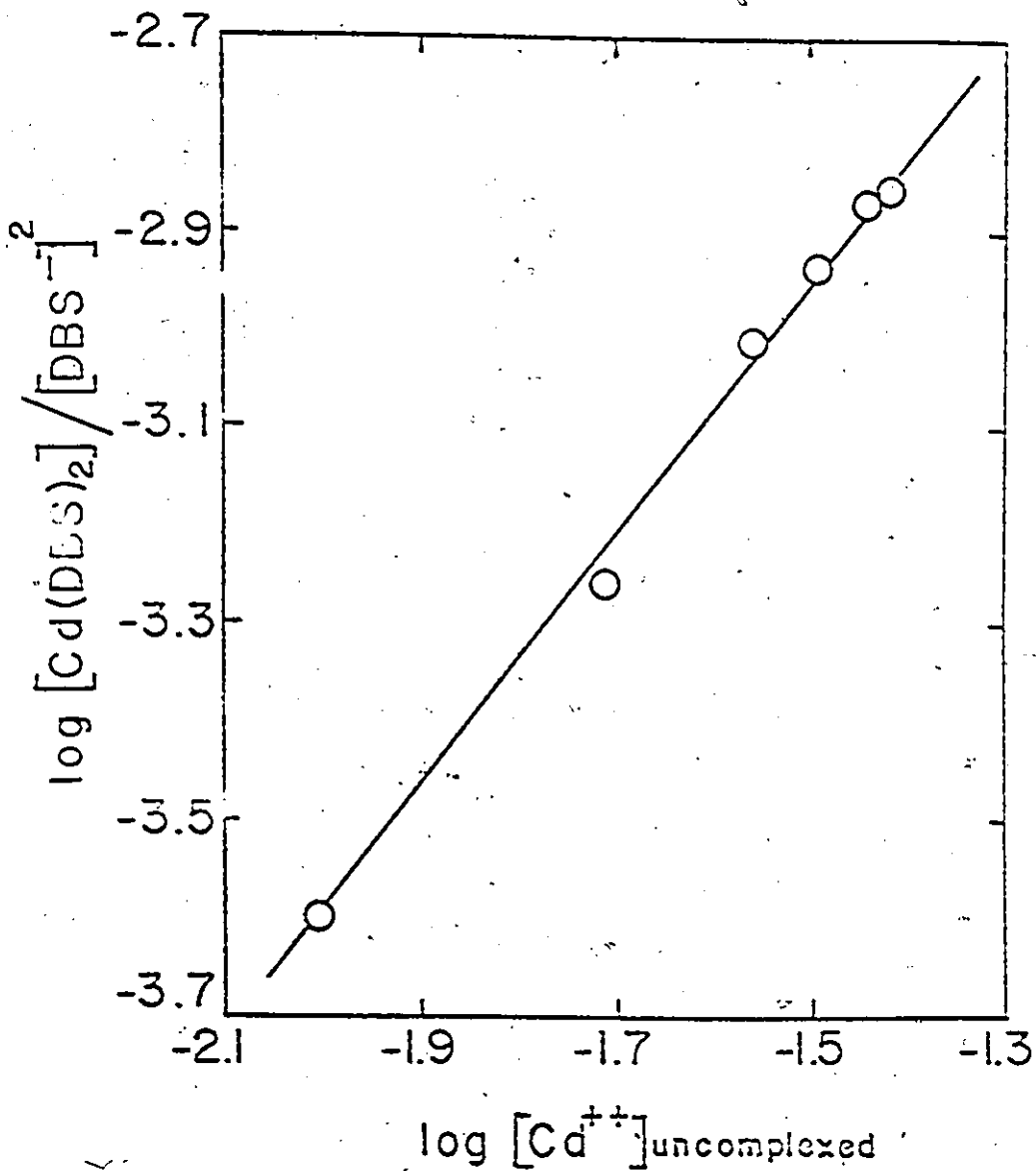


Figure 7. Spectrophotometric Analysis for the Determination of  $k_p$  of Cd-NaDBS System.

Table 5. Equilibrium Constant  $k_c$  of HDBS.

hydrogen ion activity, a	optical density			$k_c \times 10^4$ ( average )
	300 m $\mu$	320 m $\mu$	340 m $\mu$	
$1.230 \times 10^{-2}$	0.4101	0.2007	0.1124	
$1.514 \times 10^{-4}$	0.4225	0.2125	0.1175	
$1.140 \times 10^{-6}$	0.4437	0.2219	0.1226	
$k_c \times 10^4$	0.8848	1.9283	1.5068	1.4400

Table 6. Slopes and Intercepts of figures 5 to 7 and the Results of  $k_b$  .

system	slope	intercept (log $k_b$ )	$k_b$
Cu-NaDBS	1.059	-1.2412	$5.739 \times 10^{-2}$
Cd-NaDBS	1.203	-1.1475	$7.121 \times 10^{-2}$
Pb-NaDBS	1.209	-0.5640	$2.729 \times 10^{-1}$

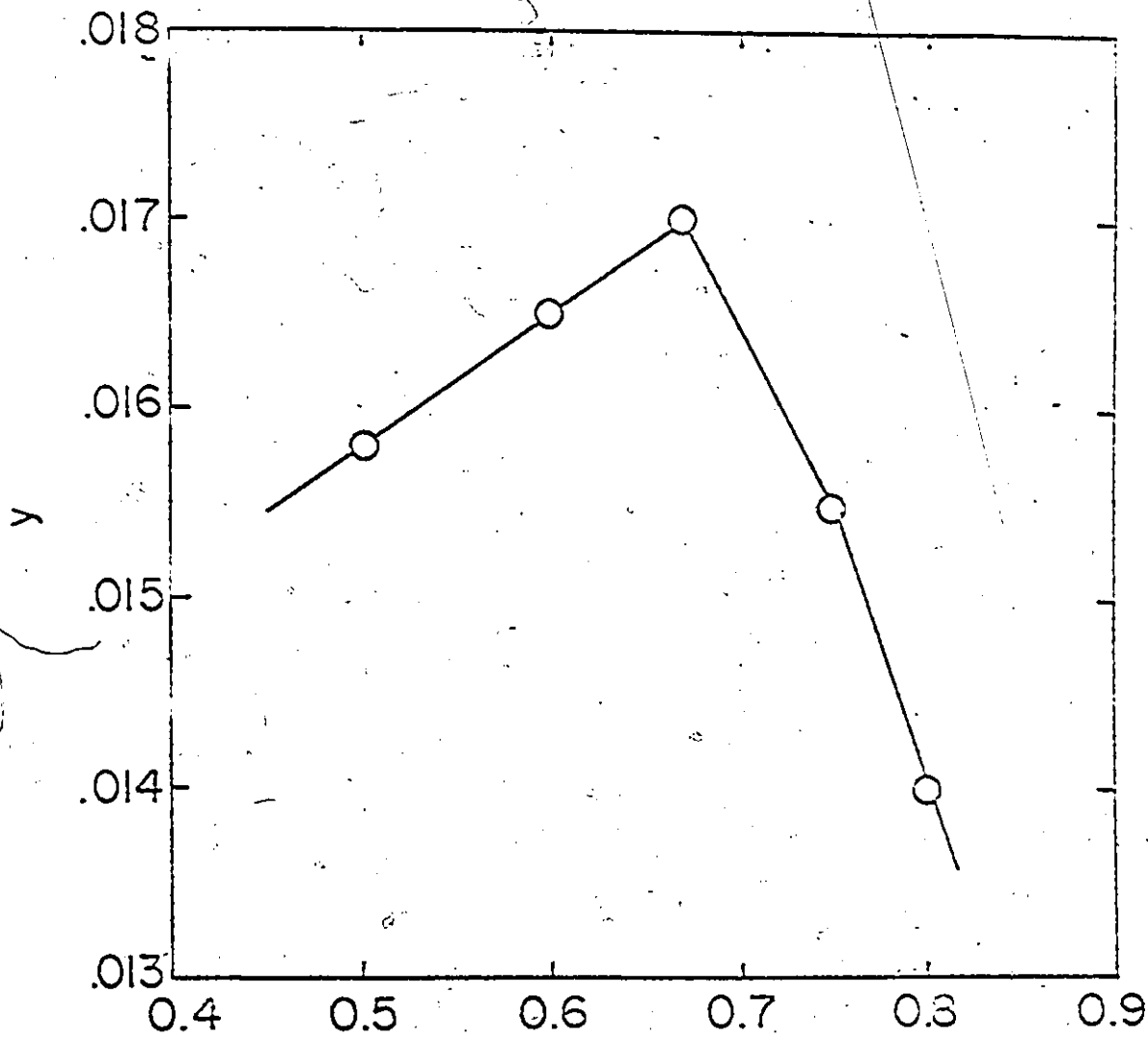


Figure 8. Method of Continuous Variation for the Determination of the Value of  $n$  in  $\text{Cd}(\text{DBS})_n$ .



enrichment ratio, which is defined as the concentration ratio of the foamate to the bulk of the ion depends upon gas flow rate and bubble size. However, it has been shown ( 50 ) that, for conditions of stable foams and constant bulk concentration during a run, the distribution factor of ions is independent of gas flow rate and bubble size. Thus, it is better to use the distribution factor rather than enrichment ratio for correlation of experimental results.

All the theoretical predictions were calculated using the same conditions at which the experiments were performed. The procedure of calculation started from an estimation of the equilibrium composition of the ionic species derived from the bulk solution reaction model. Next, the surface potential of the ions at their distance of closest approach was calculated followed by the calculation of their distribution factor using equation ( 3.45 ). The surface excess of NaDBS used in all the calculations is equal to  $3.10 \times 10^{-10}$  moles / cm<sup>2</sup> (61). The effective radii of hydrated ions are available in the literature (62) ( see appendix A.7 ) and are summarized in table 7.

A number of experimental runs were performed to obtain data for comparison with the theoretical predictions. Figures 9 to 11 show the results of distribution factor as a function of solution pH for the systems containing one metal ion. When bulk concentration is a variable, the results are shown in figures 12 to 14. Figures 15 to 17 show the results of a set of experiments to measure and predict the separability of the metal ions with respect to each other. The experimental results have been shown in a form similar to the familiar x-y diagram used in vapor-liquid equilibrium studies.

In figures 15 to 17 the ordinate is treated as the mole fraction of the smaller ion in foam (vapor) phase and the abscissa is that in bulk liquid phase. The solid lines in these figures are the theoretical predictions. Selective separation coefficients of both experimental results and theoretical predictions were also determined and are tabulated in tables B-18 to B-20. Comparison of the selective separation coefficients measured in the mixture systems and that calculated from the pure component systems at the same operating conditions is also presented in table 8.

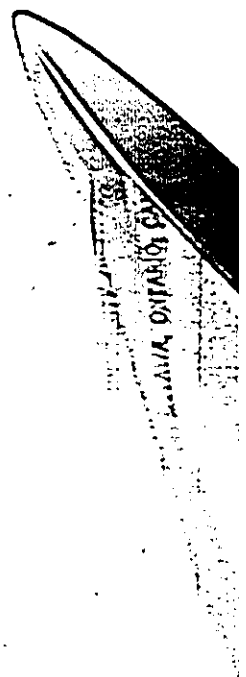
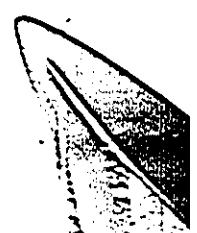


Table 7. The Effective Radii of Hydrated Ions.

element	effective radius ( $\times 10^8$ cm. )
Na <sup>+</sup>	4.7
Cu <sup>++</sup>	6.8
Cd <sup>++</sup>	6.4
Pb <sup>++</sup>	5.9



00

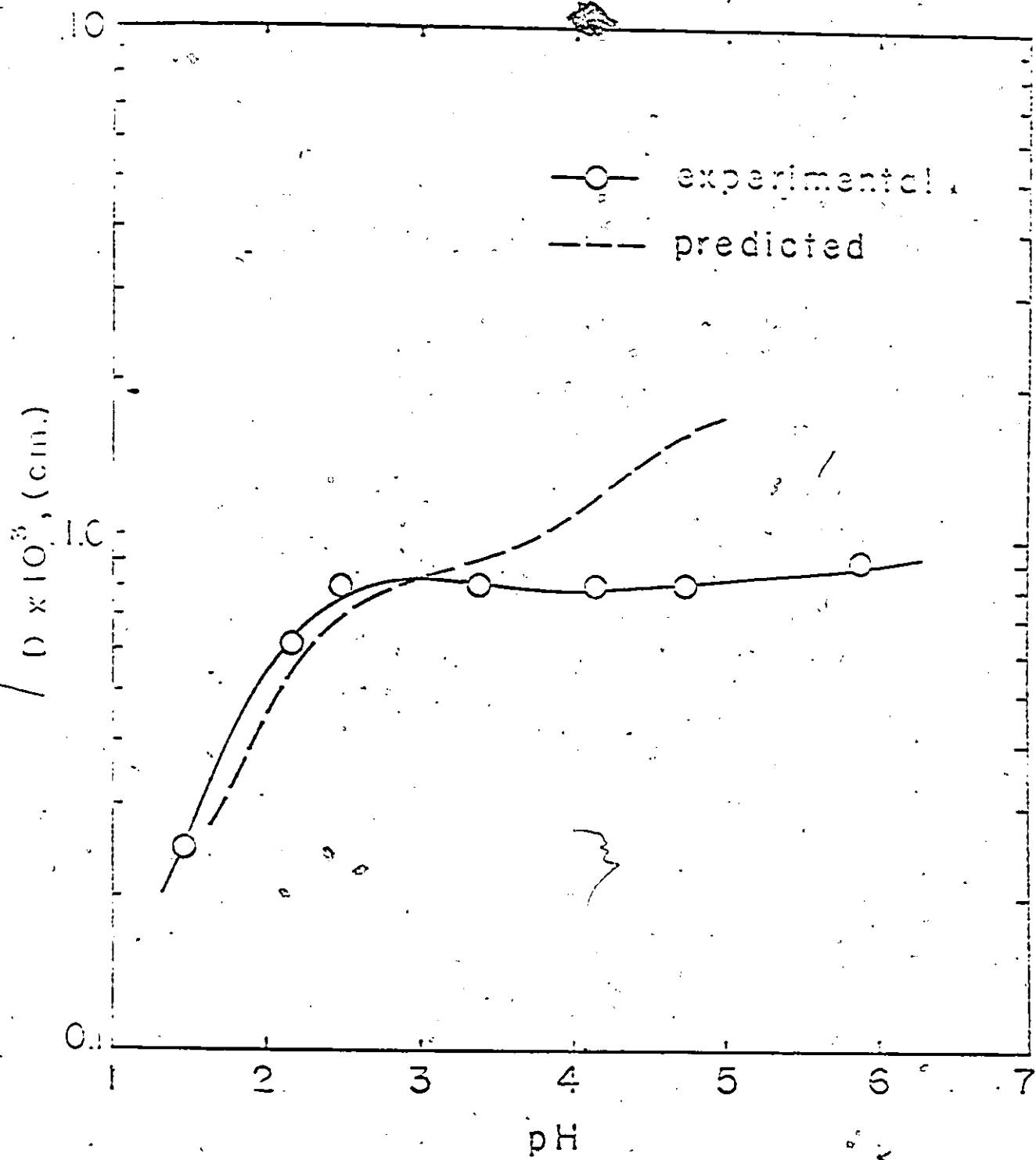


Figure 9. Effect of pH on the Distribution Factor of Copper,  
[Cu] = 10 ppm, [NaDES] = 0.50 gm/l.

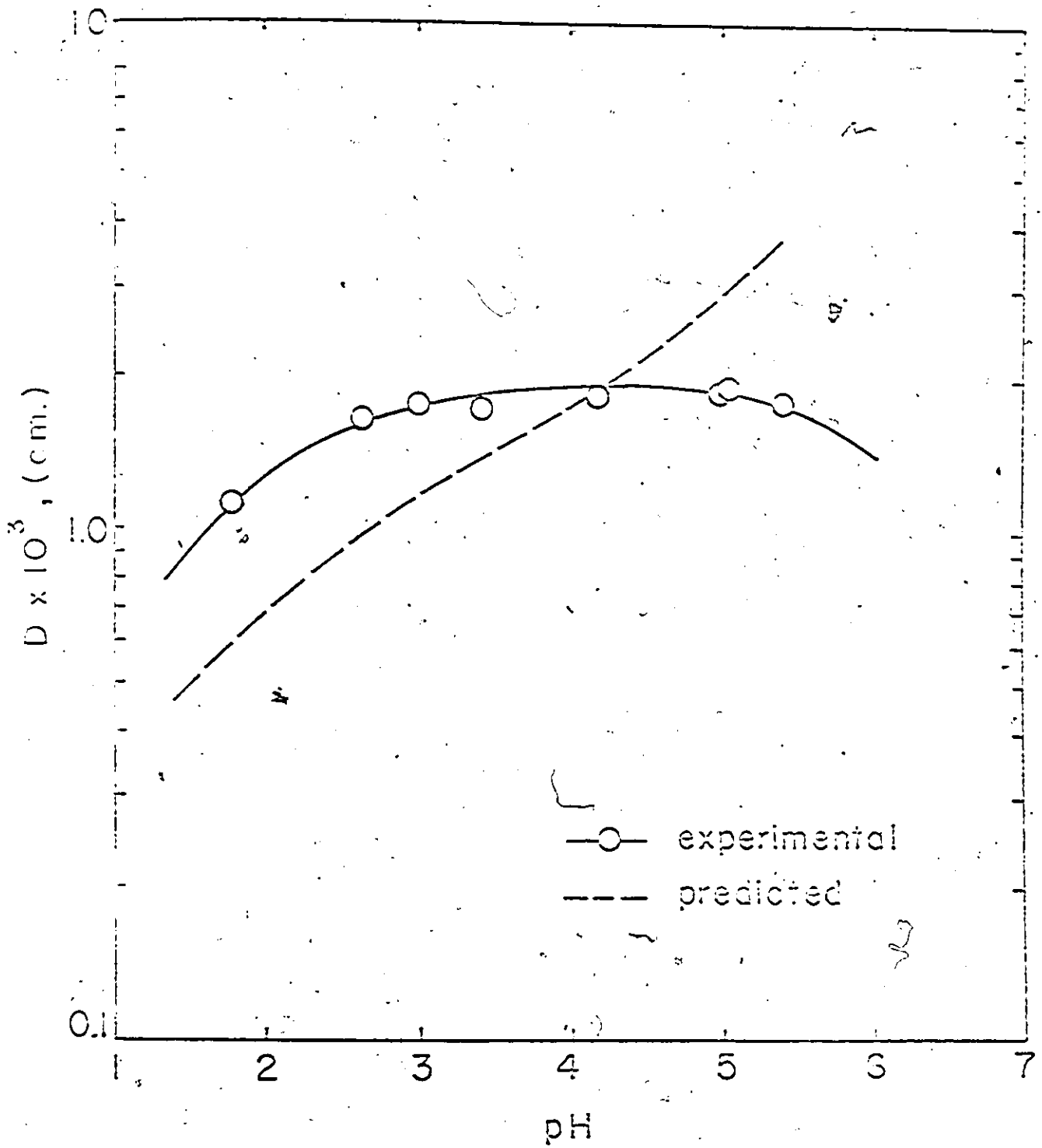


Figure 10. Effect of pH on the Distribution Factor of Cadmium, [Cd] = 10 ppm, [NaDBS] = 0.50 gm/l.

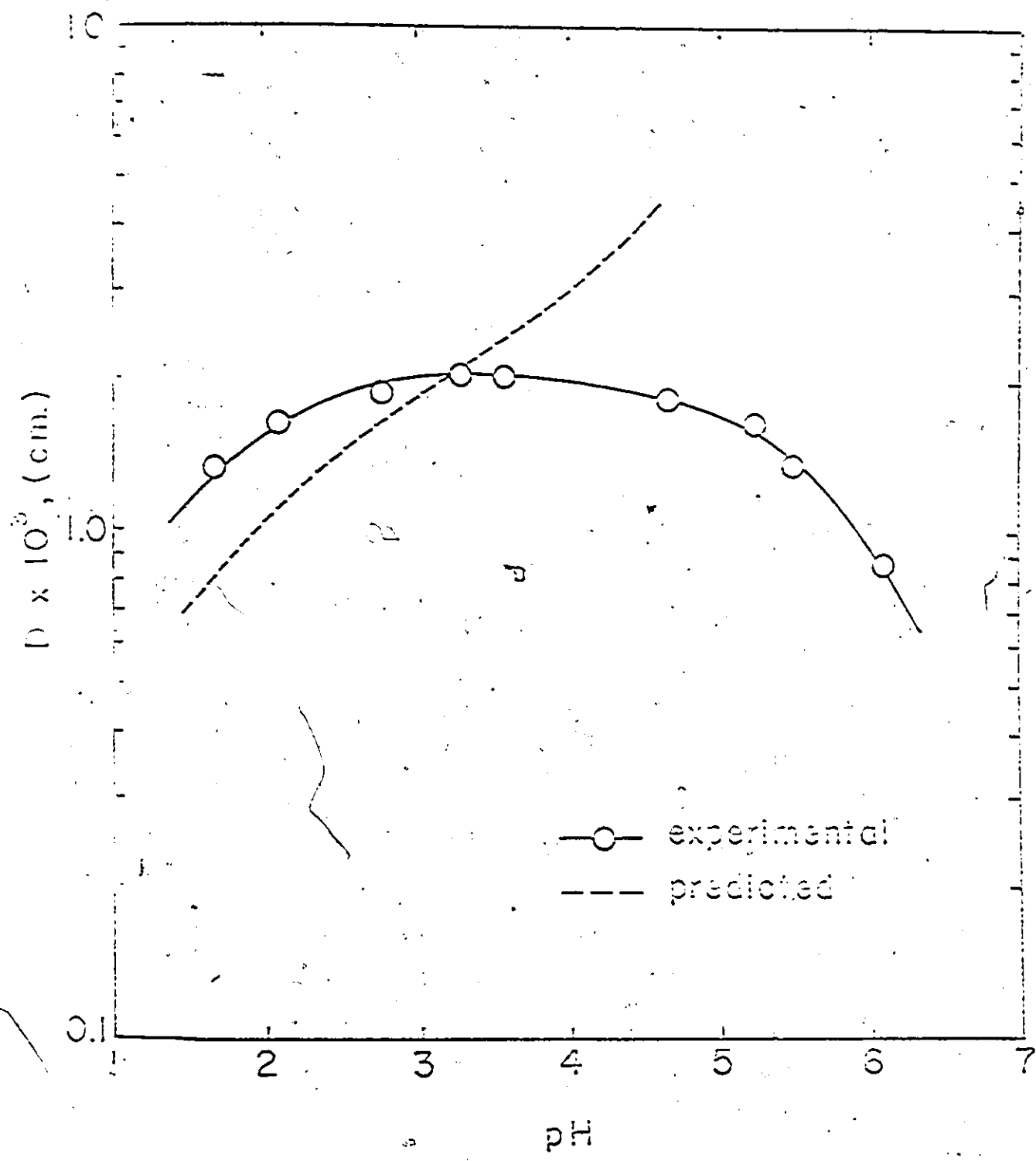


Figure 11. Effect of pH on the Distribution Factor of Lead.  
[Pb] = 10 ppm, [NaDEBS] = 0.50 gm/l.

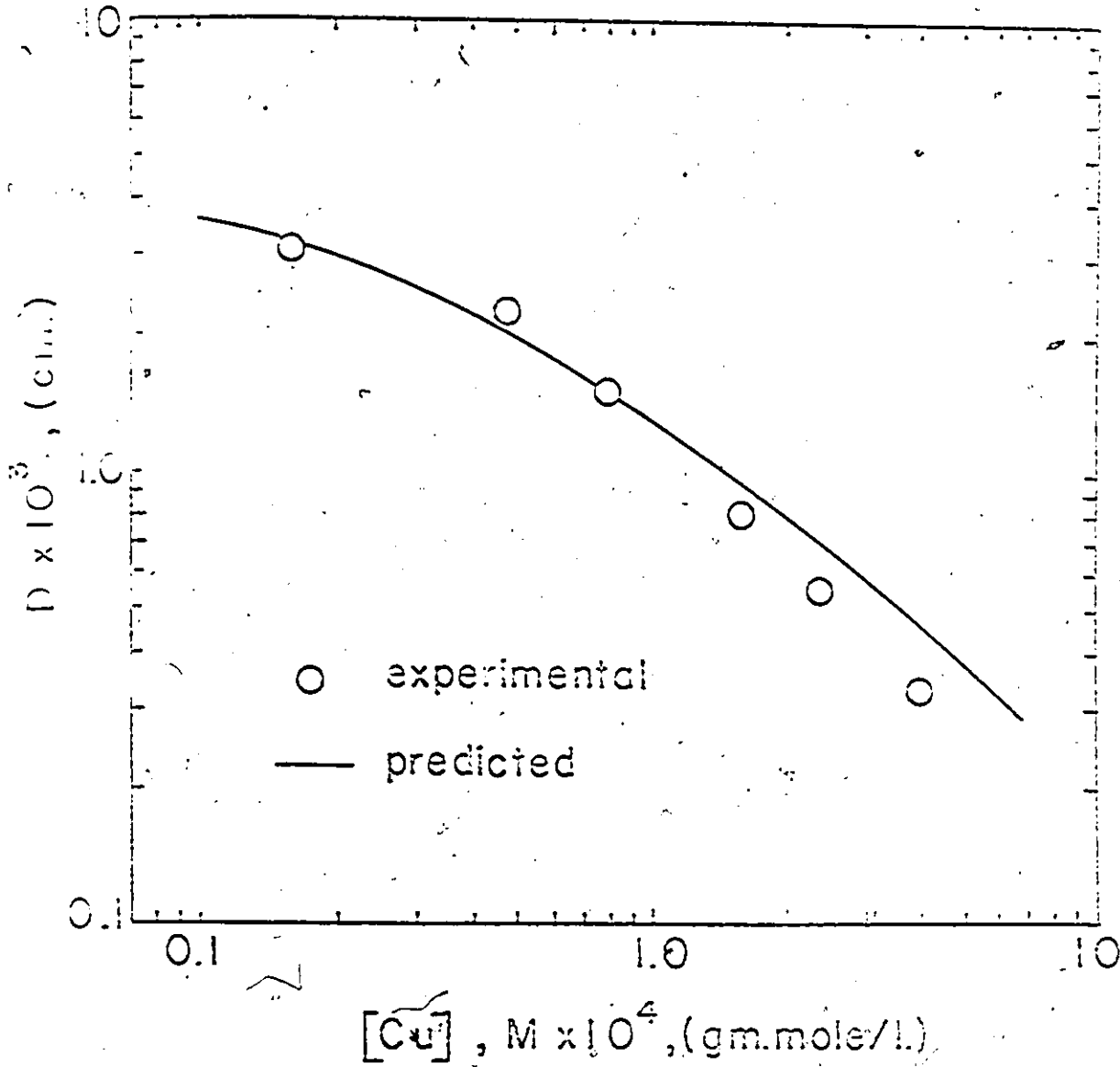


Figure 12. Effect of Bulk Copper Concentration on Distribution Factor,  $pH = 4.70 \pm 0.05$ ,  $[NaDEG] = 0.50$ .

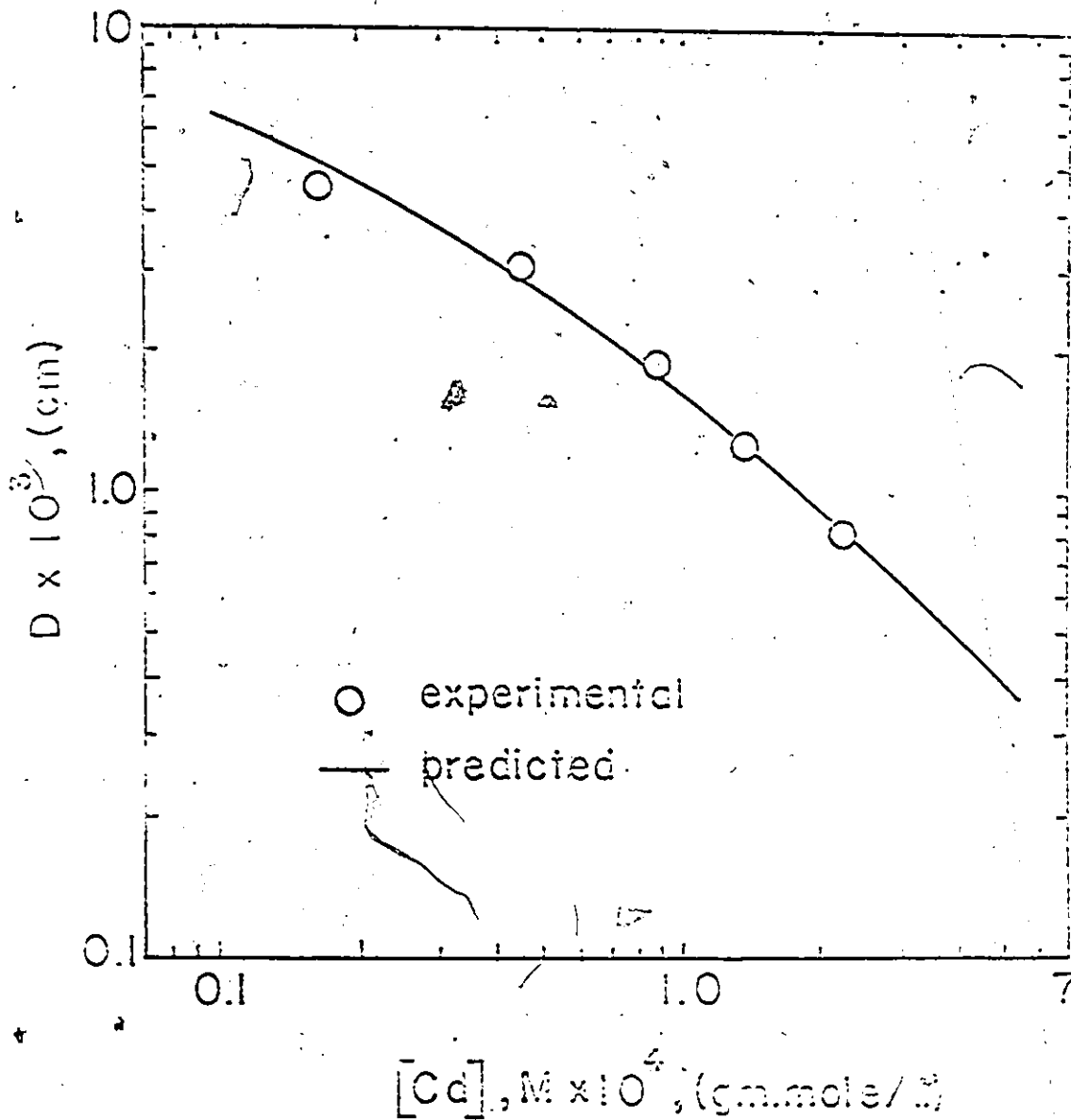


Figure 13. Effect of Bulk Cadmium Concentration on Distribution Factor,  $pH = 5.00 \pm 0.05$ ,  $[NaDES] = 0.50$  g/L.



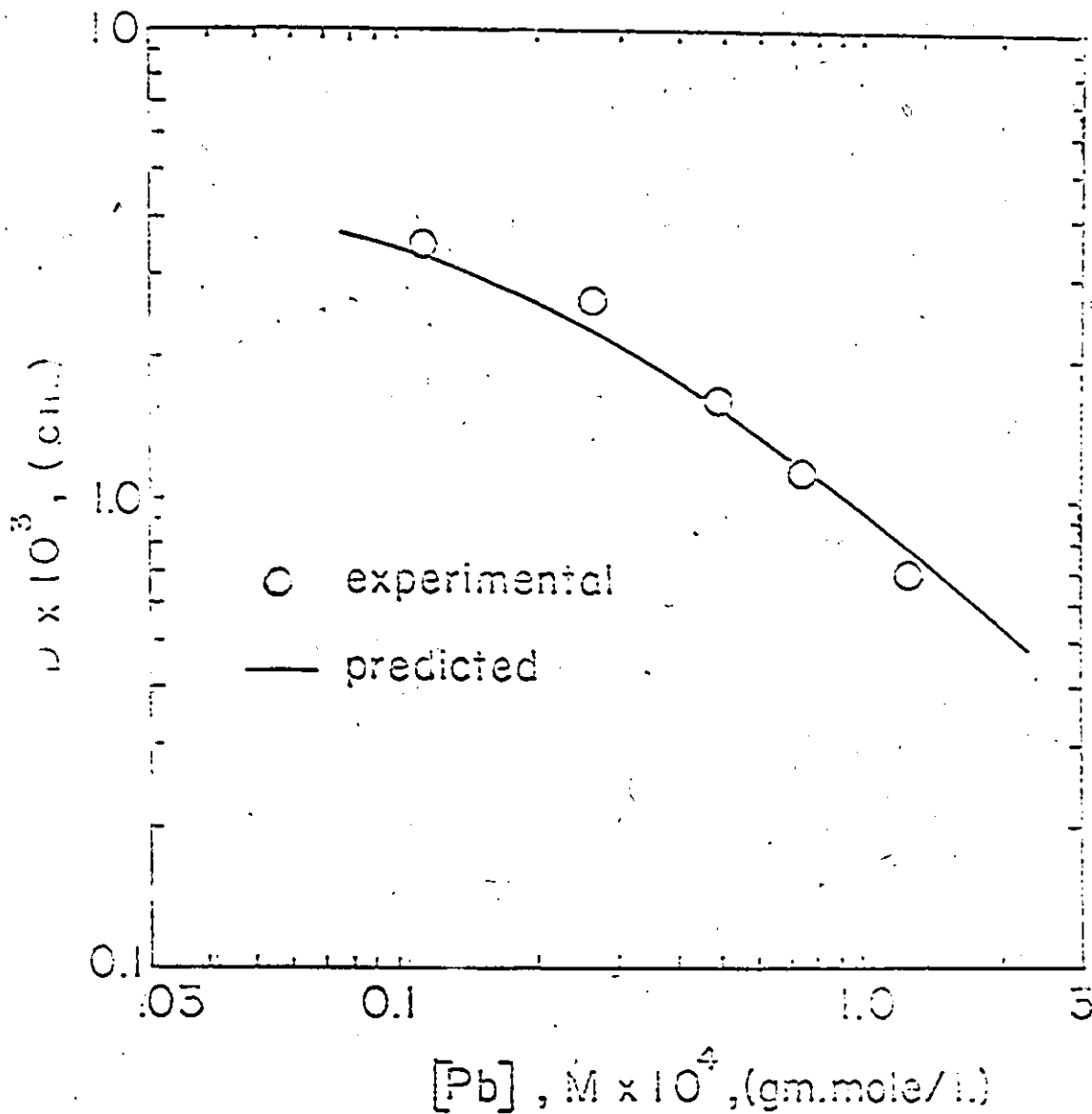


Figure 14. Effect of Bulk Lead Concentration on Distribution Factor,  $\text{pH} = 5.15 \pm 0.07$ ,  $[\text{NaDBS}] = 0.50 \text{ gm/l.}$

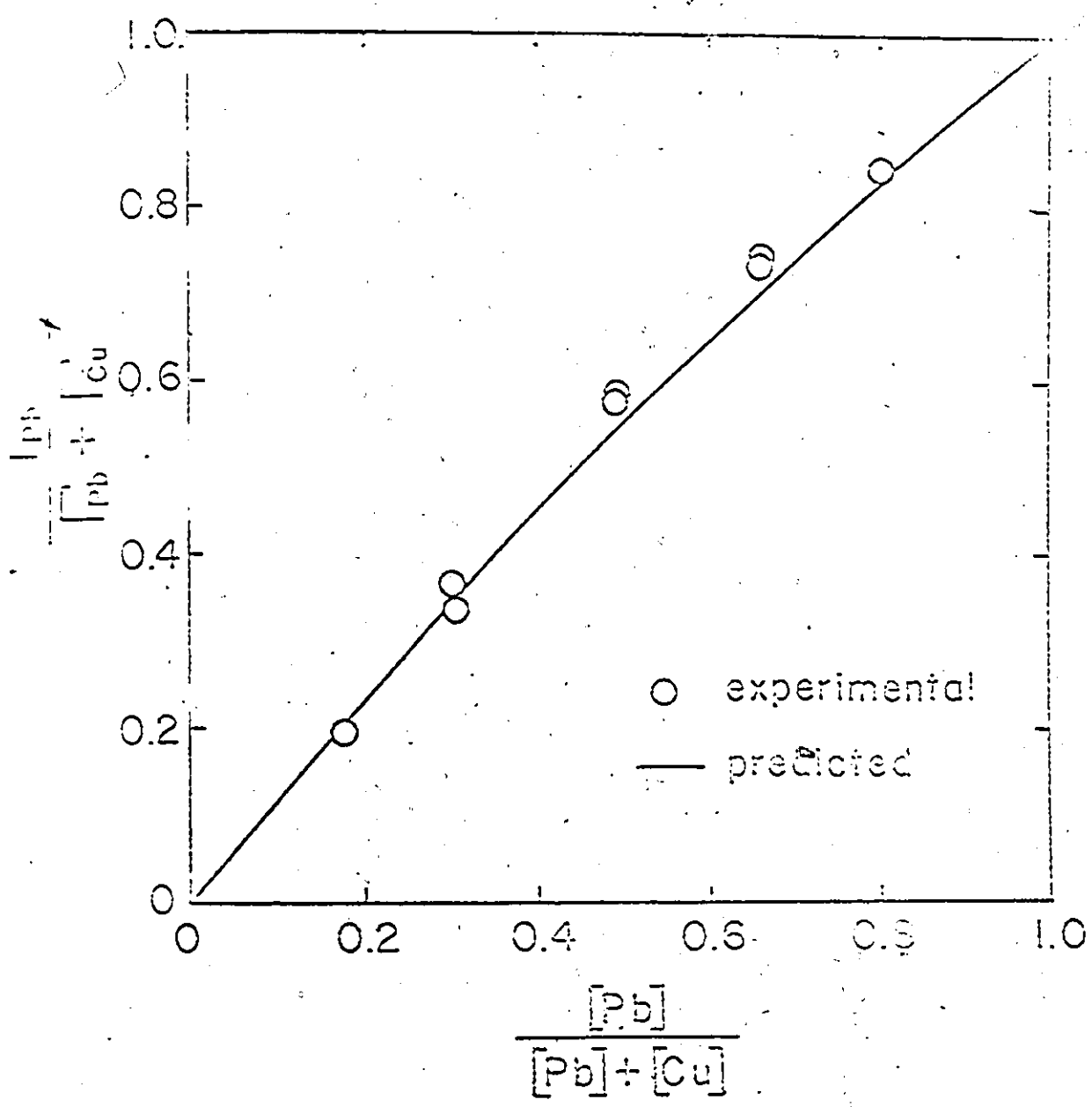


Figure 15. Comparison of Predicted and Measured Selectivity Coefficients of Pb-Cu-NaDES System, pH = 4.10 ± 0.05, [NaDES] = 0.50 gm/l.

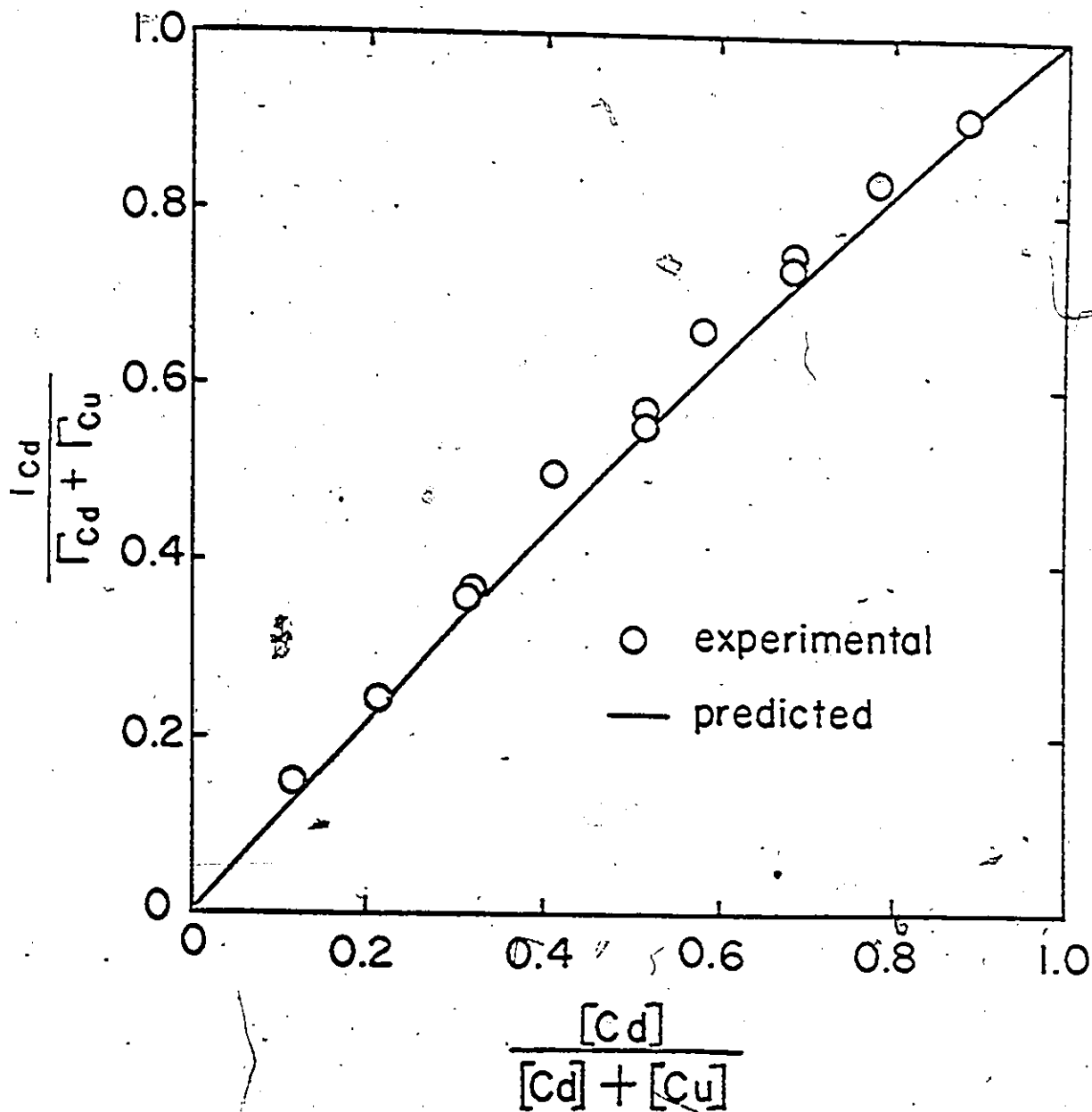


Figure 16. Comparison of Predicted and Measured Selectivity Coefficients of Cd-Cu-NaDBS System, pH = 4.10 ± 0.05, [NaDBS] = 0.50 gm/l.

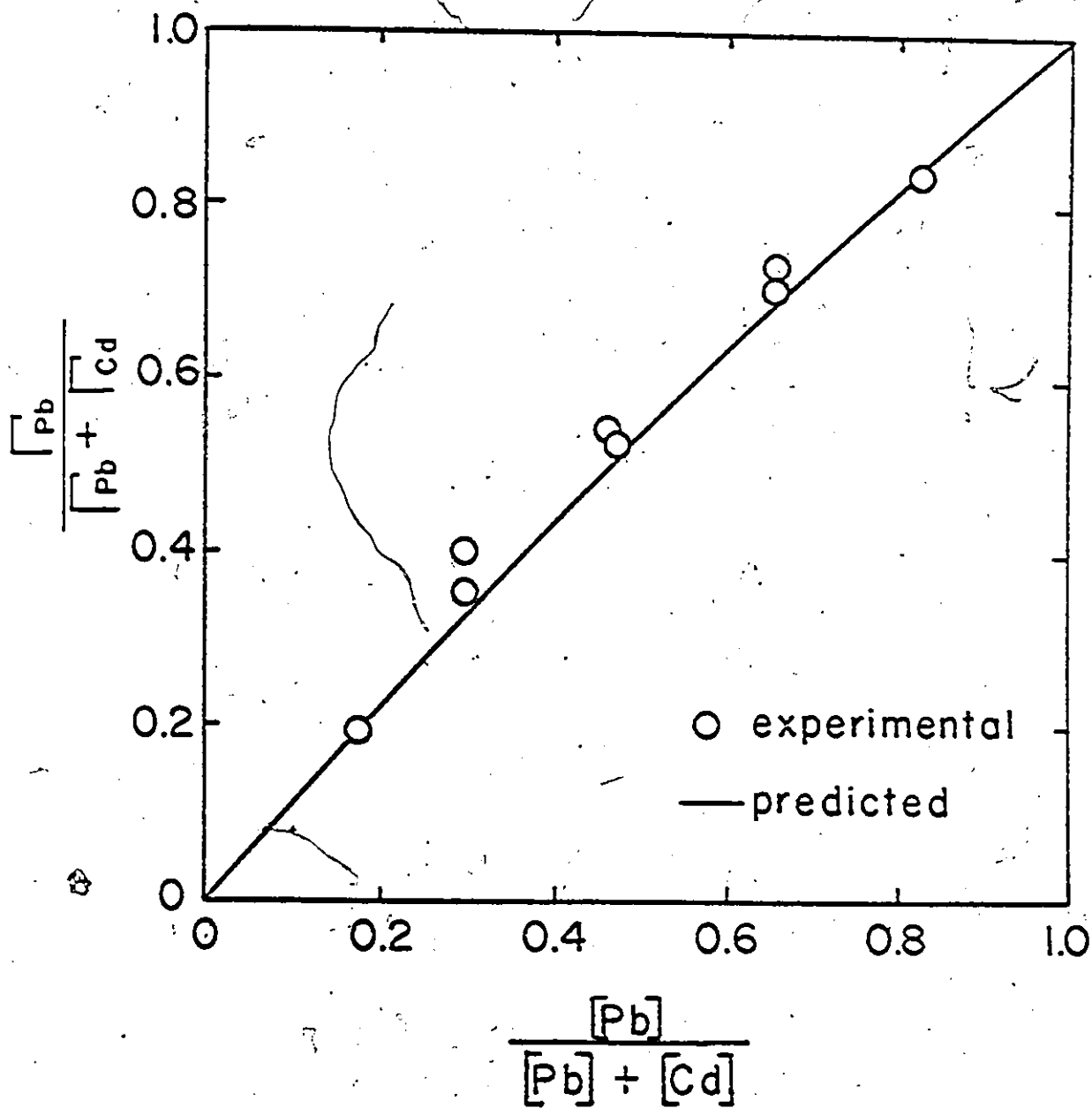


Figure 17. Comparison of Predicted and Measured Selectivity Coefficients of Pb-Cd-NaDBS System, pH = 4.10 ± 0.05, [NaDBS] = 0.50 gm/l.

Table 8. Comparison of Selectivity Coefficients Measured from Mixture Systems and That Calculated from Pure Component Systems.

system	pH	$\alpha_{\text{measured}}$	$(\Gamma/x)_1 / (\Gamma/x)_2$
Pb/Cu	4.1	1.28	3.50
Pb/Cd	4.1	1.16	1.75
Cd/Cu	4.1	1.08	2.00

CHAPTER 6

DISCUSSION

Figures 9 to 11 show the distribution factor of metal ions as a function of bulk solution pH. The concentration of metal ions was kept constant at 10 ppm; the concentration of surfactant was at 0.50 gm/l. It is observed that the theoretically predicted distribution factor is in good agreement with that measured experimentally for pH less than 4.0. At a pH greater than 4.0, deviation of the predicted and experimental results becomes unacceptable. This deviation is due to the fact that the equilibrium model assumed in this study does not account for the complex reactions occurring in this pH region.

Figures 12 to 14 show the results for the changes of distribution factor with respect to bulk metal concentrations at constant pH. In these figures, the theoretical curves were normalized by adjusting the distance of closest approach of metal ions. The data are shown in tables B-12 to B-17, in which the operating pH of each system is also indicated. It is noted that the pH of solution foamed is higher than the applicable pH range of equilibrium model and therefore the radius of hydrated ion is greater. The figures confirm the trend of the theoretical prediction. A similar observation

has been reported by Jorne and Rubin ( 9 ) for a different system.

From the results of systems containing one metal ion, it is observed that the magnitude of distribution factor is in the order of  $DF_{Pb^{++}} > DF_{Cd^{++}} > DF_{Cu^{++}}$  : The sequence is just the reverse of the order of their effective radii of hydrated ions. It can then be understood that the smaller the hydrated ion, the more the preferential adsorption on the interface, if they have the same ionic charge. This conclusion is supported by equation (3.44) which reveals the fact that the smaller ion possess a higher surface potential. Experimental proof, therefore, was conducted to examine the effect of ionic size on the separation in a system containing two different metal ions.

The results of systems containing two metal ions are shown in figures 15 to 17. Experiments were performed at constant surfactant concentration at 0.50 gm/l. and pH at  $4.10 \pm 0.05$ . The predicted and measured selectivity coefficients agree very well. The experimental results are expressed in a form similar to the familiar x-y diagram used in vapor-liquid equilibrium studies. It is because the similarity of the two separation processes, foam fractionation and distillation, have long been well known. The analogous features of the two processes are worth summarizing ( 3 ). For example : (1) the liquid phase in distillation is analogous to the bulk liquid

which the foam is generated in foam fractionation, (2) the vapor phase in distillation is analogous to the interfacial area in foam fractionation, (3) the vapor plus entrained liquid in distillation is analogous to the foam overflow in foam fractionation, (4) the heat input in distillation is analogous to the gas flow in foam fractionation (5) the pressure in distillation is analogous to the surfactant concentration in foam fractionation (11). In foam fractionation, the concentration of solute in foam ( vapor ) phase is expressed as the surface excess, and in liquid phase , that is the molar concentration.

If the vapor is richer in the more volatile substance, the curve, on the  $x$ - $y$  diagram, will be above the diagonal. The greater the distance between the equilibrium curve and the diagonal, the greater the difference in liquid and vapor compositions and more readily is the separation made. In foam fractionation process, an ion having a smaller ionic size is richer in the foam.

The results ( figures 15 to 17 ) show that cadmium ion is preferentially separable in Cd-Cu-NaDBS system and the same for lead ion in both Cu-Pb-NaDBS and Cd-Pb-NaDBS systems. The differences in values of selective separation coefficients of the three systems studied could be explained as the relative differences of the effective radii of hydrated ions. It was therefore proved that the ionic size determines the selectivity. Other evidence can be found in the work ( 4 ) which reported



that the order of increased selectivity is:  $H^+ < Na^+ < K^+ < NH_4^+$ , which is the order of decreased hydration number.

Another important finding of the foaming results was that the pH of foamate was higher than that of the bulk in the high pH region. This was observed by measuring the pH of both foamate and bulk solutions and the results are present graphically in figures 18 to 20 and in tables B-24 to B-29. This result is not from the hydrolysis of anionic surfactant but from the preferential removal of  $MOH^+$  ion in solution. For no pH change in foamate, both  $DBS^-$  hydrolysis and preferential removal of  $MOH^+$  must have equal weight or both are negligible, that is no hydrolysis of surfactant and no preferential removal of  $MOH^+$ . But, the experimental evidence shows that it is not the case. In view of the preferential adsorption of  $MOH^+$  ion, the pH change will shift to the opposite direction to that reported by Rubín and Jorñe ( 63 ). The latter will be discussed later. The distribution factor of  $MOH^+$  ion of six systems studied is also calculated based on the pH and the ionic concentration of metals and surfactant in both bulk and foamate solutions. The equilibrium model is applied on both solutions to obtain the composition of each species. The distribution factor of  $MOH^+$  can then be calculated and the results are tabulated in tables B-6 to B-17, in which the preferential adsorption of  $MOH^+$  over hydrated metal ion can be observed. It is noted that the pH change in the foamate is caused by the

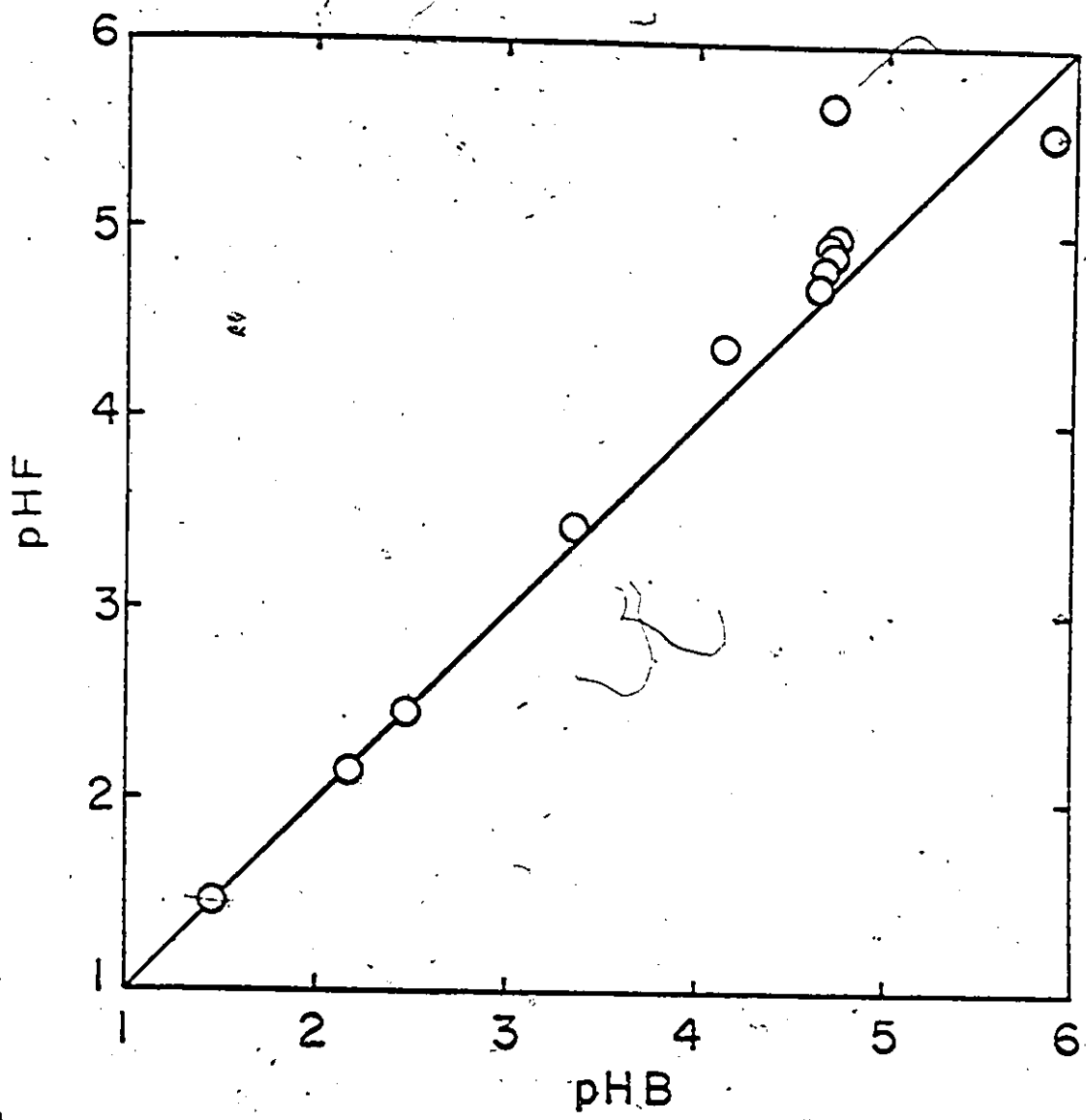


Figure 18. pH Change of Cu-NaDBS System : pHF, pH of Foamate; pHB, pH of Bulk.

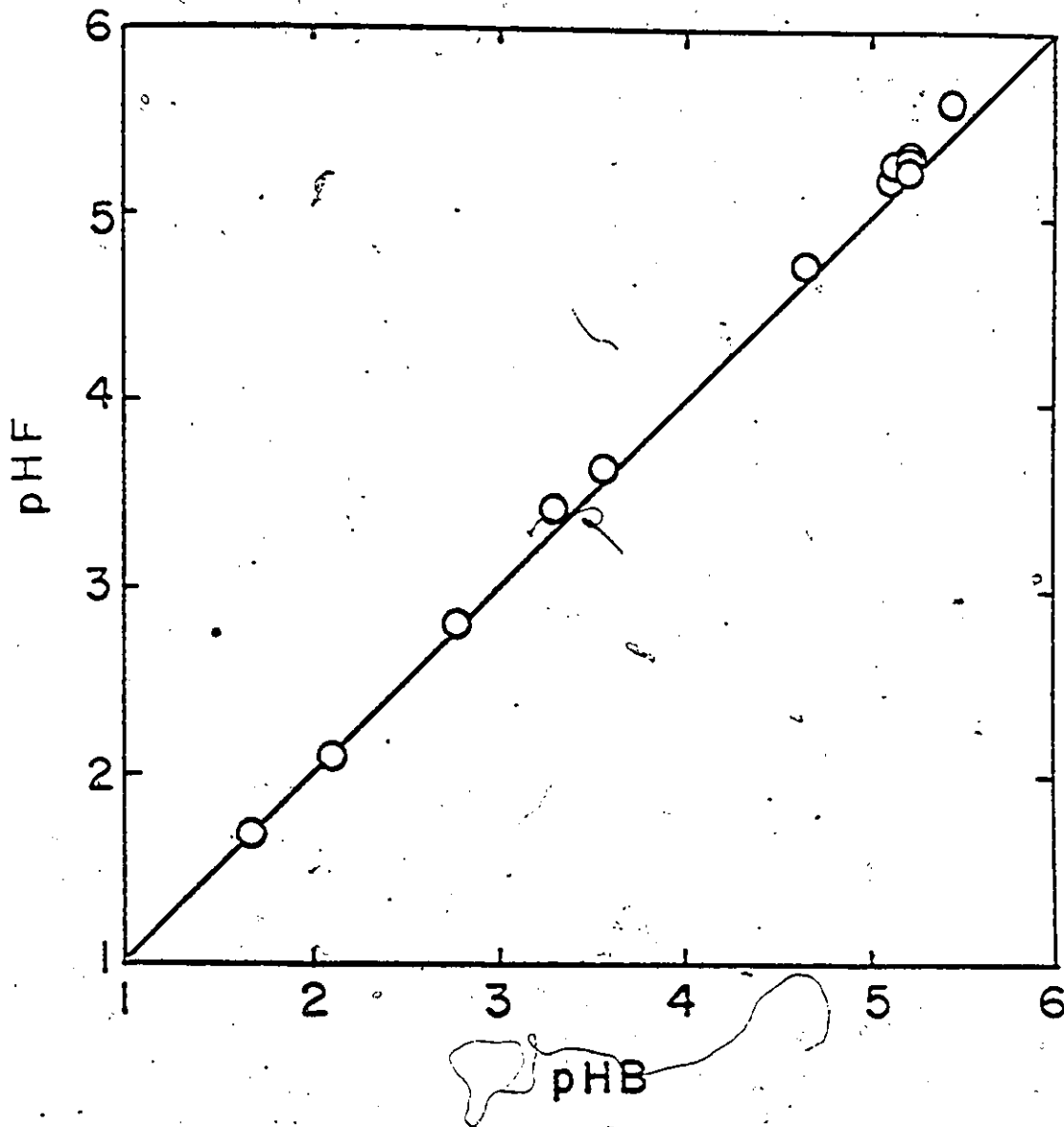


Figure 19. pH Change of Pb-NaDBS System : pHF, pH of Foamate; pHB, pH of Bulk.

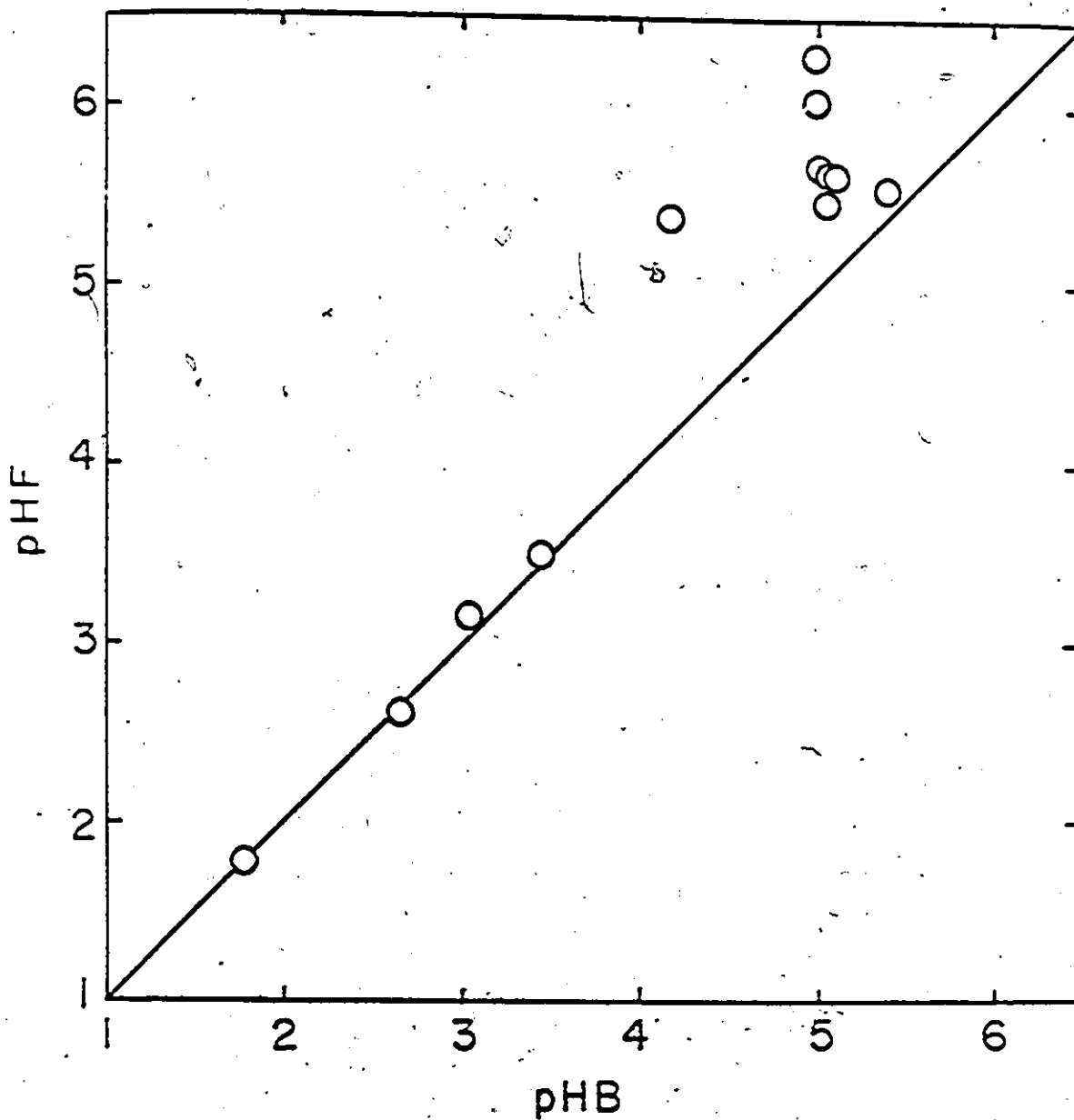
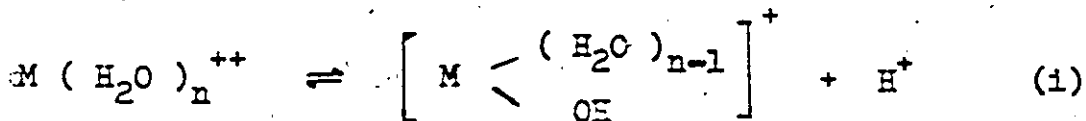


Figure 20. pH Change of Cd-NaDBS System : pHF, pH of Foamate; pHB, pH of Bulk.

surplus of hydroxyl ion, in the form of  $\text{MOH}^+$ , carried over by the foam.

It was found in figures 18 to 20 that at pH below 3.0, no pH change was observed. This is because at conditions of low pH and dilute solution, soluble metal hydroxides are not formed or make up only an insignificant fraction of the total. In this region, it can also be imagined that hydrogen ions dominate the separation role, suppressing the charge density of anionic surfactant on the air-liquid interface and therefore the distribution factor of metal ions ( see figures 9 to 11 ).

However at higher pH. it is well known that the metal ion does not exist in solution as a naked ion, but is surrounded by water dipoles which form the so called hydration sheath. If the central ion is small, i.e., the charge density is high, these coordinated water molecules can exhibit acidic properties, owing to the charge attraction exerted by the central ion on the electrons of the associated water dipoles. For example, at least one of these waters of  $\text{M}(\text{H}_2\text{O})_n^{++}$  will tend to lose its proton to a base, i.e., behave as an acid (-la), or



Should there be enough base to accept the protons offered, this type of ionization can continue so that further water molecules ionise to a stage at which the metal hydroxide can be expected to be precipitated. However, before that happens, another effect comes into operation. This is the tendency for the polynuclear species *to* form through an oxygen bridge.

The degree of bridging is comparatively little and the ions are comparatively small, but with increasing pH they tend to grow until finally such a large molecule is produced that it can no longer remain in solution and precipitates out. It should be noted that the formation of a precipitate can often be considered the final stage in the formation of polynuclear complexes. It has been mentioned ( 64 ) that the tendency to form metal-metal bonds increases with increasing atomic number within a family. Ringbom ( 37a ) and Sillén ( 65 ) discussed in detail on the behavior and character of polynuclear species.

It is not yet clear that whether, at any fixed pH before precipitation, a specific species of exact formulation exists or whether, given time, a range of different sizes is produced. But it is clear that the formation of polynuclear species, which is so complicated that was not considered in the equilibrium model, causes the deviation between the theoretical prediction and experimental results. In region pH below 4,

the hydrolytic reaction of metal ion is minimised and the agreement is considered reasonably well.

Hydrolytic reaction of the anionic surfactant ion on the air-liquid interface is also an important factor in the foam fractionation process. It has been pointed out by Cook and Talbot ( 66 ) that free acid was formed by the surface hydrolysis. They studied the surface hydrolysis of sodium lauryl sulfate ( SLS ) at different ionic strengths by pH measurements of foamed solutions and by the pH dependence of surface tension. The latter showed that an increase in pH resulted in an increase in surface tension explains that there is adequate surface hydrolysis to account for the observed collector properties of SLS solutions by hydrolytic adsorption. They found that foaming a solution of SLS produced a measurable increase in the pH of the substrate. This can only mean that the ratio of  $( \text{HLS} / \text{LS}^- )$  at surface was appreciable as a result of which the continuous removal and reforming of the surface phase caused an accumulation of  $\text{OH}^-$  in the bulk solution. This can be accounted for the fact that the reaction is shifting toward the right ( due to extraction of  $( \text{HLS} )_s$  ) of the equilibrium



Here the subscripts s refers to the surface. Therefore, it

is suggested that, if the ratio (  $HLs / LS^-$  ) were the same in the surface as in the solution, foam extraction would not affect the pH of the solution. In this report, it was found that the degree of surface hydrolysis was 1 to 4%.

Rubin and Jorne ( 63 ) also reported the surface hydrolysis effects on foam separation, in which the results indicated that the pH of the foamate was lower than that of the bulk liquid. The system they studied was foaming a solution of NaDBS alone. Hydrolysis implies, for anionic surfactants, the preferential adsorption of hydrogen ions over the counterions ( sodium in this system ) of the surfactant salt, with or without the formation of un-ionized acid.

Two runs were conducted foaming NaDBS solution alone with the apparatus used in this study. The results shown in table 9 indicate that the pH of foamate is lower than that of bulk solution. This is to support the result of Rubin and Jorne.

It should be noted, however, that the system studied in this work is much more complicated than those mentioned above. Furthermore, the apparatus designed and the systems studied were not for the purpose of investigating the effect of surface hydrolysis of surfactant. But the formation of HDDBS on the air-liquid interface does reduce the surface charge density, and according to the diffuse double layer theory, the distribution factor of metal ions is decreased. The phenomenon is important and is worthwhile to be extensively investigated.



Table 9. pH Change of Foaming NaDBS Solution without Metal Ions.

Run No.	NaDBS (gm/l.)	pHB	pHF
43	1.75	7.18	6.93
44	0.50	6.82	6.63

### 6.1 Error Analysis

In general, the results of several independently measured quantities are combined to give the desired result of the experiments. Suppose a set of measurements is made and the uncertainty in each measurement may be expressed with the same odds. Therefore, the uncertainty in the calculated result can be estimated on the basis of the uncertainties in the primary measurements. Suppose the result  $R$  is a given function of the independent variables  $x_1, x_2, x_3, \dots, x_n$ . Thus,

$$R = R(x_1, x_2, x_3, \dots, x_n) \quad (6.1)$$

Let  $w_R$  be the uncertainty in the result and  $w_1, w_2, \dots, w_n$  be the uncertainties in the independent variables. If the uncertainties in the independent variables are all given with the same odds, then the uncertainty in the result having these odds is given ( 67,68 ) as

$$w_R = \left[ \left( \frac{\partial R}{\partial x_1} w_1 \right)^2 + \left( \frac{\partial R}{\partial x_2} w_2 \right)^2 + \dots + \left( \frac{\partial R}{\partial x_n} w_n \right)^2 \right]^{\frac{1}{2}} \quad (6.2)$$

Particular notice should be given to the fact that the uncer-

ainty propagation in the result  $w_R$  depends on the square of the uncertainties in the independent variables  $w_n$ . This means that if the uncertainty in one variable is significantly larger than the uncertainties in the other variables, then it is the largest uncertainty which predominates and the others may probably be neglected.

The desired result of the experiments in this study is the distribution factor which has the expression as

$$DF = \frac{Q (C_f - C_b)}{C_b S} = \frac{Q (C_f / C_b - 1)}{(36 n \pi N G^2)^{1/3}} \quad (6.3)$$

The independent variables are  $Q$ ,  $C_f$ ,  $C_b$ ,  $N$  and  $G$ . The partial derivatives of distribution factor with respect to each independent variable are as follows :

$$\frac{\partial (DF)}{\partial Q} = \frac{(C_f / C_b - 1)}{(36 n \pi N G^2)^{1/3}} \quad (6.4)$$

$$\frac{\partial (DF)}{\partial C_f} = \frac{Q}{C_b (36 n \pi N G^2)^{1/3}} \quad (6.5)$$

$$\frac{\partial (DF)}{\partial C_b} = \frac{-Q C_f}{C_b^2 (36 n \pi N G^2)^{1/3}} \quad (6.6)$$

$$\frac{\partial (DF)}{\partial N} = \frac{-Q (C_f / C_b - 1)}{3 (36 n \pi N^4 G^2)^{1/3}} \quad (6.7)$$

and

$$\frac{\partial (DF)}{\partial G} = \frac{-2Q (C_f / C_b - 1)}{3 (36 n \pi N G^5)^{1/3}} \quad (6.8)$$

The uncertainties in the independent variables are assumed to be 1 per cent for both concentration measurements, 5 per cent for gas flow rate, 3 per cent for the bubble emission frequency, and 0.1 per cent for the weight of foamate, or

$$C_b = C_b \pm 1\%$$

$$C_f = C_f \pm 1\%$$

$$G = G \pm 5\%$$

$$N = N \pm 3\%$$

and

$$Q = Q \pm 0.1\%$$

The uncertainty of the distribution factor calculated on these bases is then in the range of 3.5% to 4.8% and the data are presented in tables B-6 to B-11.

CHAPTER 7

CONCLUSIONS

In conclusion, the distribution factor of copper, cadmium and lead ions measured by foam fractionation can be predicted by the modified theory of Gouy-Chapman diffuse double layer for the system studied below a pH of 4. Comparison of the results, when bulk concentration was a variable, was also in a good qualitative agreement.

It may also conclude that the surfactant adsorbed on air-liquid interface partly is in the form of whole molecules rather than complete in ionic form, usually caused by hydrolytic adsorption.

The results of the systems containing two metal ions showed that the ionic size determines the selectivity, i.e., for the same ionic charge, smaller ion is preferentially separable.

Because of the effect of hydronium ions at low pH and the hydrolytic reaction at high pH, the optimum conditions for the foam fractionation of aqueous solutions of metal ions with NaDBS were found to be as follows : pH range between 3.0 and 5.7 for copper, 3.0 and 5.5 for cadmium, 3.0 and 4.5 for lead, and NaDBS concentration of 0.50 gm/l.

CHAPTER 8

RECOMMENDATIONS FOR FUTURE WORK

From the fact that the ionic size determines the selectivity between ions, it is practical to separate a particular element from a multicomponent system. This could be achieved by controlling the conditions of the system, i.e., by ways of physical or chemical treatment, to enlarge the relative difference of the ionic size.

A further work is recommended to expand the applicability of the equilibrium model over a wide pH range by taking into account the complex reaction occurring in the high pH region. It is also recommended to explore the extent of surface hydrolysis of anionic surfactant ion either by measuring surface tension versus pH of solution or by designing a new apparatus to measure the composition of species right on the bubble surface.

REFERENCES

- (1) Sebba, F., "Ion Flotation", Elsevier, New York (1962). (a), pp. 40.
- (2) Lemlich, R., "Adsorptive Bubble Separation Techniques", Academic Press, New York (1972). (a), pp. 270. (b), pp. 36.
- (3) Rubin, E., and Gaden, E.L., Jr., Foam Separation in "New Chemical Engineering Separation Technique", H.M. Schoen, ed., Interscience, New York (1962), chapter 5.
- (4) Walling, C., Ruff, E.E., and Thornton, J.C., Jr., J. Phys. Chem., 61, 486 (1957).
- (5) Rubin, A.J., Johnson, J.D., and Lamb, J.C., I & EC Process Design and Develop., 5 (4), 368(1966).
- (6) Rubin, A.J., and Johnson, J.D., Analytical Chemistry, 39(3), 298(1967).
- (7) Rubin A.J., J. Amer. Water Work Assoc., 60 (7), 832(1968).
- (8) Dick, W.L., and Talbot, F.D., Ind. Eng. Chem. Fundam., 10(2), 309(1971).
- (9) Jorne, J., and Rubin, E., Separation Science, 4(4), 313(1969).
- (10) Somasundaran, P., Separation and Purification Methods, 1(1), 117(1972).
- (11) Banfield, D.L., Newson, I.H., and Alder, P.J., A.I.Ch.E. - I.Chem. E. Symposium Series No. 1, 1:5(1965).
- (12) Schoen, H.M., Rubin, E., and Ghosh, D., Journal WPCF, 34(10), 1026(1962).
- (13) Schonfeld, E., Stanford, R., Mazzella, G., Ghosh, D., and Eppok, F., Report NYO-9577/1960 ( New York : Radiation Application Inc. ).
- (14) Grievos, R.B., British Chem. Eng., 15(1), 77(1968).

- (15) Barocas, A., Jacobelli-Turi, C., and Terenzi, S., I & EC Process Design and Develop., 6, 161(1967).
- (16) Rubin, A.J., and Lapp, W.L., Analytical Chemistry, 41(8), 1133(1969).
- (17) Grieves, R.B., and Bhattacharyya, D., Separation Science, 1, 81(1966).
- (18) Grieves, R.B., and Aronica, R.C., Int. J. Air Water Pollut. 10, 31(1965).
- (19) Grieves, R.B., and Aronica, R.C., Nature, 210, 901(1966).
- (20) Grieves, R.B., and Wilson, T.E., Nature, 205, 1066 (1965).
- (21) Grieves, R.B., and Schwartz, S.M., J. Appl. Chem., 16, 14(1966).
- (22) Grieves, R.B., and Bhattacharyya, D., J. Appl. Chem., 19, 115(1969).
- (23) Grieves, R.B., and Bhattacharyya, D., Canad. J. Chem. Eng., 43, 286(1965).
- (24) Bretz, H.W., Wang, S.L., and Grieves, R.B., Appl. Microbiol. 14, 778(1966).
- (25) Grieves, R.B., and Wang, S.L., Appl. Microbiol., 15, 76(1967).
- (26) Grieves, R.B., and Crandall, C.J., Water Sewage Works, 113, 432(1966).
- (27) Grieves, R.B., and Chouinard, E.F., J. Appl. Chem., 19, 60(1969).
- (28) Robertson, G.H., Ph.D. thesis, University of California, Berkeley, 1970.
- (29) Sebba, F., Nature, 184, 1062(1959).
- (30) Sebba, F., and Lusher, J.A., J. Appl. Chem., 15, 577 (1965).
- (31) Sebba, F., and Pice, N.W., J. Appl. Chem., 15, 105 (1965).



- (32) Schnepf, R.W., and Gaden, E.L., Jr., Chem. Eng. Progr., 55, 42(1959).
- (33) Hass, P.A., thesis, Oak Ridge National Laboratory Report No. ORNL-3527, June, 1965.
- (34) Gouy, J., Phys. Radium, 9, 457(1910).
- (35) Chapman, D.L., Phil. Mag., 25, 475(1913).
- (36) Lemlich, R., Principle of Foam Fractionation from "Progress in Separation and Purification", Vol. 1, E.S. Perry, ed., Interscience, New York (1968).
- (37) Ringborn, A., "Complexation in Analytical Chemistry", Interscience, New York (1963), pp. 298. (a), pp. 31.
- (38) Flexser, L.A., Hammett, L.P., and Dingwall, A., J. Am. Chem. Soc., 57, 2103 (1935).
- (39) Job, P., Ann. Chim., 9(10), 113(1928).
- (40) Vosburgh, W.C., and Cooper, G.R., J. Am. Chem. Soc., 63, 437(1941).
- (41) Bent, H.E., and French, C.L., J. Am. Chem. Soc., 63, 568(1941).
- (42) Kingery, W.D., and Hume, D.N., J. Am. Chem. Soc., 71, 2393(1949).
- (43) Sugie, H., personal communication, Department of Industrial Chemistry, University of Nagoya, Japan.
- (44) Grahame, D.C., Chemical Reviews, 41, 441(1947).
- (45) Kruyt, H.R., "Colloid Science", Vol. 1, Elsevier, New York (1952), pp. 126.
- (46) Ruckenstein, J.J., "Physical Surface", Academic Press, New York (1970), pp. 370.
- (47) Bockris, J.D., and Reddy, A.K.N., "Modern Electrochemistry", Plenum Press, New York (1970), pp. 718. (a), pp. 725.
- (48) Davies, J.T., and Rideal, E.K., "Interfacial Phenomena", Academic Press, New York(1961), pp. 64.

- (49) Wace, P.E., and Banfield, D.C., Chem. & Process Eng., 47, 70(1966).
- (50) Rubin, E., Ph.D. thesis, Columbia University, New York (1962).
- (51) ASTM Standards on Water; Atmospheric Analysis, prepared by ASTM Committee D-2330-68, part 23, American Society for Testing and Materials, Philadelphia (1968), pp.737.
- (52) ASTM Standards on Soaps and Other Detergents, prepared by ASTM Committee D-12, 9th ed., American Society for Testing and Materials, Philadelphia (1960), pp. 144.
- (53) Manual of the Atomic Absorption Spectrophotometer, Unicam SP 90, Unicam Instruments, Ltd., Cambridge, England.
- (54) Owen, B.B., and Gurry, R.W., J. Am. Chem. Soc., 60, 3074(1938).
- (55) Denham, H.G., and Marris, N.A., Trans. Faraday Soc., 24, 515(1928).
- (56) Fuerstenan, M.C., and Atak, S., Trans. A.I.M.E., 232, 24(1965).
- (57) Nasanen, R., and Tamminen, V., J. Am. Chem. Soc., 71, 1994(1949).
- (58) Tate, J.F., and Jones, M.M., J. Phys. Chem., 65, 1661 (1961).
- (59) Biggs, A.I., Parton, H.N., and Robinson, R.A., J. Am. Chem. Soc., 77, 5844(1955).
- (60) King, E.J., Qualitative Analysis and Electrolytic Solutions, Harcourt, Brace & World, Inc., New York (1959), pp. 143.
- (61) Wace, P.F., Alder, P.J., and Banfield, D.L., Chem. Eng. Progress Symposium Series, No. 91, Vol. 65. pp. 19(1969).
- (62) Kielland, J., J. Am. Chem. Soc., 59, 1675(1937).
- (63) Rubin, E., and Jorne, J., J. of Colloid and Interface Science, 55(2), 208(1970).

- (64) Douglas, B.E., and McDaniel, D.H., "Concepts and Models of Inorganic Chemistry", Blaisdell Publishing Company, Toronto (1965), pp. 328.
- (65) Stillén, L.G., Quarterly Reviews (London), 13, 146 (1959).
- (66) Cook, M.A., and Talbot, E.L., J. Phys. Chem., 56, 412(1952).
- (67) Kline, S.J., and McClintock, F.A., Mech. Eng., pp. 3, Jan. (1953).
- (68) Holman, J.P., "Experimental Methods for Engineers", McGraw-Hill Book Company, New York (1966), pp. 57.
- (69) Hodgman, C.D., "Handbook of Chemistry and Physics", Chemical Rubber Publishing Co., 30 th ed., pp. 1941 (1948).
- (70) Brull, L., Chemical Abstract, 29, 1309(1935).
- (71) Bonino, G.B., and Centola, G., Mem. Accad. Italia, 4, 445(1933).
- (72) Brull, L., Gazz. Chim. ital., 64, 624(1934).
- (73) Ulich, E., Z. Elektrochem., 36, 497(1930).
- (74) Kielland, J., J. Chem. Education, 14, 412(1937).
- (75) Kunz, K. S. } "Numerical Analysis". McGraw-Hill.  
p. 4. (1957).
- (76) Lapidus, L. } "Digital Computation for Chemical Engineers", McGraw-Hill. p. 286. (1962).

GLOSSARY

adsorption = the adhesion of a thin film of molecules to a surface.

anionic surfactant = a surface-active material that ionizes in aqueous solution. The ion that bears a negative charge has a pronounced tendency to concentrate at the interface between two phases.

collector = surfactant or an agent used in ore flotation to promote attachment of solid particles to air bubbles.

counterion ( colligend ) = an ion with electrical charge opposite to the charge on the surface of an aggregate.

electric double layer = the excess of ions of one charge type present at an interface and the equivalent amount of ions of opposite charge present in one liquid phase, generally water. In the diffuse double layer, it is assumed that the charges in the liquid phase are distributed in accordance with a Boltzmann relation.

foam = bubbles of gas whose walls are thin liquid films.

foam fractionation = the separation of solutes by frothing.

selective adsorption = the tendency for one adsorbable species to concentrate at a surface or interface in preference to another.

surface-active agent = a substance that exhibits a marked tendency to adsorb at a surface or interface.

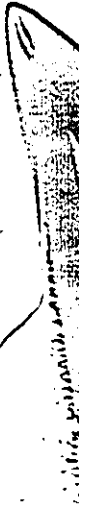
surface charge density = the excess of ions of one charge type per unit area of surface.

surface excess = the difference between the concentration of solute in the surface region and in the interior of the solution.

surface potential = the charge in the potential difference between a liquid and air arising from the presence of a surface film.

surface tension = a force with the dimensions of dynes/cm. that is a measure of the work required to increase the area of a surface by one square cm.

surfactant = a surface-active agent.



APPENDIX A

- A.1 A Mathematical Model of the System Containing Two Metal Ions.
- A.2 Derivation of Equation (3.7).
- A.3 Method of Continuous Variation.
- A.4 Derivation of Equation (3.34).
- A.5 Derivation of Equation (3.42).
- A.6 Derivation of Equation (3.44).
- A.7 Determination of the Effective Radii of Hydrated Ions.



APPENDIX A.1

A Mathematical Model of the System Containing Two Metal Ions

Equilibrium reaction of the system containing copper and cadmium ions are presented here. The equilibrium constants, CONC, of the three binary systems studied are tabulated in table A-1. The following notations are made for the system :  
A(1) = [Cu<sup>++</sup>], A(2) = [CuOH<sup>+</sup>], A(3) = [Cu(DBS)<sub>2</sub>], A(4) = [DBS<sup>-</sup>],  
A(5) = [HDBS], A(6) = [NO<sub>3</sub><sup>-</sup>], A(7) = [CuNO<sub>3</sub><sup>+</sup>], A(8) = [Cd<sup>++</sup>], A(9) = [CdOH<sup>+</sup>],  
A(10) = [Cd(DBS)<sub>2</sub>], and A(11) = [CdNO<sub>3</sub><sup>+</sup>]. It is noted that the larger hydrated ion, copper in this case, is chosen as the number one ion. The equilibrium model of the system can be obtained as follows :



$$\frac{A(2) [\text{H}^+]}{A(1) \text{ CONC}(1)} = 1.0 \quad (\text{A.1-1})$$



$$\frac{A(9) [\text{H}^+]}{A(8) \text{ CONC}(2)} = 1.0 \quad (\text{A.1-2})$$



Table A-1. Equilibrium Constants of the Model of Mixture Systems.

equilibrium constant	Cu / Cd	Cu / Pb	Cd / Pb
CONC(1)	$3.400 \times 10^{-7}$	$3.400 \times 10^{-7}$	$4.565 \times 10^{-9}$
CONC(2)	$4.565 \times 10^{-9}$	$6.760 \times 10^{-7}$	$6.76 \times 10^{-7}$
CONC(3)	$5.390 \times 10^{-2}$	$5.390 \times 10^{-2}$	$6.645 \times 10^{-2}$
CONC(4)	$6.645 \times 10^{-2}$	$2.208 \times 10^{-1}$	$2.208 \times 10^{-1}$
CONC(5)	$4.237 \times 10^{-17}$	$4.237 \times 10^{-17}$	$7.413 \times 10^{-1}$
CONC(6)	$7.413 \times 10^{-1}$	2.291	2.291
CONC(7)	$1.136 \times 10^{-5}$	$1.136 \times 10^{-5}$	$1.136 \times 10^{-5}$

CONC(8) = concentration of larger ion

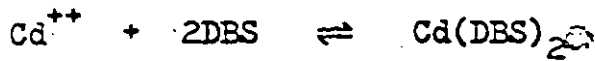
CONC(9) = concentration of smaller ion

CONC(10) = surfactant concentration

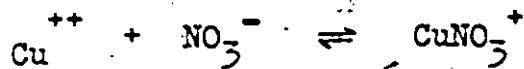
CONC(11) =  $\text{NO}_3^-$  concentration



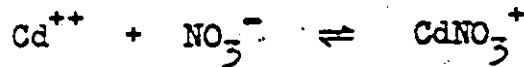
$$\frac{A(3)}{A(1) \cdot A(4)^2 \text{ CONC}(3)} = 1.0 \quad (\text{A.1-3})$$



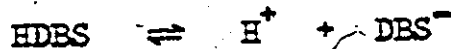
$$\frac{A(10)}{A(8) \cdot A(4)^2 \text{ CONC}(4)} = 1.0 \quad (\text{A.1-4})$$



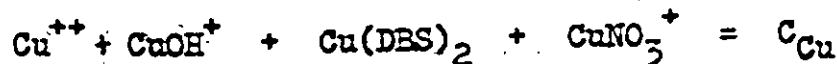
$$\frac{A(7)}{A(1) \cdot A(6) \text{ CONC}(5)} = 1.0 \quad (\text{A.1-5})$$



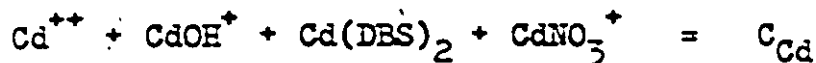
$$\frac{A(11)}{A(8) \cdot A(6) \text{ CONC}(6)} = 1.0 \quad (\text{A.1-6})$$



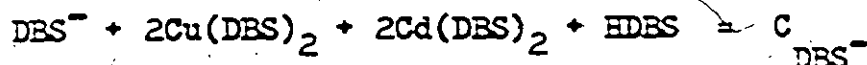
$$\frac{A(4) [\text{H}^+]}{A(5) \text{ CONC}(7)} = 1.0 \quad (\text{A.1-7})$$



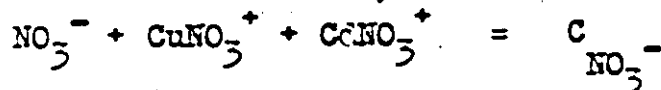
$$\frac{A(1) + A(2) + A(3) + A(7)}{\text{CONC}(8)} = 1.0 \quad (\text{A.1-8})$$



$$\frac{A(8) + A(9) + A(10) + A(11)}{\text{CONC}(9)} = 1.0 \quad (\text{A.1-9})$$



$$\frac{A(4) + 2A(5) + 2A(10) + A(5)}{\text{CONC}(10)} = 1.0 \quad (\text{A.1-10})$$



$$\frac{A(6) + A(7) + A(11)}{\text{CONC}(11)} = 1.0 \quad (\text{A.1-11})$$

Manipulating above equations, a set of equations for the use of the Regula-falsi iterative process is obtained as follows :

$$A(2)^{F+1} = \frac{1}{2} A(2)^F \left[ 1.0 + A(1) \text{CONC}(1)/A(2)[\text{H}^+] \right]^F \quad (\text{A.1-12})$$

$$A(9)^{r+1} = \frac{1}{2} A(9)^r [1.0 + A(8) \text{ CONC}(2)/A(9) [H^+]]^r \quad (\text{A.1-13})$$

$$A(3)^{r+1} = \frac{1}{2} A(3)^r [1.0 + A(1) A(4)^2 \text{ CONC}(3)/A(3)]^r \quad (\text{A.1-14})$$

$$A(10)^{r+1} = \frac{1}{2} A(10)^r [1.0 + A(8) A(4)^2 \text{ CONC}(4)/A(10)]^r \quad (\text{A.1-15})$$

$$A(7)^{r+1} = \frac{1}{2} A(7)^r [1.0 + A(1) A(6) \text{ CONC}(5)/A(7)]^r \quad (\text{A.1-16})$$

$$A(11)^{r+1} = \frac{1}{2} A(11)^r [1.0 + A(8) A(6) \text{ CONC}(6)/A(11)]^r \quad (\text{A.1-17})$$

$$A(4)^{r+1} = \frac{1}{2} A(4)^r [1.0 + A(5) \text{ CONC}(7)/A(4) [H^+]]^r \quad (\text{A.1-18})$$

$$A(1)^{r+1} = \frac{1}{2} A(1)^r [1.0 + \text{CONC}(8)/(A(1)+A(2)+A(3)+A(7))]^r \quad (\text{A.1-19})$$

$$A(8)^{r+1} = \frac{1}{2} A(8)^r [1.0 + \text{CONC}(9)/(A(8)+A(9)+A(10)+A(11))]^r \quad (\text{A.1-20})$$

$$A(5)^{r+1} = \frac{1}{2} A(5)^r [1.0 + \text{CONC}(10)/(A(4)+2A(3)+2A(10)+A(5))]^r \quad (\text{A.1-21})$$

and

$$A(6)^{r+1} = \frac{1}{2} A(6)^r [1.0 + \text{CONC}(11)/(A(6)+A(7)+A(11))]^r \quad (\text{A.1-22})$$

APPENDIX A.2

Derivation of Equation (3.7)

Consider a monobasic acid reaction  $HA \rightleftharpoons H^+ + A^-$ , and the two conjugate forms, HA and  $A^-$ , coexist in the solution. According to the Beer's law, the optical density of the solution can be expressed as :

$$OD = l \epsilon_n C_n \quad (A.2-1)$$

where  $\epsilon_n$  is the extinction coefficient of the mixture, a characteristic intensive factor of the absorbing species, and  $C_n$  is the sum of the concentrations of the light absorbing species and is equal to

$$C_n = C_{A^-} + C_{HA} \quad (A.2-2)$$

And if, as seems generally to be the case, each substance absorbs independently of the presence of the other, then the optical density is equal to

$$OD = ( \epsilon_r C_{A^-} + \epsilon_s C_{HA} ) l \quad (A.2-3)$$

where  $\epsilon_r$  is the extinction coefficient of species  $A^-$  and

$\epsilon_{\beta}$  is that of species HA. From above three equations, it follows that

$$\frac{C_{HA}}{C_{A^{-}}} = \frac{\epsilon_{\gamma} - \epsilon_{\alpha}}{\epsilon_{\alpha} - \epsilon_{\beta}} \quad (\text{A.2-4})$$

By combination of equation (A.2-4) with the common expression of the reaction

$$k_c = \frac{a_{\alpha} C_{A^{-}}}{C_{HA}} \quad (\text{A.2-5})$$

the following general equation is then derived.

$$a_{\alpha} \epsilon_{\alpha} \left( \frac{1}{k_c} \right) - a_{\alpha} \left( \frac{\epsilon_{\beta}}{k_c} \right) - (\epsilon_{\gamma}) = -\epsilon_{\alpha} \quad (5.7)$$

APPENDIX A.3

Method of Continuous Variation

The formation of complex ion can be represented by the equation



in which A is a metallic ion and B is an anion. To determine n, solution of A and B of the same molar concentration, M, are mixed in varying proportions, and optical density of the resulting solutions is measured. Let the mixture be made by the addition of p liter of B to (1-p) liter of A ( p < 1 ), with no appreciable volume change on mixing. Let C<sub>1</sub>, C<sub>2</sub> and C<sub>3</sub> be the concentration of A, B and AB<sub>n</sub>, respectively. For the mixture - the following equations apply

$$C_1 = M(1-p) - C_3 \quad (A.3-1)$$

$$C_2 = Mp - nC_3 \quad (A.3-2)$$

$$C_1 C_2^n = K C_3 \quad (A.3-3)$$

The condition for a maximum in the curve of C<sub>3</sub> plotted against p is that

$$\frac{dC_3}{dp} = 0 \quad (A.3-4)$$

Differentiating equations (A.3-1), (A.3-2) and (A.3-3) with respect to  $p$ ,

$$C_1' = -M - C_3' \quad (\text{A.3-5})$$

$$C_2' = M - n C_3' \quad (\text{A.3-6})$$

$$C_2^n C_1' + C_1 n C_2^{n-1} C_2' = K C_3' \quad (\text{A.3-7})$$

and considering the equation (A.3-4), we obtain

$$C_1' = -M \quad (\text{A.3-8})$$

$$C_2' = M \quad (\text{A.3-9})$$

$$C_2 C_1' + n C_1 C_2' = 0 \quad (\text{A.3-10})$$

or

$$-C_2 M + n C_1 M = 0 \quad (\text{A.3-11})$$

Substituting the relation  $C_1 = C_2 / n$  into equation (A.3-1) and combining with equation (A.3-2), we immediately deduce the equation (A.3-12).

$$n = \frac{p}{1-p} \quad (\text{A.3-12})$$

APPENDIX A.4

Derivation of Equation (3.34)

The identity

$$\frac{1}{2} \frac{d}{d\phi} \left( \frac{d\phi}{dx} \right)^2 = \frac{d^2\phi}{dx^2} \quad (3.35)$$

can be used in the differential equation (3.32) to give

$$\frac{d}{d\phi} \left( \frac{d\phi}{dx} \right)^2 = -\frac{8\pi}{\epsilon} \sum_1 n_1^0 z_1 e_0 \exp(-z_1 e_0 \phi / kT) \quad (A.4-1)$$

which can be integrated to give

$$\begin{aligned} \left( \frac{d\phi}{dx} \right)^2 &= -\frac{8\pi}{\epsilon} \int \sum_1 n_1^0 z_1 e_0 \exp(-z_1 e_0 \phi / kT) d\phi \\ &= \frac{8\pi kT}{\epsilon} \sum_1 n_1^0 \exp(-z_1 e_0 \phi / kT) + C \quad (A.4-2) \end{aligned}$$

The integration constant C can be evaluated by considering that, deep in the bulk of the solution, i.e., at  $x \rightarrow \infty$ , not only is the volta potential zero,  $\phi_{x \rightarrow \infty} = 0$ , but the field  $d\phi / dx$  is also zero. Under these conditions,



$$C = -\frac{8\pi kT}{\epsilon} \sum_1 n_1^0 \quad (\text{A.4-3})$$

By introducing this value of the integration constant into equation (A.4-2), the result is

$$\left(\frac{d\phi}{dx}\right)^2 = \frac{8\pi kT}{\epsilon} \sum_1 n_1^0 [\exp(-z_1 e_0 \phi / kT) - 1] \quad (\text{A.4-4})$$

or

$$\frac{d\phi}{dx} = \pm \left(\frac{8\pi kT}{\epsilon}\right)^{\frac{1}{2}} \left[\sum_1 n_1^0 (v^{z_1} - 1)\right]^{\frac{1}{2}} \quad (3.34)$$

APPENDIX A.5

Derivation of Equation (3.42)

Equation (3.38) shows that

$$\alpha = - \left( \frac{kT \epsilon}{2 \pi} \right)^{\frac{1}{2}} \left[ \sum_i n_i^0 \left( e^{-z_i e_0 \phi / kT} - 1 \right) \right]^{\frac{1}{2}}$$

Consider a z-z electrolyte, and

$$\begin{aligned} \alpha &= - \left( \frac{kT \epsilon}{2 \pi} \right)^{\frac{1}{2}} \left[ n_1^0 \left( e^{z e_0 \phi / kT} - 1 + e^{-z e_0 \phi / kT} - 1 \right) \right]^{\frac{1}{2}} \\ &= - \left( \frac{kT \epsilon}{2 \pi} \right)^{\frac{1}{2}} \left[ n_1^0 \left[ e^{z e_0 \phi / kT} - 2 \left( e^{z e_0 \phi / 2kT} \right) \right. \right. \\ &\quad \left. \left. \left( e^{-z e_0 \phi / 2kT} \right) + e^{-z e_0 \phi / kT} \right] \right]^{\frac{1}{2}} \\ &= - \left( \frac{kT \epsilon n_1^0}{2 \pi} \right)^{\frac{1}{2}} \left( e^{z e_0 \phi / 2kT} - e^{-z e_0 \phi / 2kT} \right) \end{aligned} \quad (A.5-1)$$

Since

$$e^{+x} - e^{-x} = 2 \sinh x$$

equation (A.5-1) then becomes

$$\alpha = - 2 \left( \frac{kT \epsilon n_1^0}{2 \pi} \right)^{\frac{1}{2}} \sinh \left( \frac{z e_0 \phi}{2kT} \right) \quad (A.5-2)$$

At  $z = z_0$

$$\alpha_M = - \alpha = \left( \frac{2kT \epsilon n_1^0}{\pi} \right)^{\frac{1}{2}} \sinh \left( \frac{z e_0 \phi}{2kT} \right) \quad (3.42)$$

APPENDIX A.6

Derivation of Equation (3.44)

From equation (3.43), we know that

$$\begin{aligned} \left(\frac{d\phi}{dx}\right)_{x_0} &= - \left(\frac{2kT}{ze_0}\right) K \sinh\left(\frac{ze_0\phi}{2kT}\right) \\ &= -\frac{K}{a} \sinh(a\phi) \end{aligned} \quad (\text{A.6-1})$$

where  $a = ze_0 / 2kT$ . By integration with the boundary conditions  $x = x_0'$ ,  $\phi = \phi_0'$ ;  $x = x_0''$ ,  $\phi = \phi_0''$ , we have

$$\int_{\phi_0'}^{\phi_0''} \frac{d\phi}{\sinh(a\phi)} = - \int_{x_0'}^{x_0''} \left(\frac{K}{a}\right) dx \quad (\text{A.6-2})$$

$$\frac{1}{a} \ln \left[ \tanh\left(\frac{a\phi}{2}\right) \right]_{\phi_0'}^{\phi_0''} = -\frac{K}{a} (x_0'' - x_0') \quad (\text{A.6-3})$$

$$\ln \left[ \frac{\tanh\left(\frac{a\phi_0'}{2}\right)}{\tanh\left(\frac{a\phi_0''}{2}\right)} \right] = K (x_0'' - x_0') \quad (\text{A.6-4})$$

or

$$\tanh\left(\frac{ze_0\phi_0'}{4kT}\right) = \exp\left[K(x_0'' - x_0')\right] \tanh\left(\frac{ze_0\phi_0''}{4kT}\right) \quad (\text{3.44})$$

APPENDIX A.7

Determination of the Effective Radii of Hydrated Ions

It has been shown by Brull ( 70 ) that the  $a_1$  parameter of the Debye-Huckel formula may be regarded as the effective diameter of the hydrated ion. It was also concluded that the  $a_1$  parameter has no definite physical significance and is only empirical corrective coefficient to make theoretical results conform to experimental data. On the other hand, the  $a_1$  parameter of the theory of Bonino ( 71 ) has an unquestionable physical significance, both because on a basis of this physical significance the parameter can be calculated from the fundamental physical constants of the ions, i.e., the true radius and the deformability, and because the same physical significance makes it possible to deduce the parameter from other experiments, e.g., mobility measurements. The expression proposed by Bonino was written as :

$$\frac{10^8 a_1}{z_1} = 0.9 ( 10^8 r_1 / 10^{24} \alpha_1 ) + 2 \quad (\text{A.7-1})$$

where  $z_1$  is ionic valence,  $r_1$  is effective ionic radius, and  $\alpha_1$  is the deformability. From the ionic mobilities,  $a_1$  can be calculated from the equation

$$10^8 a_1 = 182 z_1 / u \quad (\text{A.7-2})$$

where  $l_{\infty}$  is the equivalent conductivity limit, or its empirical modification given by Brull ( 72 )

$$10^8 a_1 = 216 z_1^{1/2} / l_{\infty} \quad (\text{A.7-3})$$

One can also determine the chemical hydration number by the entropy deficiency method ( 73,74 ) and calculate  $a_1$  from this and effective radius of the ion. The results has been partly revised, using the recent entropy values of aqueous ions, by Kielland ( 62 ) and the values of effective radii of hydrated ions from this work were used in this study.

APPENDIX B

TABLES OF EXPERIMENTAL AND CALCULATED DATA AND

SAMPLE CALCULATION

Table B-1. Spectrophotometric Analysis for the Determination of  $k_p$  of Cu-NaDBS System.

$\log[\text{Cu}^{++}]_{\text{uncomplexed}}$	$\log[\text{Cu}(\text{DBS})_2] / [\text{DBS}^-]^2$
- 2.060	- 3.415
- 1.796	- 3.157
- 1.656	- 2.996
- 1.606	- 2.949
- 1.564	- 2.882

Table B-2. Spectrophotometric Analysis for the Determination of  $k_b$  of Pb-NaDBS System.

$\log[\text{Pb}^{++}]_{\text{uncomplexed}}$	$\log[\text{Pb}(\text{DBS})_2] / [\text{DBS}^-]^2$
- 2.643	- 3.778
- 2.360	- 3.390
- 2.083	- 3.081
- 1.932	- 2.875
- 1.869	- 2.856



Table B-5. Spectrophotometric Analysis for the Determination of  $k_p$  of Cd-NaDBS System.

$\log[\text{Cd}^{++}]_{\text{uncomplexed}}$	$\log[\text{Cd}(\text{DBS})_2] / [\text{DBS}^-]^2$
- 2.055	- 3.597
- 1.711	- 3.260
- 1.559	- 3.010
- 1.492	- 2.952
- 1.442	- 2.870
- 1.420	- 2.858

Table B-5. Spectrophotometric Measurements of HDBS Solution.

solution	transmittance			
	pH	300 mμ	320 mμ	340 mμ
1	1.910	0.389	0.630	0.772
2	3.820	0.378	0.613	0.763
3	5.945	0.360	0.600	0.754

[HDBS] =  $5.4 \times 10^{-5}$  M

Table B-6. Effect of pH on the Distribution Factor of  $\text{Cu}^{++}$  and  $\text{CuOH}^+$ .

Run No.	pH	$\text{DF}_{\text{Cu}^{++}}$ ( $10^3$ cm)	$\pm\text{DF}_{\text{Cu}^{++}}$ ( $10^3$ cm)	$\text{DF}_{\text{CuOH}^+}$ ( $10^3$ cm)	$\pm\text{DF}_{\text{CuOH}^+}$ ( $10^3$ cm)
31	5.877	0.916	0.036	0.259	0.012
32	4.728	0.806	0.032	1.420	0.055
33	4.141	0.800	0.032	1.610	0.062
34	3.357	0.802	0.032	0.963	0.038
35	2.167	0.613	0.025	0.560	0.023
36	2.467	0.793	0.032	0.763	0.031
37	1.470	0.244	0.011	0.227	0.011

[Cu] = 10 ppm

[NaDBS] = 0.50 gm/l.

Table B-7. Effect of Bulk Copper Concentration on the Distribution Factor of  $\text{Cu}^{++}$  and  $\text{CuOH}^+$  :

Run No.	$[\text{Cu}] \times 10^4$ (mole/l.)	$\text{DF}_{\text{Cu}^{++}}$ ( $10^3$ cm)	$\text{DF}_{\text{Cu}^{++}}$ ( $10^3$ cm)	$\text{DF}_{\text{CuOH}^+}$ ( $10^3$ cm)	$\text{DF}_{\text{CuOH}^+}$ ( $10^3$ cm)
32	1.574	0.806	0.032	1.420	0.055
38	2.361	0.556	0.023	0.664	0.027
39	3.935	0.333	0.015	0.624	0.025
40	0.787	1.500	0.059	2.230	0.086
41	0.472	2.240	0.086	4.070	0.155
42	0.157	3.120	0.119	51.900	1.200

pH =  $4.70 \pm 0.05$

$[\text{NaDBS}] = 0.50$  gm/l.

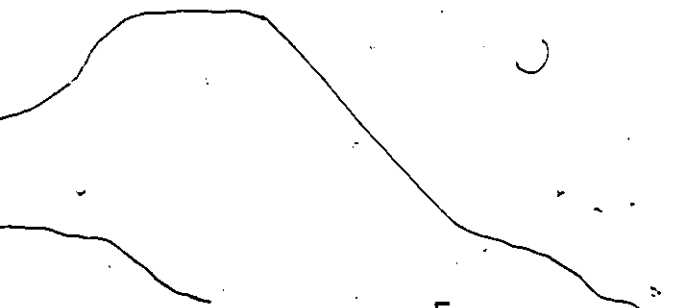
Table B-8. Effect of pH on the Distribution Factor of  $Pb^{++}$  and  $PbOH^+$ .

Run No.	pH	$DF_{Pb^{++}}$ ( $10^3$ cm)	$\pm DF_{Pb^{++}}$ ( $10^3$ cm)	$DF_{PbOH^+}$ ( $10^3$ cm)	$\pm DF_{PbOH^+}$ ( $10^3$ cm)
82	3.570	2.010	0.078	2.400	0.093
83	6.090	0.834	0.034	0.498	0.022
84	2.762	1.890	0.073	2.080	0.080
85	2.085	1.620	0.063	1.630	0.063
86	1.670	1.320	0.052	1.320	0.052
87	5.443	1.360	0.054	2.240	0.086
88	4.654	1.840	0.072	2.340	0.090
89	3.288	2.040	0.079	2.870	0.110
94	5.215	1.640	0.064	2.090	0.081

[Pb] = 10 ppm

[NaDBS] = 0.50 gm/l.

Table B-9. Effect of Bulk Lead Concentration on the Distribution Factor of  $Pb^{++}$  and  $PbOH^+$ .



Run No.	$[Pb] \times 10^5$ (mole/l.)	$DF_{Pb^{++}}$ ( $10^3$ cm)	$\frac{+DF_{Pb^{++}}}{-DF_{Pb^{++}}}$ ( $10^3$ cm)	$DF_{PbOH^+}$ ( $10^3$ cm)	$\frac{+DF_{PbOH^+}}{-DF_{PbOH^+}}$ ( $10^3$ cm)
90	2.664	2.650	0.102	3.340	0.128
91	1.158	3.490	0.133	4.600	0.175
92	7.480	1.110	0.044	1.500	0.059
93	12.310	0.699	0.029	0.832	0.034
94	4.826	1.640	0.064	2.090	0.081

pH =  $5.00 \pm 0.05$

$[NaDBS] = 0.50$  gm/l.

Table B-10. Effect of pH on the Distribution Factor of  $\text{Cd}^{++}$  and  $\text{CdOH}^+$ .

Run No.	pH	$\text{DF}_{\text{Cd}^{++}}$ ( $10^3$ cm)	$\frac{+}{-}\text{DF}_{\text{Cd}^{++}}$ ( $10^3$ cm)	$\text{DF}_{\text{CdOH}^+}$ ( $10^2$ cm)	$\frac{+}{-}\text{DF}_{\text{CdOH}^+}$ ( $10^2$ cm)
95	4.982	1.890	0.074	4.510	0.170
96	4.168	1.860	0.072	3.640	0.137
97	3.420	1.720	0.067	0.207	0.008
98	3.007	1.770	0.069	0.262	0.010
99	2.625	1.650	0.064	0.158	0.006
100	1.761	1.110	0.044	0.113	0.004
101	5.400	1.800	0.070	0.268	0.010
106	5.001	1.890	0.073	1.010	0.038

[Cd] = 10 ppm

[NaDBS] = 0.50 gm/l.

Table B-11. Effect of Bulk Cadmium Concentration on the Distribution Factor of  $\text{Cd}^{++}$  and  $\text{CdOH}^+$ .

Run No.	$[\text{Cd}] \times 10^4$ (mole/L.)	$\text{DF}_{\text{Cd}^{++}}$ ( $10^3$ cm)	$\pm\text{DF}_{\text{Cd}^{++}}$ ( $10^3$ cm)	$\text{DF}_{\text{CdOH}^+}$ ( $10^2$ cm)	$\pm\text{DF}_{\text{CdOH}^+}$ ( $10^2$ cm)
102	1.379	1.290	0.051	0.542	0.021
103	2.206	0.816	0.033	1.450	0.055
104	0.445	3.030	0.116	1.230	0.046
105	0.165	4.540	0.173	1.370	0.052
106	0.890	1.890	0.073	1.010	0.038

pH =  $5.00 \pm 0.05$

$[\text{NaDBS}] = 0.50$  gm/L.



Table B-12. Theoretical Prediction of Distribution Factors of  $\text{Cu}^{++}$  and  $\text{CuOH}^+$  vs. Bulk Concentration.

Run No.	$r_{\text{eff}}$ ( $10^8$ cm)	$DF_{\text{Cu}^{++}}$ ( $10^3$ cm)	$DF_{\text{CuOH}^+}$ ( $10^3$ cm)
32	6.8	1.575	2.025
	8.8*	0.990	1.352
38	6.8	1.098	1.463
	8.8*	0.717	1.016
39	6.8	0.728	0.957
	8.8*	0.496	0.687
40	6.8	2.532	3.325
	8.8*	1.487	2.109
41	6.8	3.633	4.732
	8.8*	2.020	2.864
42	6.8	6.737	9.118
	8.8*	3.318	5.067

\* effective radius of hydrated ion used in the normalization curve in figures 12 to 14.

Table B-13. Theoretical Prediction of Distribution Factors of  $\text{Cu}^{++}$  and  $\text{CuOH}^+$  vs. pH.

Run No.	$r_{\text{eff}}$ ( $10^8$ cm)	$\text{DF}_{\text{Cu}^{++}}$ ( $10^3$ cm)	$\text{DF}_{\text{CuOH}^+}$ ( $10^3$ cm)
31	6.8	2.623	2.776
	8.8*	1.591	1.710
32	6.8	1.575	2.025
	8.8*	0.990	1.352
33	6.8	1.169	2.033
	8.8*	0.742	1.442
34	6.8	0.858	2.969
	8.8*	0.548	2.261
35	6.8	0.506	8.601
	8.8*	0.325	6.918
36	6.8	0.607	6.412
	8.8*	0.389	5.108

\* as noted before

Table B-14. Theoretical Prediction of Distribution Factors of  $Pb^{++}$  and  $PbOH^+$  vs. pH .

Run No.	$r_{eff}$ ( $10^8$ cm)	$DF_{Pb^{++}}$ ( $10^3$ cm)	$DF_{PbOH^+}$ ( $10^3$ cm)
82	5.9	2.365	5.481
	11.7*	0.536	2.112
84	5.9	1.659	9.033
	11.7*	0.387	4.172
85	5.9	1.062	16.26
	11.7*	0.256	8.211
86	5.9	0.834	24.44
	11.7*	0.209	12.92
87	5.9	11.71	12.22
	11.7*	2.155	2.370
88	5.9	4.739	5.697
	11.7*	0.999	1.469
89	5.9	2.146	6.484
	11.7*	0.487	2.684
94	5.9	8.405	8.984
	11.7*	1.630	1.893

\* as noted before

Table B-15. Theoretical Prediction of Distribution Factors of  $Pb^{++}$  and  $PbOH^+$  vs. Bulk Concentration.

Run No.	$r_{eff}$ ( $10^8$ cm)	$DF_{Pb^{++}}$ ( $10^3$ cm)	$DF_{PbOH^+}$ ( $10^3$ cm)
90	5.9	12.62	13.60
	11.7*	2.075	2.493
91	5.9	25.65	27.46
	11.7*	3.234	3.919
92	5.9	5.468	5.878
	11.7*	1.213	1.411
93	5.9	3.313	3.594
	11.7*	0.850	0.995
94	5.9	8.405	8.984
	11.7*	1.630	1.893

\* as noted before

Table B-16. Theoretical Prediction of Distribution Factors of  $\text{Cd}^{++}$  and  $\text{CdOH}^+$  vs. pH.

Run No.	$r_{\text{eff}}$ ( $10^8$ cm)	$D_{\text{Cd}^{++}}^2$ ( $10^5$ cm)	$D_{\text{CdOH}^+}^2$ ( $10^5$ cm)
95	6.4	3.132	7.616
	8.6*	1.722	5.176
96	6.4	1.896	13.29
	8.6*	1.065	9.860
97	6.4	1.354	28.26
	8.6*	0.768	21.54
98	6.4	1.176	44.34
	8.6*	0.668	34.01
99	6.4	0.997	—
	8.6*	0.568	—
100	6.4	0.578	—
	8.6*	0.335	—
101	6.4	3.841	6.627
	8.6*	2.091	4.232
106	6.4	3.166	7.554
	8.6*	1.740	5.120

\* as noted before

Table B-17. Theoretical Prediction of Distribution Factors of  $\text{Cd}^{++}$  and  $\text{CdOH}^+$  vs. Bulk Concentration.

Run No.	$r_{\text{eff}}$ ( $10^8$ cm)	$DF_{\text{Cd}^{++}}$ ( $10^3$ cm)	$DF_{\text{CdOH}^+}$ ( $10^3$ cm)
102	6.4	2.234	5.133
	8.6*	1.293	3.567
103	6.4	1.394	3.801
	8.6*	0.855	2.777
104	6.4	5.830	12.66
	8.6*	2.920	8.017
105	6.4	11.96	26.01
	8.6*	5.216	15.22
106	6.4	3.166	7.554
	8.6*	1.740	5.120

\* as noted before

Table B-18. Experimental and Predicted Selectivity Coefficient of Cd-Cu-NaDBS System.

Run No.	$\frac{[Cd]}{[Cd]+[Cu]}$	$\frac{[Cd]}{[Cd]+[Cu]}^E$	$(\alpha_{Cd,Cu})_E$	$\frac{[Cd]}{[Cd]+[Cu]}^T$	$(\alpha_{Cd,Cu})_T$
107	0.113	0.150	1.370	0.121	1.073
108	0.210	0.245	1.217	0.222	1.072
109	0.310	0.360	1.247	0.326	1.072
110	0.410	0.499	1.425	0.428	1.071
111	0.512	0.552	1.168	0.530	1.071
112	0.580	0.664	1.430	0.597	1.072
113	0.683	0.738	1.303	0.700	1.072
114	0.783	0.838	1.430	0.796	1.072
115	0.783	0.838	1.430	0.796	1.072
116	0.312	0.366	1.267	0.328	1.072
117	0.512	0.575	1.284	0.530	1.071
118	0.683	0.740	1.317	0.700	1.072

pH =  $4.10 \pm 0.05$       [NaDBS] = 0.50 gm/l.



Table B-19. Experimental and Predicted Selectivity Coefficient of  
Pb-Cu-NaDBS System.

Run No.	$\frac{[Pb]}{[Pb]+[Cu]}$	$\left(\frac{[Pb]}{[Pb]+[Cu]}\right)_E$	$(\alpha_{Pb,Cu})_E$	$\left(\frac{[Pb]}{[Pb]+[Cu]}\right)_T$	$(\alpha_{Pb,Cu})_T$
121	0.804	0.844	1.324	0.836	1.254
122	0.661	0.748	1.527	0.709	1.253
123	0.492	0.580	1.436	0.546	1.251
124	0.304	0.368	1.338	0.352	1.251
125	0.174	0.193	1.146	0.207	1.251
126	0.304	0.337	1.170	0.352	1.251
127	0.492	0.586	1.470	0.546	1.251
128	0.661	0.749	1.539	0.708	1.253

pH = 4.10 ± 0.05

[NaDBS] = 0.50 gm/l.



Table B-21. Spectrophotometric Measurements of Cu-NaDBS System.

	wavelength, m $\mu$							[Cu]
	260	270	280	290	300	310	320	(10 <sup>2</sup> M)
TM	0.930	0.928	0.850	0.776	0.737	0.770	0.873	0.91
OD	0.0315	0.0232	0.0706	0.1102	0.1325	0.1135	0.0590	
TM	0.860	0.860	0.737	0.632	0.576	0.622	0.778	1.67
OD	0.0655	0.0655	0.1325	0.1993	0.2396	0.2062	0.1090	
TM	0.742	0.770	0.638	0.517	0.449	0.502	0.691	2.31
OD	0.1296	0.1135	0.1952	0.2865	0.3478	0.2993	0.1605	
TM	0.700	0.745	0.605	0.480	0.410	0.462	0.662	2.59
OD	0.1549	0.1278	0.2182	0.3188	0.3872	0.3354	0.1791	
TM	0.620	0.653	0.529	0.413	0.353	0.411	0.618	2.86
OD	0.2076	0.1851	0.2766	0.3840	0.4522	0.3862	0.2090	

[NaDBS] =  $1.436 \times 10^{-3}$  M

[HClO<sub>4</sub>] = 0.50 M

asymptotic limit at 300 m $\mu$  : OD = 0.495,  $\epsilon$  = 344.706



Table B-23. Spectrophotometric Measurements of Cd-NaDBS System.

	wavelength, mμ						[Cd]	
	260	270	280	290	300	310	320	(10 <sup>2</sup> M)
TM	1.000	0.975	0.878	0.790	0.741	0.770	0.870	0.91
OD	0.0000	0.0110	0.0565	0.1024	0.1302	0.1135	0.0605	
TM	1.000	0.920	0.733	0.598	0.522	0.570	0.740	2.00
OD	0.0000	0.0362	0.1349	0.2233	0.2823	0.2441	0.1308	
TM	0.726	0.658	0.498	0.375	0.314	0.362	0.545	2.86
OD	0.1391	0.1818	0.3028	0.4260	0.5031	0.4413	0.2636	
TM	0.638	0.573	0.415	0.301	0.250	0.296	0.477	3.34
OD	0.1952	0.2418	0.3819	0.5215	0.6021	0.5287	0.3215	
TM	0.600	0.533	0.365	0.253	0.202	0.243	0.413	3.75
OD	0.2219	0.2733	0.4377	0.5969	0.6946	0.6144	0.3840	
TM	0.600	0.533	0.360	0.245	0.193	0.235	0.412	3.94
OD	0.2219	0.2733	0.4437	0.6108	0.7144	0.6289	0.3851	

[NaDBS] =  $1.436 \times 10^{-3}$  M

[HClO<sub>4</sub>] = 0.50 M

asymptotic limit at 300 mμ : OD = 0.740 , ε = 515.3203

TABLE B-24 EXPERIMENTAL DATA OF CU - NADDS SYSTEM

RUN NO.    COLLECTION TIME, MIN    GAS RATE (HL/MIN)    WEIGHT OF FOAMATE, GH (NO./MIN)    BUBBLE RATE (PPH)    BULK CONC., PPM (GM/L.)    PHD    PPH

31	15.00	66.67	7.9975	2574.0	10.00	37.30	0.50	5.88	5.53
32	15.00	66.67	9.3619	2584.0	10.00	34.40	0.50	4.73	4.91
33	15.00	66.67	9.2615	2562.0	10.00	34.20	0.50	4.14	4.38
34	15.00	66.67	8.5090	2570.0	10.00	36.30	0.50	3.36	3.42
35	15.00	66.67	7.9508	2576.0	10.00	31.50	0.50	2.17	2.14
36	15.00	66.67	9.3149	2577.0	10.00	33.80	0.50	2.47	2.45
37	15.00	66.67	8.0907	2566.0	10.00	18.40	0.50	1.47	1.46
38	15.00	66.67	8.5854	2572.0	15.00	42.20	0.50	4.64	4.70
39	15.00	66.67	8.1556	2570.0	25.00	53.90	0.50	4.72	4.89
40	15.00	66.67	10.0553	2568.0	5.00	26.00	0.50	4.67	4.82
41	15.00	66.67	9.8426	2568.0	3.00	22.30	0.50	4.71	4.94
42	15.00	66.67	9.6792	2572.0	1.00	11.40	0.50	4.70	5.67

TABLE D-25. EXPERIMENTAL DATA OF PB - NADDS SYSTEM

RUN NO. COLLECTION TIME (MIN) GAS RATE (ML/MIN) HEIGHT OF FOAMATE, CM BUBBLE RATE (NO./MIN) BULK CONC. (PPH) FOAMATE CONC. (GM/L.) OBS. BULK PHB (PHF)

82	15.00	66.84	11.6690	3000.0	10.15	61.70	0.50	3.57	3.64
83	15.00	66.84	13.6603	3000.0	10.02	24.75	0.50	6.09	5.96
84	15.00	66.84	10.9722	3000.0	10.94	66.40	0.50	2.76	2.80
85	15.00	66.84	10.6523	3000.0	11.26	61.75	0.50	2.08	2.09
86	15.00	66.84	10.4904	3000.0	10.80	51.00	0.50	1.67	1.67
87	15.00	66.84	12.3855	3000.0	10.00	45.55	0.50	5.44	5.62
88	15.00	66.84	12.4258	3000.0	10.00	54.00	0.50	4.65	4.74
89	15.00	66.84	11.1780	3000.0	10.00	63.80	0.50	3.29	3.42
90	15.00	66.84	12.8853	3000.0	5.52	39.70	0.50	5.12	5.21
91	15.00	66.84	12.6593	3000.0	2.40	22.40	0.50	5.14	5.25
92	15.00	66.84	10.4464	3000.0	15.50	65.60	0.50	5.22	5.32
93	15.00	66.84	11.3092	3000.0	25.50	72.50	0.50	5.20	5.25
94	15.00	66.84	12.4437	3000.0	10.00	50.00	0.50	5.21	5.30

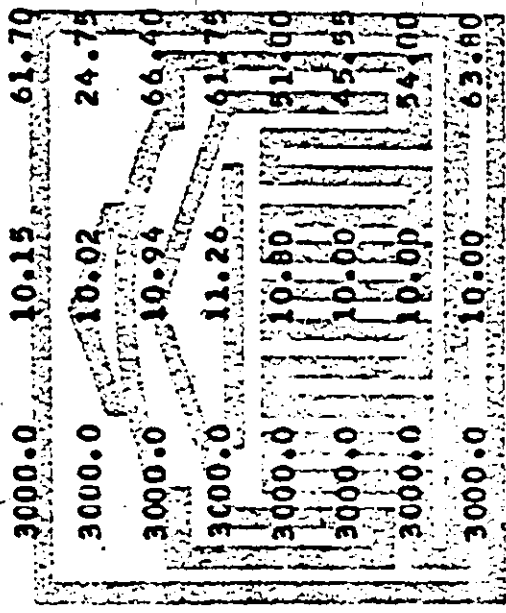


TABLE B-26. EXPERIMENTAL DATA OF CD - NADBS SYSTEM

RUN NO. COLLECTION TIME, MIN GAS RATE (ML/MIN) HEIGHT OF FOAMATE, GH (NO./MIN) BUBBLE RATE (PPH) CONC., PPM DBS, BULK PHB PHF (GH/L.)

95	15.00	66.67	12.2066	3000.0	10.00	56.00	0.50	4.98	6.28
96	15.00	66.67	11.8948	3000.0	10.00	56.00	0.50	4.17	5.38
97	15.00	66.67	10.9960	3000.0	10.00	56.00	0.50	3.42	3.49
98	15.00	66.67	11.3177	3000.0	10.00	56.00	0.50	3.01	3.15
99	15.00	66.67	11.2782	3000.0	10.00	53.00	0.50	2.63	2.61
100	15.00	66.67	10.4837	3000.0	10.00	41.00	0.50	1.76	1.77
101	15.00	66.67	12.3328	3000.0	10.00	53.00	0.50	5.40	5.54
102	15.00	66.67	11.6560	3000.0	15.50	66.00	0.50	5.08	5.62
103	15.00	66.67	11.1566	3000.0	24.80	78.50	0.50	4.94	6.04
104	15.00	66.67	12.3931	3000.0	5.00	41.00	0.50	5.05	5.62
105	15.00	66.67	14.8411	3000.0	1.85	18.50	0.50	5.04	5.49
106	15.00	66.67	12.0862	3000.0	10.00	56.00	0.50	5.00	5.66

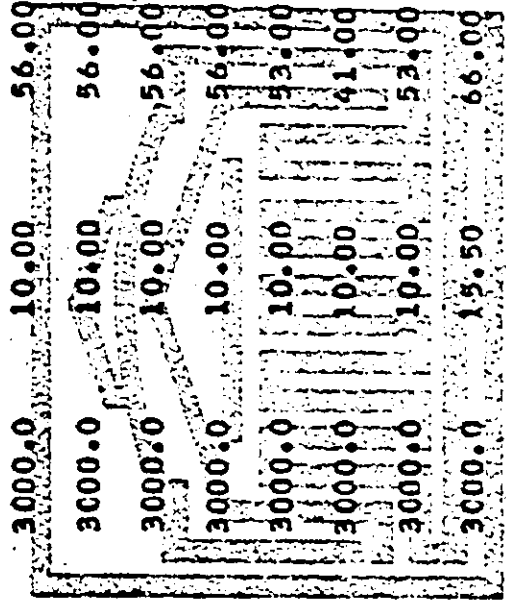


TABLE B-27. EXPERIMENTAL DATA OF CU - CD - NADDS SYSTEM

RUN NO.	COLLECTION TIME, MIN	GAS RATE (HL/HIN)	WEIGHT OF FOAMATE, GH	BUBBLE RATE (NO./MIN)	CUB MOLE/L X10**5	COB MOLE/L X10**5	CUF MOLE/L X10**5	MOLE/L X10**5	CDF MOLE/L X10**5	PHB GH/L	PHF
107	14.60	71.43	10.0540	2500.0	27.00	3.45	65.00	10.00	0.50	4.11	4.62
108	14.00	71.43	9.6750	2500.0	24.70	6.55	59.00	17.50	0.50	4.06	4.52
109	14.00	71.43	9.8559	2500.0	21.80	9.80	49.50	25.00	0.50	4.10	4.70
110	14.00	71.43	10.1882	2500.0	19.20	13.35	40.50	33.50	0.50	4.14	4.94
111	14.00	71.43	9.8853	2500.0	16.00	16.80	36.05	41.00	0.50	4.09	4.61
112	14.00	71.43	10.1380	2500.0	13.05	18.00	28.75	47.75	0.50	4.09	4.90
113	14.00	71.43	10.3970	2500.0	9.75	21.00	20.75	51.50	0.50	4.10	4.52
114	14.00	71.43	10.0770	2500.0	6.65	24.00	14.00	60.50	0.50	4.09	4.87
115	14.00	71.43	10.1130	2500.0	3.45	27.00	7.75	68.50	0.50	4.09	4.82
116	14.00	71.43	10.3393	2500.0	21.80	9.88	48.50	25.00	0.50	4.06	4.56
117	14.00	71.43	10.3672	2500.0	16.00	16.80	33.50	40.00	0.50	4.07	4.59
118	14.00	71.43	10.0663	2500.0	9.75	21.00	20.75	51.50	0.50	4.13	4.71



TABLE B-28, EXPERIMENTAL DATA OF CU - PB - NADBS SYSTEM

RUN NO.	COLLECTION TIME, MIN	GAS RATE (ML/MIN)	WEIGHT OF FOAMATE, GM	BUBBLE RATE (NO./MIN)	CUB MOLE/L X10**5	PBB MOLE/L X10**5	CUF MOLE/L X10**5	PBF MOLE/L X10**5	DBSD PHB GM/L	PHF
121	14.00	76.93	12.7070	1970.0	1.10	4.50	3.67	18.50	0.50	4.11 4.29
122	14.00	76.93	13.4953	1970.0	1.95	3.80	6.25	16.62	0.50	4.04 4.14
123	14.00	76.93	13.2930	1970.0	3.00	2.90	12.75	16.50	0.50	4.11 4.36
124	14.00	76.93	13.6617	1970.0	4.12	1.80	19.37	10.75	0.50	4.10 4.26
125	14.00	76.93	13.2550	1970.0	5.00	1.05	28.25	6.75	0.50	4.06 4.76
126	14.00	76.93	13.5868	1970.0	4.12	1.80	20.25	10.12	0.50	4.10 4.53
127	14.00	76.93	13.3338	1970.0	3.00	2.90	12.50	16.50	0.50	4.10 4.48
128	14.00	76.93	13.1250	1970.0	1.95	3.80	6.30	16.95	0.50	4.13 4.51

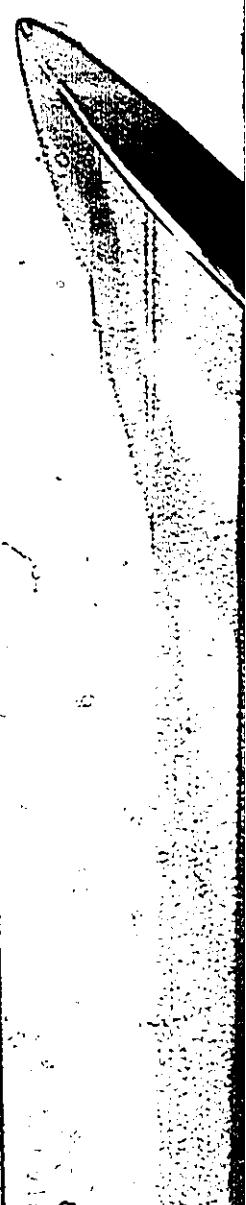
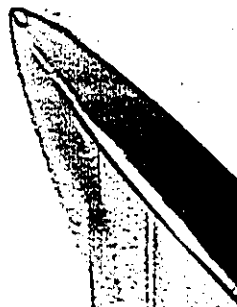


TABLE B-29. EXPERIMENTAL DATA OF CD - PB - NADBS SYSTEM

RUN NO.	COLLECTION TIME, MIN	GAS RATE (ML/MIN)	WEIGHT OF FOAMATE, GM	BUBBLE RATE (NO./MIN)	CD8 MOLE/L X10**5	PBB MOLE/L X10**5	CDF MOLE/L X10**5	PDF MOLE/L X10**5	DBS8 PH8 GM/L	PHF
129	14.00	76.93	12.9634	1970.0	0.95	4.50	3.67	19.00	0.50	4.13 4.38
130	14.00	76.93	13.5861	1970.0	3.11	2.80	13.00	13.87	0.50	4.13 4.31
131	14.00	76.93	12.8742	1970.0	1.97	3.80	7.50	17.50	0.50	4.12 4.46
132	14.00	76.93	13.5617	1970.0	4.27	1.80	21.25	11.37	0.50	4.15 4.38
133	14.00	76.93	13.4769	1970.0	4.90	1.05	31.12	7.62	0.50	4.13 4.66
134	14.00	76.93	13.3989	1970.0	1.97	3.80	7.77	20.75	0.50	4.12 4.83
135	14.00	76.93	13.7335	1970.0	3.11	2.70	13.75	15.50	0.50	4.15 4.33
136	14.00	76.93	13.5915	1970.0	4.27	1.80	21.25	13.50	0.50	4.10 4.71



PSHE POTYAM  
SHERPORMS



Sample Calculation of the Predicted Value of Distribution Factor  
in Figures 10, 13 and 16.

Runs 96, 102 and 109, representing one point in each of figures 10, 13 and 16, are chosen for the sample calculation of cadmium ion. The following constants were used for all the calculations.

- XK - Boltzmann constant.  $1.38 \times 10^{-16}$  erg/molecule. °K
- XT - Absolute temperature. 298 °K
- XA - Dielectric constant of water. 81
- XE - Electronic charge,  $4.803 \times 10^{-10}$  esu
- XN - Avogadro number.  $6.023 \times 10^{23}$  molecules/g-mole
- XG - Surface excess of NaDBS.  $3.10 \times 10^{-10}$  moles/cm<sup>2</sup>

Step 1 Solve for equilibrium concentration of all ions in the solution.

From the known equilibrium constants of the reactions and the total amount of metal ions and surfactant used, the equilibrium concentration of all ions in the solution were calculated from the equilibrium model. The results are presented in table B-30.

Step 2 Solve for surface potential of the smallest ion in the solution.

Based on the above equilibrium concentration and equation (3.38) and (3.39), the surface potential of Na<sup>+</sup> was calculated. The values are tabulated in table B-31 as  $V_{Na^+}$ .

Step 3 Solve for the surface potential for other metal ions:

Since we are only interested in the separation of metal ions, the surface potential of other larger size of metal ions were calculated based on equation (3.44). The results are shown in table B-31 as  $V_{Cd^{++}}$  and  $V_{Cu^{++}}$ . The term  $(kT\epsilon / 8\pi e_0^2) = 758.1$

Step 4 Integrate for the distribution factor.

The distribution factor of cadmium ion was calculated by using the value of its surface potential, the equilibrium composition of all ions and equation (3.45). For the smaller metal ion, equation

(3.46) was used. The results are presented in table B-31 as DTF  $\text{Cd}^{++}$ . Since the surface excesses of cadmium and copper ions are needed in figure 16, they are calculated and shown as

$$\Gamma_{\text{Cd}^{++}} \quad \text{and} \quad \Gamma_{\text{Cu}^{++}}$$

Table B-30. Equilibrium Concentration of all ions in the solution.

Run	$Cd^{++}$	$CdOH^+$	$DBS^-$	$Na^+$	HDBS	$H^+$	$NO_3^-$	$CdNO_3^+$
96	$8.894 \times 10^{-5}$	$5.978 \times 10^{-9}$	$9.758 \times 10^{-4}$	$1.436 \times 10^{-3}$	$4.602 \times 10^{-4}$	$6.792 \times 10^{-5}$	$2.374 \times 10^{-4}$	$1.565 \times 10^{-8}$
102	$1.378 \times 10^{-4}$	$7.597 \times 10^{-8}$	$1.358 \times 10^{-3}$	$1.436 \times 10^{-3}$	$7.800 \times 10^{-5}$	$8.279 \times 10^{-6}$	$2.046 \times 10^{-4}$	$2.090 \times 10^{-8}$

Run 109

$Cu^{++} = 2.171 \times 10^{-4}$      $Cd^{++} = 9.796 \times 10^{-5}$      $CuOH^+ = 9.291 \times 10^{-7}$      $Na^+ = 1.436 \times 10^{-3}$

$CdOH^+ = 5.630 \times 10^{-9}$      $H^+ = 7.943 \times 10^{-5}$      $NO_3^- = 4.769 \times 10^{-4}$      $CuNO_3^+ = 4.387 \times 10^{-24}$

$DBS^- = 9.255 \times 10^{-4}$      $CdNO_3^+ = 3.463 \times 10^{-8}$

Table B-3L Sample Calculation. [NaDBS] = 0.50 gm/L

figure no.	10	13	16
Run no.	96	102	109
[Cd] (Cu)	10 ppm	$1.379 \times 10^{-4} M$	$9.80 \times 10^{-5} M$ ( $2.18 \times 10^{-5} M$ )
V <sub>Na<sup>+</sup></sub>	523.7	422.3	280.3
V <sub>Cd<sup>++</sup></sub> (V <sub>Cu<sup>++</sup></sub> )	18.48	13.79	14.26 (13.78)
DTF <sub>Cd<sup>++</sup></sub> (DTF <sub>Cu<sup>++</sup></sub> )	$1.892 \times 10^{-3}$	$1.290 \times 10^{-3}$	$7.540 \times 10^{-4}$ ( $7.035 \times 10^{-4}$ )
$\Gamma_{Cd^{++}}$ ( $\Gamma_{Cu^{++}}$ )	---	---	$0.739 \times 10^{-10}$ ( $1.527 \times 10^{-10}$ )
X <sub>Cd<sup>++</sup></sub> (X <sub>Cu<sup>++</sup></sub> ) (cm)	$6.40 \times 10^{-8}$	$8.60 \times 10^{-8}$	$6.40 \times 10^{-8}$ ( $6.80 \times 10^{-8}$ )
pH	4.168	5.00	4.10

APPENDIX C

Two computer programs for the calculation of distribution factor are presented here separately; one is for the system containing one metal ion, the other is for that containing two metal ions. The notation and the method of use are interpreted as the comment in the computer program.

PURPOSE OF THIS PROGRAM  
CALCULATES THE THEORETICAL AND EXPERIMENTAL VALUES OF DISTRIBUTION  
FACTOR OF IONS FOR THE SYSTEMS CONTAINING ONE METAL ION.  
THE INDEPENDENT VARIABLES ARE THE PH AND TOTAL METAL CONC.  
THE THEORETICAL BACKGROUND IS BASED ON THE GILY-CHAPMAN DIFFUSE  
DOUBLE LAYER THEORY.

DESCRIPTION OF PARAMETERS

PH : PH OF THE SOLUTION FCAPED, PRESET VALUE  
Z : VALANCE OF SPECIES I IN THE SOLUTION  
B : CORRELATED CONSTANTS FOR THE AMOUNT OF HNO3 VS PH  
XK, XT, XA, XE, XN AND XG : BOLTZMANN CONSTANT, ABSOLUTE TEMPERATURE,  
DIELECTRIC CONSTANT, ELECTRONIC CHARGE, AVERAGE NUMBER AND  
SURFACE EXCESS OF SURFACTANT, NADDS.  
CONC : EQUILIBRIUM CONSTANTS FOR THE SIMULTANEOUS EQUATIONS  
GOVERNING THE EQUILIBRIUM RELATION IN THE SOLUTION.  
X1 TO X3 : EFFECTIVE RADII OF SPECIES I IN THE SOLUTION  
DTF1 TO DTF5 : DISTRIBUTION FACTOR OF SPECIES I IN THE SOLUTION.

METHOD OF USE

1. THEORETICAL PART :  
READ IN ALL THE CONSTANTS & CONDITIONS PRESET THEN COMPUTER  
WILL AUTOMATICALLY CALCULATE SURFACE POTENTIAL OF SPECIES  
IN THE SOLUTION. THE DISTRIBUTION FACTOR IS CALCULATED FROM  
THE INTEGRATION OF EQUATION USING THE SURFACE POTENTIAL AS  
THE LOWER LIMIT.

2. EXPERIMENTAL PART  
CALL SUBROUTINE LTK RIGHT AFTER ALL THE EXPERIMENTAL DATA  
ARE READ IN TO GIVE ALL THE RESULTS ANTICIPATED.

IMPLICIT REAL\*8(A-H,I,C-Y)  
DIMENSION SUBRAT(30),DTF2(10),CCN(10),KM(5),CC(10),SH(10),S(30),FI  
130),FL(30),G(30),GI(30),GB1(30),GB2(30),GF1(30),GF2(30),OBSB(30),D  
285F(30),CLB(30),CLF(30),PHF(30),PHR(30),WTF(30),GAS(30),TIME(30),C  
31A(30),SURFAS(30),ND(30),E(10),DTF1(10),A(10),B(10),C(10),H(30),AC  
4(10),PH(10),D(10),CCNC(9),V(15),CCBS(30)

0001  
0002

```

00C3      INTEGER, Z(20)
00C4      M=6
00C5      WM(1)=63.54
00C6      WM(2)=207.21
00C7      WM(3)=112.41
00C8      X4=4.7CCD-08
0009      READ(1,50) (Z(I),I=1,7)
0010      REAC(1,49) (PT(I),I=1,3)
0011      READ(1,49) (SH(I),I=1,6)
0012      READ(1,52) XK,XT,X6,XE,XN,XG
0013      READ(1,51) (CCN(I),I=1,M)
0014      DO 2 MK=1,3
0015      READ(1,50) II
0016      READ(1,51) CAA
0017      REAC(1,52) (B(I),I=1,7)
0018      REAC(1,51) (CCNC(I),I=1,7)
0019      DO 5 I=1,II
0020      READ(1,60) NO(I),PHB(I),PHF(I),TIME(I),CUB(I),GAS(I),HTF(I)
1, BUBRAT(II), CSEB(I), CSEF(I)
60 FORMAT(I3,2F5.3,F4.1,3F5.2,F7.4,F6.1,2010.3)
0021      DIA(I)=(6.*GAS(I))/(3.14159*5.*BUBRAT(I))*0.33333
0022      SURFAS(I)=5.*3.14159*BUBRAT(I)*DIA(I)*CIA(I)
0024      V(I)=HTF(I)/TIME(I)
0025      CUF(I)=CUF(I)/(WM(MK)*1.0D 03)
0026      CUB(I)=CUR(I)/(KM(MK)*1.0C 03)
0027      DO 61 N=1,II
0028      F(N)=1./10.**(PHB(N))
0029      FI(N)=1./10.**(PHF(N))
0030      G(N)=10.**(B(1)+B(2)+PHB(N)+B(3)+PHB(N)**2)
0031      GI(N)=10.**(B(1)+B(2)+PHF(N)+B(3)+PHF(N)**2)
0032      61 CONTINUE
0033      DO 62 N=1,II
0034      CCNC(1)=CUF(N)
0035      CONC(6)=CUB(N)+G(N)
0036      CALL EQUILB (Z,F,B,CONC,G,A,C,AC,N,1,PCT)
0037      GB1(N)=AC(1)
0038      GB2(N)=AC(2)
0039      CCNC(1)=CUF(N)

```

C  
C

```

CC40      CONC(6)=CUF(N)+G1(A)
CC41      CALL FCILBM (Z,F1,B,CONC,G1,A,C,AC,N,1,PCT)
CC42      GF1(A)=AC(1)
CC43      GF2(N)=AC(2)
CC44      62 CONTINUE
CC45      IF(MK-2) 15,16,17
CC46      15 WRITE(3,20)
CC47      GC TC 4
CC48      16 WRITE(3,21)
CC49      GO TO 4
CC50      17 WRITE(3,22)
CC51      4 CALL LIK(GB1,GB2,GF1,GF2,II,WTF,GAS,TIME,CIA,CUB,PH8,PFF,CUF,SURFA
        15,NO,CBSB,CBSF,CDBS)
        WRITE(3,40)
CC52      CALL RCH(V,GAS,UBBRAT,GD1,GF1,II,NC)
CC53      CALL RCF(V,GAS,UBBRAT,CB2,GF2,II,NC)
CC54      READ(1,52) X1,X2
CC55      WRITE(3,11) X1,X2,X4
CC56      WRITE(3,9)
CC57      YX1=X1
CC58      YX2=X2
CC59      DO 250 LL=1,11
CC60      WRITE(3,97)
CC61      CONC(1)=CUB(LL)
CC62      CONC(6)=CUB(LL)+G(LL)
CC63      CALL FCILBM (Z,F,B,CONC,G,A,C,AC,LL,MK,PCT)
CC64      CALL RCON (Z,AC,XK,XT,XA,XE,XN,XG,V114,YK1)
CC65      DO 3 LG=1,20
CC66      CALL WIKF (XK,XT,XE,X1,X2,X4,Z,V114,YK1,V111,V112)
CC67      CALL INTEG(Z,AC,XK,XT,XA,XE,XN,V111,P,TF,V111,1)
CC68      DTF1(LL)=TF*F
CC69      CALL INTEG(7,AC,XK,XT,XA,XE,XN,V111,P,TF,V112,2)
CC70      DTF2(LL)=TF*(P+2.*DSQRT(1./((1.0D-03*AC(2)*XN)))*(DSQRT(V112))-DSQRT(
        1/V111)))
CC71      WRITE(3,91) NC(LL),X1,DTF1(LL),DTF2(LL)
CC72      CLDX1=X1
CC73      IF(MK.EC.2) GC TC 101
CC74

```

C  
C







CCCC

SUBROUTINE FCILPM (Z,P,B,CCNC,C,A,C1AC,K1L,PCT)

CALCULATES THE EQUILIBRIUM CONCENTRATION OF THE EXISTING SPECIES IN THE SOLUTION BASED ON THE MODIFIED REGULA-FALSI POSITION METHOD.

A & AC : CONCENTRATION OF SPECIES IN THE SOLUTION.  
CONC : EQUILIBRIUM CONSTANT  
H : HYDROGEN CONCENTRATION

IMPLICIT REAL\*8(A-H,C-Y)  
DIMENSION A(10),B(10),C(10),H(30),AC(10),PH(10),D(10),CCNC(9)

INTEGER Z(20)

A(1)=1.00D-05

A(2)=1.00D-05

A(3)=1.00D-05

A(4)=1.00D-05

A(5)=1.00E-05

A(6)=1.00D-05

A(7)=1.00D-05

DC 300 J=1,100

A(2)=0.5\*A(2)\*((CCNC(3)\*A(1))/(A(2)\*H(K)))+1.0)

A(3)=0.5\*A(3)\*((CCNC(4)\*A(1)\*A(4)\*A(4)/A(3))+1.0)

A(4)=0.5\*A(4)\*((CCNC(5)\*A(5)/(H(K)\*A(4)))+1.0)

A(7)=0.5\*A(7)\*((CCNC(7)\*A(1)\*A(6)/A(7))+1.0)

A(6)=0.5\*A(6)\*((CCNC(6)/(A(6)+A(7)))+1.0)

A(1)=0.5\*A(1)\*((CCNC(1))/(A(1)+A(2)+A(3)+A(7)))+1.0)

A(5)=0.5\*A(5)\*((CCNC(2)/(A(4)+A(5)+2.\*A(3)))+1.0)

300 CONTINUE

C(1)=A(1)+A(2)+A(3)+A(7)

C(2)=A(4)+2.\*A(3)+A(5)

C(3)=A(2)\*H(K)/A(1)

C(4)=A(3)/(A(1)\*A(4)\*A(4))

C(5)=H(K)\*A(4)/A(5)

C(6)=A(6)+A(7)

C(7)=A(7)/(A(1)+A(6))

AC(1)=A(1)

AC(2)=A(2)

CCCC

C  
C  
C  
CC20 AC(3)=2.\*A(3)+A(4)+A(5)  
CC21 AC(4)=CCNC(2)  
CC22 AC(5)=H(K)  
0033 AC(6)=A(6)  
CC24 AC(7)=A(7)  
CC25 AC(3)=A(4)  
0036 PCT=A(4)/CONC(2)  
0037 1 RETURN  
0038 END

COC1 SUBROUTINE RCOT (Z,AC,XK,XT,XE,XA,XG,VII<sup>4</sup>,YK1)

CCCC IMPLICIT REAL\*8(A-T,C-Y)  
CCCC DIMENSION AC(10)

CCCC INTEGER Z(20)

CCCC Z(3)=-Z(3)

CCCC Z(6)=-Z(6)

CCCC YK=8.\*3.14159\*Z(4)\*Z(4)\*XE\*XE\*1.0D-03\*ZN\*AC(4)/(XA\*YK\*XT)

CCCC YK1=DSQRT(YK)

CCCC H=1

CCCC TT1=XE\*XC\*ZN

CCCC TT=XK\*XT\*XA\*ZN\*1.0D 00/(2.\*3.14159)

CCCC V1=15.0

CCCC V2=100.0

CCCC SUM1=0.0

CCCC SUM2=0.0

CCCC DO 10 N=1,7

CCCC SUM1=SUM1+AC(N)\*(V1\*\*Z(N)-1.0C)\*1.0D-03

CCCC SUM2=SUM2+AC(N)\*(V2\*\*Z(N)-1.0C)\*1.0D-03

CCCC T1=DSQRT(TT\*SUM1)

CCCC T2=DSQRT(TT\*SUM2)

CCCC F1=T1-TT1

CCCC F2=T2-TT1

CCCC FF=F1\*F2

CCCC IF(FF) 12,13,13

CCCC V2=V2+50.

CCCC IF(H.GT. 500) GO TO 19

CCCC M=M+1

CCCC GO TO 5

CCCC 12 M=1

CCCC 11 Y=(V2-V1)\*CABS(F1)/(CABS(F1)+LEPS(F2))

CCCC V3=V1+Y

CCCC SUM3=0.0

CCCC DO 14 N=1,7

CCCC SUM3=SUM3+AC(N)\*(V3\*\*Z(N)-1.0C)\*1.0D-03

CCCC T3=DSQRT(TT\*SUM3)

CCCC F3=T3-TT1

C  
C  
C

```

0037 AA1=DAOS(Y/V3)
0038 IF(AA1 .LE. 1.0C-06) GO TO 15
0039 FF=FI*F3
0040 IF(FF) 16,15,17
0041 16 V2=V3
0042 SUM2=0.0
0043 DO 8 N=1,7
0044 8 SUM2=SUM2+AC(N)**(V2**Z(N)-1.0)*1.0C-03
0045 18 M=M+1
0046 IF(M .GT. 558) GO TO 19
0047 GO TO 11
0048 17 V1=V3
0049 SUM1=0.0
0050 DO 7 N=1,7
0051 7 SUM1=SUM1+AC(N)**(V1**Z(N)-1.0)*1.00-03
0052 GO TO 18
0053 19 WRITE(3,47) M
0054 47 FORMAT(5X, ' NO CONVERGENCY, NUMBER OF ITERATION = ',15)
0055 GO TO 1
0056 15 V114=V3
0057 Z(3)=-Z(3)
0058 Z(6)=-Z(6)
0059 1 RETURN
0060 END

```

CCCC1 SUBROUTINE INTEG (Z, AC, XK, XT, XA, XF, XN, V222, P, TF, V333, KK)

0002 IMPLICIT REAL\*8(A-F, O-Y)  
CCCC3 DIMENSION AC(10), U(5000), C(5000)

0004 INTEGER Z(20)  
0005 Z(3)=-Z(3)  
CCCC6 Z(6)=-Z(6)

0007 L=1  
0008 U(1)=1.0001  
CCCC5 DV=(V222-U(1))\*4.00E-03

0010 26 W1=0.0  
0011 DO 30 N=1,7  
0012 30 W1=W1+AC(N)\*(U(1)+Z(N)-1.)\*1.00E-03

0013 IF(W1) 10,10,11  
0014 10 WRITE(3,9) W1  
0015 9 FORMAT(5X, ' THE VALUE OF W1 = ', D12.5)

0016 W1=-W1  
0017 11 W1=DSQRT(W1)  
0018 Q(L)=(V233\*\*Z(KK)-1.0)/(U(1)+W1)

0019 IF(U(1).GE.V222) GO TO 40  
0020 UCL=U(1)  
0021 L=L+1

0022 U(1)=UOLD+DV  
0023 GO TO 36  
0024 40 CALL GSF (DV, C, L, L)

0025 P=U(L)  
0026 1 P=F/DSQRT(XN)  
0027 TF=(XK\*XT\*XA)/(E\*\*3.14159\*XE\*XE)

0028 TF=DSQRT(TF)  
0029 Z(3)=-Z(3)  
0030 Z(6)=-Z(6)

0031 RETURN  
0032 END

SUBROUTINE MIKE (XK,XT,XE,XI,X2,X4,Z,V114,YK1,V111,V112)

```
CCCC2 IMPLICIT REAL*8(A-F,O-Y)
CCCC3 INTEGR Z(20)
CCCC4 FY4=-DLOG(V114)+XK*XT/XE
CCCC5 TN4=CTANR(Z(4)+XE*FY4/(4.*XK*XT))
CCCC6 TN1=TN4/DEXP(YK1+(X1-X4))
CCCC7 TN2=TN4/DEXP(YK1+(X2-X4))
CCCC8 FY=DLOG((1+TN1)/(1-TN1))/2.
CCCC9 FYY=DLOG((1+TN2)/(1-TN2))/2.
CCCC10 FY1=FY*4.*XK*XT/(Z(1)*XE)
CCCC11 FY2=FY*4.*XK*XT/(Z(2)*XE)
CCCC12 V111=DEXP(-XE*FY1/(XK*XT))
CCCC13 V112=DEXP(-XE*FY2/(XK*XT))
CCCC14 RETURN
CCCC15 END
```

CCCC SUBROUTINE QSF (M,Y,Z,ADIM)  
 CCCCC IMPLICIT REAL\*8(A-F,D-Z)  
 CCCCC DIMENSION Y(5000),Z(5000)

C C PARAMETERS JI-THE INCREMENT OF ARGUMENT VALUES, Y-THE INPUT VECTOR  
 C C OF FUNCTION VALUES, Z-THE RESULTING VECTOR OF INTEGRAL VALUES. Z  
 C C MAY BE IDENTICAL WITH Y

C C METHOD BEGINNING WITH Z(1)=0.0 EVALUATION OF VECTOR Z IS DONE  
 C C BY MEANS OF SIMPSONS RULE TOGETHER WITH NEWTONS 3/8 RULE OR A  
 C C COMBINATION OF THESE TWO RULES. TRUNCATION ERROR IS OF ORDER H\*\*5  
 C C ( I.E., FOURTH ORDER METHOD). ONLY IN CASE NDIM=3 TRUNCATION ERROR  
 C C OF Z(2) IS OF ORDER H\*\*4

CCCC NT=.3333333\*+  
 CCCCC IF (NDIM .EQ. 5) NT=.1  
 C C NDIM IS GREATER THAN 5. PREPARATION OF INTEGRATION LOOP

CCCC 1 SUM1=Y(2)+Y(2)  
 CCCCC SUM1=SUM1+SUM1  
 CCCCC SUM1=NT\*(Y(1)+SUM1+Y(3))  
 CCCCC AUX1=Y(4)+Y(4)  
 CCCCC AUX1=AUX1+AUX1  
 CCCCC AUX1=SUM1+NT\*(Y(3)+AUX1+Y(5))  
 CCCCC AUX2=NT\*(Y(1)+3\*.875\*(Y(2)+Y(5))+2.625\*(Y(3)+Y(4))+Y(6))  
 CCCCC SUM2=Y(5)+Y(5)  
 CCCCC SUM2=SUM2+SUM2  
 CCCCC SUM2=AUX2-NT\*(Y(4)+SUM2+Y(6))  
 CCCCC Z(1)=0.0  
 CCCCC AUX=Y(3)+Y(3)  
 CCCCC AUX=AUX+AUX  
 CCCCC Z(2)=SUM2-NT\*(Y(2)+AUX+Y(4))  
 CCCCC Z(3)=SUM1  
 CCCCC Z(4)=SUM2  
 CCCCC IF (NDIM.EQ. 5) Z(2)  
 C C INTEGRATION LOOP

CCCC 2 DO 4 I=7,NDIM+2  
 CCCCC SUM1=AUX1

CCCC C  
 CCCCC C  
 CCCCC C



```

0025 SUM2=LX2
0026 AUX1=Y(I-1)+Y(I-1)
0027 AUX1=ALX1+ALX1
0028 AUX1=SLP2+HT*(Y(I-2)+ALX1+Y(I))
0029 Z(I-2)=SUM1
0030 IF(I-NDIM) 3,6,6
0031 3 AUX2=Y(I)+Y(I)
0032 AUX2=AUX2+AUX2
0033 AUX2=SUP2+HT*(Y(I-1)+ALX2+Y(I+1))
0034 4 Z(I-1)=SUM2
0035 5 Z(NDIM-1)=AUX1
0036 Z(NDIM)=AUX2
0037 RETURN
0038 6 Z(NDIM-1)=SUP2
0039 Z(NDIM)=AUX1
0040 RETURN
C END OF INTEGRATION LOOP
C 7 IF(NDIM-3) 12,11,8
C NDIM IS EQUAL TO 4 OR 5
0041 8 SUM2=1.125*HT*(Y(I)+Y(2)+Y(2)+Y(2)+Y(3)+Y(3)+Y(3)+Y(4))
0042 SUM1=Y(2)+Y(2)
0043 SUM1=SUM1+SUM1
0044 SUM1=HT*(Y(1)+SUM1+Y(3))
0045 Z(I)=0.0
0046 AUX1=Y(3)+Y(3)
0047 AUX1=AUX1+ALX1
0048 Z(2)=SUP2-FT*(Y(2)+AUX1+Y(4))
0049 IF(NDIM-5) 10,9,9
0050 9 AUX1=Y(4)+Y(4)
0051 AUX1=ALX1+AUX1
0052 Z(5)=SUM1+FT*(Y(3)+AUX1+Y(5))
0053 10 Z(3)=SUM1
0054 Z(6)=SUP2
0055 RETURN
C NDIM IS EQUAL TO 3
0057 11 SUM1=HT*(1.25*Y(1)+Y(2)+Y(2)-C.25*Y(3))
0058 SUP2=Y(2)+Y(2)
C
C
C

```



```

0059 SUM2=SUM2+SUM2
0060 Z(3)=HT*(Y(1)+SUM2*(3))
0061 Z(1)=C.C
0062 Z(2)=SUM1
0063 -12 RETURN
0064 END

```

```

C
C
C
CCC1 SUBROUTINE LTK(CUF1, CUF2, CLF1, CUF2, I1, WTP, GAS, TIME, DIA, CUB, CFB, PPF
1, CUF, SURFAS, NO, CBSB, DSSF, GAMAG)
C CALCULATES THE DISTRIBUTION FACTOR CF SPECIES I FROM THE
C EXPERIMENTAL RESULTS.
C
CCC2 IMPLICIT REAL*8(A-F, C-Z)
CCC3 DIMENSION CGAS1(30), CGAS2(30), WTF(30), GAS(30), TIME(30), CUF1(30), CU
1D1(30), CUF2(30), CUB2(30), GAMA1(30), GAMAG2(30), DIA(30), SURFAS(30), CU
2FC(30), CUF(30), NC(30), ERRCR(30), CUF(30), CFI(30), PHF1(30), PHR(30), P
3HF(30), CBSR(30), DSSF(30), GAMAG3(30), GAMAG4(30), C1(30), D2(30), D3(30),
4D4(30)
C DO 84 N=1, 11
C SURFACE CONCENTRATION OF CU**
CGAS1(M)=WTF(M)*(CUF1(M)-CUB1(M))/(6.*1.0D03*GAS(M)*TIME(M))
C SURFACE CONCENTRATION CF CUCH*
CGAS2(M)=WTF(M)*(CUF2(M)-CUB2(M))/(6.*1.0D03*GAS(M)*TIME(M))
C GAMAG TO GAMAG : SURFACE EXCESS CF SPECIES I
GAMA1(M)=CGAS1(M)*DIA(M)
GAMA2(M)=CGAS2(M)*DIA(M)
C UFC(M)=CUB(M)+6.*1.0D03*(GAS(M)*(GAMA1(M)+GAMA2(M))*TIME(M)/(DIA(M)
1)*WTF(M))
ERRCR(M)=100.*(CUFC(M)-CUF(M))/CUF(M)
C THE OH- CCAC IN FCAPATE
DPH(M)=1.0D-14*(IC.*(PHB(M))+GAMA2(M)*TIME(M)*SURFAS(M)/1.0D03
DPF(M)=1.0E-14/DPH(M)
PHF1(M)=DLCGIC(CFH(M))
GAMA3(M)=WTF(M)*(CUF(M)-CUB(M))/(SURFAS(M)*TIME(M)*1.0D02)
GAMA4(M)=WTF(M)*(EPSF(M)-[CBSB(M)]/(SURFAS(M)*TIME(M)*1.0D03)
C D1 TO D5 : DISTRIBUTION FACTOR CF SPECIES I
D1(M)=GAMA1(M)*1.0D03/CUB1(M)
D2(M)=GAMA2(M)*1.0D03/CUB2(M)
D3(M)=GAMA3(M)*1.0D03/CUB(M)
D4(M)=GAMA4(M)*1.0D03/CBSB(M)
C6 CONTINUE
WRITE(3,90)
DC 88 N=1, 11
DC 88 WRITE(3,87) NC(M), CGAS1(M), CC6S2(M), GAMA1(M), GAMA2(M), GAMAG3(M), D1(
C
C
C

```



```

1M1, D2(M), D3(M), GAM/4(M), D4(M), FPROR(M), PFR(M), PHF(M), PHS(M)
67 FORMAT(14, 10C10.3, /F7.3)
5C FORMAT(///, ' RUN, 1X, 'CU++ GAS, 2X, 'CLCH+ GAS, 1X, 'GAMA CU++, 1X, '
1GAMA CUDT+, 1X, 'GAMA CUT, 1X, 'DSF CU++, 2X, 'DSF CUPH+, 1X, 'DSF CLT
2, 3X, 'GAMA DES, 3X, 'DSF CBS, 2X, 'DEV CUF, 2X, 'PHR, 3X, 'PF, 2X, 'CA
31. PHF, //)

```

```

CC26 RETURN
CC27 END

```



SUBROUTINE RCF(V,GAS,PUBRAT,CUF,CUF,I,NCI)  
 ERROR ANALYSIS (CALCULATE THE ABSOLUTE VALUE OF DISTRIBUTION FACTOR  
 OF EXPERIMENTAL RESULTS.

```

CCCC
CCCC IMPLICIT REAL*8(A-H,O-Z)
CCCC DIMENSION V(15),GAS(15),BUBRAT(15),CUB(15),CUFF(15),ERROR(15),WF(15)
CCCC 1),WF1(15),HG(15),HGI(15),HN(15),WNI(15),WX(15),WY(15),HX(15),HY(15),
CCCC 215),DF(15),ERR(15),NO(15)
CCCC DC 10 I=1,11
CCCC CUB(I)=CUB(I)*1.0D-03
CCCC CUF(I)=CUF(I)*1.0D-03
CCCC WF1(I)=V(I)*0.001
CCCC WNI(I)=BUBRAT(I)*0.03
CCCC HGI(I)=GAS(I)*0.05
CCCC HX1(I)=CLB(I)*0.01
CCCC WY1(I)=CUF(I)*0.01
CCCC WF(I)=(CUF(I)/CUB(I)-1.0)/((565.488*BUBRAT(I)*GAS(I)**2.0)**0.3333)
CCCC WN(I)=-V(I)*(CUF(I)/CUB(I)-1.0)/(565.488*BUBRAT(I)**4.0*GAS(I)
CCCC 1)**2.0)**0.3333)
CCCC HG(I)=-2.0*V(I)*(CUF(I)/CUB(I)-1.0)/(3.0*(565.488*BUBRAT(I)*GAS(I)
CCCC 1)**5.0)**0.3333)
CCCC WY(I)=V(I)/(CUB(I)*(565.488*BUBRAT(I)*GAS(I)**2.0)**0.3333)
CCCC WX(I)=-V(I)*CUF(I)/((565.488*BUBRAT(I)*GAS(I)**2.0)**0.3333)*CUB(
CCCC 11)**2.0)
CCCC ERROR(I)=(WF(I)*WF1(I)*WF1(I)*WF1(I)*WF1(I)*WF1(I)*WF1(I)*WF1(I)*WF1(I)
CCCC 1)*HG(I)*HG1(I)*HG1(I)*HN(I)*HN(I)*HN(I)*HN(I)*WX(I)*WX(I)*WX(I)*
CCCC 2*HX1(I))**C.5
CCCC DF(I)=V(I)*(CUF(I)/CUB(I)-1.0)/((565.488*BUBRAT(I)*GAS(I)**2.0)**C.
CCCC 13333)
CCCC ERR(I)=ERROR(I)/DF(I)
CCCC 10 CONTINUE
CCCC WRITE(3,5) (AC(I),I=1,11)
CCCC WRITE(3,7) (DF(I),I=1,11)
CCCC WRITE(3,6) (ERRCR(I),I=1,11)
CCCC WRITE(3,8) (ERR(I),I=1,11)
CCCC 5 FORMAT(2X,' RUN NO',IX,12I10)
CCCC 6 FOPMAT(1X,' DF(DEV)',IX,12C10.3)
CCCC 7 FOPMAT(2X,' DF',IX,12C10.3)
CCCC 8 FOPMAT(2X,' ERFCR',IX,12C10.3)
CCCC RETURN
CCCC END
  
```

PURPOSE OF THIS PROGRAM

CALCULATES THE THEORETICAL AND EXPERIMENTAL VALUES OF DISTRIBUTION FACTOR OF IONS FOR THE SYSTEMS CONTAINING TWO METAL IONS. THE INDEPENDENT VARIABLE IS THE MOLAR FRACTION OF LIGHT METAL. THE THEORETICAL BACKGROUND IS BASED ON THE GOUY-CHAPMAN DIFFUSE DOUBLE LAYER THEORY.

DESCRIPTION OF PARAMETERS

PH : PH OF THE SOLUTION FOAMED, PRESET VALUE  
Z : VALANCE OF SPECIES 1 IN THE SOLUTION  
B : CORRELATED CONSTANTS FOR THE AMOUNT OF HNO<sub>3</sub> VS PH  
XK, XT, XA, XE, XN AND XG : POLTZMANN CONSTANT, ABSOLUTE TEMPERATURE, DIELECTRIC CONSTANT, ELECTRONIC CHARGE, AVOGADRO NUMBER AND SURFACE EXCESS OF SURFACTANT, NAORS.  
CCNC : EQUILIBRIUM CONSTANTS FOR THE SIMULTANEOUS EQUATIONS GOVERNING THE EQUILIBRIUM RELATION IN THE SOLUTION.  
CONC1 & CONC2 : PRESET METAL CONCENTRATIONS  
X1 TO X5 : EFFECTIVE RADII OF SPECIES 1 IN THE SOLUTION  
DTF1 TO DTF5 : DISTRIBUTION FACTOR OF SPECIES 1 IN THE SOLUTION.  
ALF21 : RELATIVE SEPARATION COEFFICIENT OF METAL 2 TO METAL 1.  
GAMA21 : RATIO OF THE SURFACE EXCESSES OF METAL 2 AND METAL 1.

METHOD OF USE

1. THEORETICAL PART :  
READ IN ALL THE CONSTANTS & CONDITIONS PRESET, THEN COMPUTER WILL AUTOMATICALLY CALCULATE SURFACE POTENTIAL OF SPECIES IN THE SOLUTION. THE DISTRIBUTION FACTOR IS CALCULATED FROM THE INTEGRATION OF EQUATION USING THE SURFACE POTENTIAL AS THE LOWER LIMIT. THE RELATIVE SEPARATION COEFFICIENT AND THE RATIO OF THE SURFACE EXCESSES OF TWO COMPONENTS ARE ALSO CALCULATED AT CERTAIN MOLAR FRACTION OF 'LIGHT' COMPONENT.  
2. EXPERIMENTAL PART  
CALL SUBROUTINE LTK RIGHT AFTER ALL THE EXPERIMENTAL DATA ARE READ IN TO GIVE ALL THE RESULTS ANTICIPATED.  
IMPLICIT REAL\*(A-H, C-Y)

```

COC2      DIMENSION BUBRAT(30),DTF2(10),CON(10),WM(5),CO(10),SH(10),S(30),F(
130),F1(30),G(30),G1(30),G2(30),G3(30),CF1(30),CF2(30),CRSB(30),D
2BSF(30),CLB(30),CUF(30),PHF(30),PHB(30),WTF(30),GAS(30),TWF(30),D
3IA(30),SURFAS(30),NO(30),E(10),DTF1(10),A(15),B(10),C(15),H(30),AC
4(15),PH(10),D(10),CCNC(15),G3(30),G5(30),GF3(30),GF5(30),CCR(30)
5,CDF(30),CON1(10),CON2(10),DTF3(10),DTF5(10),ALF21(10),GAMA21(10),
6CON21(10),V(15),GAMA1(15),GAMA2(15),GAMA5(15),GABS(30)
INTEGER Z(20)
0004 READ(1,3) (Z(I),I=1,10)
0005 READ(1,1) (E(I),I=1,3)
0006 READ(1,1) XK,XT,XA,XE,XN,XG
DO 11 J=1,3
0008 READ(1,1) (CONC(I),I=1,7)
0009 READ(1,1) X1,X2,X3,X4,X5
0010 READ(1,3) II
0011 DO 25 I=1,II
0012 READ(1,60) NO(I),PHB(I),PHF(I),WTF(I),TIME(I),GAS(I),BUBRAT(I)
0013 READ(1,1) CUF(I),CUR(I),CDF(I),CCB(I),DBSF(I),DBSD(I)
0014 60 FORMAT(I3,2F5.3,F7.4,2F5.2,F6.1)
0015 DIA(I)=(6.*GAS(I))/(3.14159*5.*BUBRAT(I))*0.3333
0016 SURFAS(I)=5.*3.14159*BUBRAT(I)*DIA(I)*DIA(I)
0017 V(I)=WTF(I)/TIME(I)
0018 25 CONTINUE
0019 DO 61 N=1,II
0020 F(N)=1./10.*(PHB(N))
0021 F1(N)=1./10.*(PF(N))
0022 G(N)=10.*(B(1)+B(2)*PHG(N)+E(3)*PHE(N))*2)
0023 G1(N)=10.*(B(1)+B(2)*PHF(N)+B(3)*PHF(N))*2)
0024 61 CONTINUE
0025 DO 62 N=1,II
0026 CONC(N)=CUB(N)
0027 CONC(9)=CCE(N)
0028 CONC(10)=CRSB(N)
0029 CONC(11)=CCNC(8)+CONC(5)+G(N)
0030 CALL ECILDM(F,CCNC,A,C,AC,N,1,PCT)
0031 G81(N)=AC(1)
0032 G82(N)=AC(2)

```

C  
C  
C

```

CC33 GB3(N)=AC(3)
CC34 GBF(N)=AC(5)
CC35 CCNC(8)=CUF(N)
CC36 CCNC(9)=CDF(N)
CC37 CCNC(10)=CDSF(N)
CC38 CCNC(11)=CCNC(8)+CCNC(9)+G1(N)
CC39 CALL EQILDM(F1,CCNC,A,C,AC,N,1,PCT)
0040 GF1(N)=AC(1)
CC41 GF2(N)=AC(2)
0042 GF3(N)=AC(3)
0043 GF5(N)=AC(5)
CC44 62 CONTINUE
0045 CALL LTK(GB1,GB2,GF1,GF2,II,ITF,GAS,TIME,CIA,CUB,PHD,PHF,CUF,SURFA
IS,NO,CBSB,CDSF,GB3,GB5,GF3,GF5,CDB,CDF,J,GDBS)
CC46 WRITE(3,16)
CC47 CALL RCH(V,GAS,UBBRAT,GB1,GF1,II,NC)
0048 CALL RCH(V,GAS,EUERAT,CB2,GF2,II,NO)
CC49 WRITE(3,9)
0050 DO 19 N=1,II
0051 WRITE(3,97)
0052 CCNC(8)=CUB(N)
0053 CCNC(9)=CEB(N)
0054 CCNC(10)=CDSB(N)
0055 CCNC(11)=CCNC(8)+CCNC(9)+G(N)
0056 CALL EQILDM(F,CCNC,A,C,AC,N,1,PCT)
CC57 IF(PCT.LT. 0.1) GC TC 95
0058 GO TO 94
CC59 95 WRITE(3,96) PCT
CC60 PCT=0.1
0061 94 DO 90 L=1,8
CC62 XG=PCT+GCB(N)
CC63 CALL PCT(2,AC,XK,XT,XA,XE,XN,XG,VII4,YK1)
CC64 CALL NIKE(XK,XT,XE,XI,X2,X3,X4,X5,Z,VII4,YK1,VIII,VIII2,VIII3,VIII5)
CC65 CALL INTEG(Z,AC,XK,XT,XA,XE,XN,VIII,P,TF,VIII,II)
CC66 CTF(L)=TF*P
0067 CALL INTEG(Z,AC,XK,XT,XE,XN,VIII,P,TF,VIII2,2)
CC68 CTF2(L)=TF*(F+2.+TSCR*(1./((1.0D-03*AC(2)+XN)))=(TSCR*(V112)-DSQRT(V
11111))

```





SUBROUTINE ESILPM (F,CCNC,/,C,AC,K,L,PC)

CALCULATES THE EQUILIBRIUM CONCENTRATION OF THE EXISTING SPECIES IN THE SOLUTION BASED ON THE MODIFIED REGULA-FALSI POSITION METHOD.

A & AC : CONCENTRATION OF SPECIES IN THE SOLUTION.  
CONC : EQUILIBRIUM CONSTANT  
H : HYDROGEN CONCENTRATION

```

0002  IMPLICIT REAL*8(A-K,O-Z)
0003  DIMENSION A(15),AC(15),H(30),CCNC(15)
0004  A(1)=1.000E-05
0005  A(2)=1.000E-05
0006  A(3)=1.000E-05
0007  A(4)=1.000E-05
0008  A(5)=1.000E-05
0009  A(6)=1.000E-05
0010  A(7)=1.000E-05
0011  A(8)=1.000E-05
0012  A(9)=1.000E-05
0013  A(10)=1.000E-05
0014  A(11)=1.000E-05
0015  DO 1 J=1,100
0016  A(2)=C.5*A(2)*(1.C+A(1)*CCNC(1)/(A(2)*H(K)))
0017  A(9)=0.5*A(9)*(1.C+A(8)*CCNC(2)/(A(9)*H(K)))
0018  A(3)=0.5*A(3)*(1.0+A(1)*A(4)*A(4)*CCNC(3)/A(3))
0019  A(10)=0.5*A(10)*(1.C+A(8)*A(4)*A(4)*CCNC(4)/A(10))
0020  A(7)=0.5*A(7)*(1.0+A(1)*A(6)*CCNC(5)/A(7))
0021  A(11)=0.5*A(11)*(1.0+A(8)*A(6)*CCNC(6)/A(11))
0022  A(4)=0.5*A(4)*(1.C+A(5)*CCNC(7)/(A(4)*H(K)))
0023  A(1)=0.5*A(1)*(1.0+CCNC(8)/(A(1)+A(2)+A(3)+A(7)))
0024  A(8)=0.5*A(8)*(1.C+CCNC(9)/(A(8)+A(9)+A(10)+A(11)))
0025  A(5)=0.5*A(5)*(1.C+CCNC(10)/(A(4)+A(3)+A(10)+A(11)))
0026  A(6)=0.5*A(6)*(1.0+CCNC(11)/(A(6)+A(7)+A(11)))
0027  1 CONTINUE
0029  C(1)=A(2)*H(K)/A(1)
0030  C(2)=A(9)*H(K)/A(8)

```

C

```

0030      C(3)=A(3)/(A(1)+A(4)+A(6)+A(7))
0031      C(4)=A(10)/(A(8)+A(2)+A(4))
0032      C(5)=A(7)/(A(1)+A(6))
0033      C(6)=A(11)/(A(8)+A(6))
0034      C(7)=A(4)+F(K)/A(5)
0035      C(8)=A(1)+A(2)+A(3)+A(7)
0036      C(9)=A(8)+A(9)+A(10)+A(11)
0037      C(10)=A(4)+A(3)+A(10)+A(10)+A(5)
0038      C(11)=A(6)+A(7)+A(11)
0039      AC(1)=A(1)
0040      AC(2)=A(8)
0041      AC(3)=A(2)
0042      AC(4)=CONC(10)
0043      AC(5)=A(9)
0044      AC(6)=H(K)
0045      AC(7)=A(6)
0046      AC(8)=A(7)
0047      AC(9)=A(4)
0048      AC(10)=A(11)
0049      PCT=A(4)/CONC(10)
0050      RETURN
0051      END

```

0001 SUBROUTINE ROOT (Z,AC,XK,XT,XA,XE,XN,XG,V114,YK1)

0002 IMPLICIT REAL\*8(A-H,C-Y)

0003 DIMENSION AC(15)

0004 INTEGER Z(20)

0005 Z(7)=-Z(7)

0006 Z(9)=-Z(9)

0007 YK=8.\*3.14159\*Z(4)\*Z(4)\*XE\*XE\*1.0D-03\*XN\*AC(4)/(XA\*XK\*XT)

0008 YK1=DSQRT(YK)

0009 M=1

0010 TT1=XE\*XG\*XN

0011 TT=XK\*XT\*XA\*XN\*1.0D 00/(2.\*3.14159)

0012 V1=15.0

0013 V2=100.0

0014 SUM1=0.0

0015 SUM2=0.0

0016 DO 10 N=1,10

0017 SUM1=SUM1+AC(N)\*(V1\*Z(N)-1.C)\*1.0D-03

0018 SUM2=SUM2+AC(N)\*(V2\*Z(N)-1.0)\*1.0D-03

0019 TT1=DSQRT(TT\*SUM1)

0020 TT2=DSQRT(TT\*SUM2)

0021 F1=TT1-TT2

0022 F2=12-TT1

0023 FF=F1\*F2

0024 IF(FF) 12,13,13

0025 V2=V2+35.

0026 IF(N.GT. 900) GO TO 19

0027 M=M+1

0028 GO TO 9

0029 12 M=1

0030 11 Y=(V2-V1)\*COS(F1)/(CABS(F1)+CABS(F2))

0031 V3=V1+Y

0032 SUP3=0.0

0033 DO 14 N=1,10

0034 14 SUM3=SUM3+AC(N)\*(V3\*Z(N)-1.C)\*1.0D-03

0035 T3=CSQRT(TT\*SUM3)

0036 F3=13-TT1

```

0037      AA1=CABS(Y/V3)
0038      IF(AA1 .LE. 1.0D-06) GC TC 15
0039      FF=F1*F2
0040      IF(FF) 16,15,17
0041      16 V2=V3
0042      SUM2=0.0
0043      DO 8 N=1,10
0044      8 SUM2=SUM2+AC(N)*(V2**Z(N)-1.0)*1.0D-03
0045      18 M=M+1
0046      IF(M .GT. 800) GC TC 15
0047      GO TC 11
0048      17 V1=V3
0049      SUM1=0.0
0050      DO 7 N=1,10
0051      7 SUM1=SUM1+AC(N)*(V1**Z(N)-1.0)*1.0D-03,
0052      GC TC 12
0053      19 WRITE(3,67) *
0054      47 FORMAT(5X,' NO CONVERGENCY, NUMBER OF ITERATION = ',I5)
0055      GC TC 1
0056      15 V114=V3
0057      Z(7)=-Z(7)
0058      Z(5)=-Z(5)
0059      1 RETURN
0060      END

```











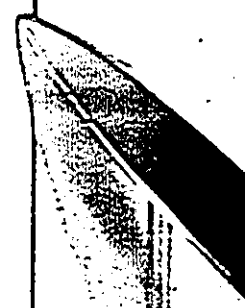
CC59 SUM2=SUM2+SUM2  
0060 Z(3)=HT\*(Y(1))+SUM2+Y(31)  
CC61 Z(1)=0.0  
CC62 Z(2)=SUM1  
0063 12 RETURN  
CC64 END

48

2

8

16



0001

SUBROUTINE LTK(CUB1,CUB2,CUF1,CUF2,I1,WTF,GAS,TIME,DIA,CUB,PHE,PHF,  
1,CUF,SCRFAS,NO,CBSB,CBSF,CUB3,CUB5,CUF3,CUF5,CDB,CCF,J,GAM/9)

CALCULATES THE DISTRIBUTION FACTOR OF SPECIES I FROM THE  
EXPERIMENTAL RESULTS.

0002

IMPLICIT REAL\*8(A-H,I,Q-Z)

DIMENSION CGAS1(30),CGAS2(30),WTF(30),GAS(30),TIME(30),CUF1(30),CU  
1B1(30),CUF2(30),CUB2(30),GAMA1(30),GAMA2(30),DIA(30),SUPFAS(30),CU  
2FC(30),CUF(30),NC(30),ERROR(30),CUB(30),CPH(30),PHF1(30),PHB(30),P  
3HF(30),DBSB(30),CBSF(30),GAMA8(30),GAMA9(30),C1(30),C2(30),C3(30),  
4D4(30),CUB3(30),CUB5(30),CUF3(30),CUF5(30),CDB(30),CCFC(30)  
5),ERROR1(30),CGAS3(30),CGAS5(30),GAMA3(30),GAMA5(30),GAMA7(30),D5(  
630),ALF21(30),GAMA21(30),CCN21(30)  
DO 1 M=1,11

0004

SURFACE CONCENTRATION OF M1++ AND M2++ (RADIUS OF M1++ > M2++ )

0005

CGAS1(M)=WTF(M)\*(CUF1(M)-CUB1(M))/(6.\*1.CC03\*GAS(M)\*TIME(M))

0006

CGAS2(M)=WTF(M)\*(CUF2(M)-CUB2(M))/(6.\*1.CC03\*GAS(M)\*TIME(M))

0007

SURFACE CONCENTRATION OF MICH+ AND M2OH+

0008

CGAS3(M)=WTF(M)\*(CUF3(M)-CUB3(M))/(5.\*1.CD03\*GAS(M)\*TIME(M))

0009

CGAS5(M)=WTF(M)\*(CUF5(M)-CUB5(M))/(6.\*1.CD03\*GAS(M)\*TIME(M))

0010

GAMA1 TO GAMA5 : SURFACE EXCESS OF SPECIES I

0011

GAMA1(M)=CGAS1(M)\*DIA(M)

0012

GAMA2(M)=CGAS2(M)\*DIA(M)

0013

GAMA3(M)=CGAS3(M)\*DIA(M)

0014

GAMA5(M)=CGAS5(M)\*DIA(M)

0015

CUFC(M)=CUB(M)+6.\*1.CD03\*GAS(M)\*(GAMA1(M)+GAMA3(M))\*TIME(M)/(DIA(M)  
1)\*WTF(M))

0016

CUFC(M)=(CDB(M)+6.\*1.CD03\*GAS(M)\*(GAMA2(M)+GAMA5(M))\*TIME(M)/(DIA(M)  
1)\*WTF(M))

0017

ERROR1(M)=100.\*(CUFC(M)-CLF(M))/CLF(M)

0018

ERROR1(M)=100.\*(CCFC(M)-CCF(M))/CCF(M)

0019

DPH(M)=1.0D-14\*(10.\*\*((PHB(M)))+(GAMA3(M)+GAMA5(M))\*TIME(M)\*SURFAS(  
1M)/1.0C 03

0020

DPH(M)=1.0D-14/CPH(M)

0021

PHF1(M)=-CLOG10(CPH(M))

0022

PHF1(M)=-CLOG10(CPH(M))

0023

PHF1(M)=-CLOG10(CPH(M))

0024

PHF1(M)=-CLOG10(CPH(M))

0025

PHF1(M)=-CLOG10(CPH(M))

0026

PHF1(M)=-CLOG10(CPH(M))

0027

PHF1(M)=-CLOG10(CPH(M))

0028

PHF1(M)=-CLOG10(CPH(M))

0029

PHF1(M)=-CLOG10(CPH(M))

0030

PHF1(M)=-CLOG10(CPH(M))

0031

PHF1(M)=-CLOG10(CPH(M))

0032

PHF1(M)=-CLOG10(CPH(M))

0033

PHF1(M)=-CLOG10(CPH(M))

0034

```

0020 GAMA7(M)=WTF(M)*(CCF(M)-CEE(M))/(SURFAS(M)*TIME(M)*1.COC3)
0021 GAMA8(M)=WTF(M)*(CUF(M)-CUP(M))/(SURFAS(M)*TIME(M)*1.OEO3)
0022 GAMA9(M)=WTF(M)*(DBSF(M)-DBSB(M))/(SURFAS(M)*TIME(M)*1.OO03)
C D1 TO D5 : DISTRIBUTION FACTOR CF SPECIES I
0023 D1(M)=GAMA1(M)*1.COC3/CUB1(M)
0024 D2(M)=GAMA2(M)*1.OEO3/CUB2(M)
0025 D3(M)=GAMA3(M)*1.COC3/CUB3(M)
0026 D4(M)=GAMA9(M)*1.COC3/DBSB(M)
0027 D5(M)=GAMA5(M)*1.OEO3/CUR5(M)
0028 ALF21(M)=D2(M)/D1(M)
0029 GAMA21(M)=GAMA2(M)/(GAMA2(M)+GAMA1(M))
0030 CON21(M)=CCB(M)/(CCB(M)+CUB(M))
0031 I CONTINUE
0032 IF(J-2) 5,6,7
0033 5 WRITE(3,2)
0034 GO TO 8
0035 6 WRITE(3,9)
0036 GO TO 8
0037 7 WRITE(3,10)
0038 8 DO 3 M=1,11
0039 WRITE(2,4) NO(M),CON21(M),GAMA21(M),ALF21(M),C1(M),D2(M),D3(M),D5(
1M),GAMA9(M),C4(M),PFB(M),PFF(M),PHE1(M)
3 WRITE(3,15) GAMA1(M),GAMA2(M),GAMA3(M),GAMA5(M)
15 FORMAT(37X,4D11.4)
4 FORMAT(14,9C11.4,2F1.3)
2 FORMAT(1H1,/,/, RUN,1X,CC/(CD+CU),2X,GAMA21,4X,ALPHA21,4X,
1DTF CU+,3X,DTF CD+,3X,DTF CUCH+,2X,DTF CCOH+,3X,GAMACBS,
2,5X,DSF CBS,3X,PFB,4X,PFF,2X,CAL PFF,/)
9 FORMAT(1H1,/,/, RUN,1X,PB/(PB+CU),2X,GAMA21,4X,ALPHA21,4X,
1DTF CU+,3X,DTF PB+,3X,DTF CUCH+,2X,DTF PBOH+,3X,GAMACBS,
2,5X,DSF CBS,3X,PFB,4X,PFF,2X,CAL PFF,/)
10 FORMAT(1H1,/,/, RUN,1X,PB/(PB+CO),2X,GAMA21,4X,ALPHA21,4X,
1DTF CD+,3X,DTF PB+,3X,DTF CDOH+,2X,DTF PROH+,3X,GAMADBS,
2,5X,DSF CBS,3X,PFB,4X,PFF,2X,CAL PFF,/)
RETURN
0046 END
0047

```

11  
08  
1



0001 SUBROUTINE PCH(V,GAS,BUBRAT,CUB,CUF,II,NC)  
 C ERROR ANALYSIS (CALCULATE THE ABSOLUTE VALUE OF DISTRIBUTION FACTOR  
 C OF EXPERIMENTAL RESULTS.

0002 IMPLICIT REAL\*8(A-F,O-Z)  
 0003 DIMENSION V(15),GAS(15),BUBRAT(15),CUB(15),CUF(15),ERROR(15),WF(15),  
 1),WFI(15),HG(15),HGI(15),HN(15),HNI(15),HX(15),HXI(15),HY(15),HYI(15),  
 215),DF(15),ERR(15),NC(30)

0004 DO 10 I=1,11  
 0005 CUB(I)=CUB(I)\*1.0D-03  
 0006 CUF(I)=CUF(I)\*1.0C-03  
 0007 WFI(I)=V(I)\*C.0C1  
 0008 HNI(I)=BUBRAT(I)\*C.C3

0009 HGI(I)=GAS(I)\*0.05  
 0010 HXI(I)=CUB(I)\*0.C1  
 0011 HYI(I)=CUF(I)\*0.C1  
 0012 HF(I)=(CUF(I)/CUB(I)-1.)/((565.488\*BUBRAT(I)\*GAS(I)\*\*2.)\*0.3333)  
 0013 WN(I)=-V(I)\*(CUF(I)/CUB(I)-1.0)/(3.C\*(565.488\*BUBRAT(I)\*\*2.0)\*GAS(I)  
 1)\*\*2.0)\*\*0.3333

0014 HG(I)=-2.0\*V(I)\*(CUF(I)/CUB(I)-1.0)/(3.0\*(565.488\*BUBRAT(I)\*GAS(I)  
 1)\*\*5.0)\*\*0.3333  
 0015 WY(I)=V(I)/(CUB(I)\*(565.488\*BUBRAT(I)\*GAS(I)\*\*2.C)\*\*C.3333)  
 0016 WX(I)=-V(I)\*CUF(I)/((565.488\*BUBRAT(I)\*GAS(I)\*\*2.0)\*\*0.3333)\*CUB(I)  
 1)\*\*2.C)

0017 ERROR(I)=(WF(I)\*WFI(I)+HG(I)\*HGI(I)+HN(I)\*HNI(I)+HX(I)\*HXI(I)+HY(I)\*HYI(I)+  
 1)\*HG(I)\*HGI(I)+WY(I)\*C.5  
 2\*WXI(I)\*\*C.5  
 DF(I)=V(I)\*(CUF(I)/CUB(I)-1.)/((565.488\*BUBRAT(I)\*GAS(I)\*\*2.0)\*\*C.  
 13333)

0019 ERR(I)=ERROR(I)/DF(I)  
 0020 IO CONTINUE

0021 WRITE(3,5) (NC(I),I=1,11)  
 0022 WRITE(3,7) (CF(I),I=1,11)  
 0023 WRITE(3,6) (EPRCR(I),I=1,11)  
 0024 WRITE(3,8) (ERR(I),I=1,11)

0025 5 FORMAT(2X, ' RUN NC', 1X, 12I10)  
 0026 6 FORMAT(1X, ' DF (CF)', 1X, 12C10.3)  
 0027 7 FORMAT(2X, ' DF', 1X, 12C10.3)  
 0028 8 FORMAT(2X, ' EPRCR', 1X, 12C10.3)  
 0029 RETURN  
 0030 END